The Human Rad52 Protein:

A Correlation of Protein Function with Oligomeric State

A Dissertation Presented

By

Janice Ann Lloyd

Submitted to the Faculty of the

University of Massachusetts

Graduate School of Biomedical Sciences

in partial fulfillment of the requirements for the degree of

Doctor of Philosophy

September 6, 2002

Biochemistry and Molecular Pharmacology

Parts of this dissertation have appeared in:

Ranatunga, W., Jackson, D., Lloyd, J.A., Forget, A.L., Knight, K.L., and Borgstahl, G.E.O. (2001) Human Rad52 exhibits two modes of self-association. *J Biol Chem* **276**(11), 15876-15880.

Lloyd, J.A., Forget A.L. and Knight, K.L. (2002) Correlation of biochemical properties with the oligomeric state of human Rad52 protein. (in press in *J Biol Chem*)

Lloyd, J.A., McGrew, D. and Knight, K.L. Essential residues for DNA binding in human Rad52 (in preparation)

The Human Rad52 Protein: The Correlation of Protein Function with Oligomeric State

A Dissertation Presented

By

Janice Ann Lloyd

Approved as to style and content by:

Dr. Anthony Carruthers, Chair of Committee

Dr. Kai Lin, Member of Committee

Dr. Craig Peterson, Member of Committee

Dr. Bill Royer, Member of Committee

Dr. Lorraine Symington, Member of Committee

Dr. Kendall Knight, Thesis Advisor

Dr. John Sullivan
Dean, Graduate School of Biomedical Science

Department of Biochemistry and Molecular Pharmacology
September 6, 2002

Acknowledgements

First, I would like to thank my parents, Kenneth and Joan Lloyd, for all of the support, love, and encouragement they gave me throughout the course of my graduate career. I credit them for the work ethic that they instilled in me. It is by their example that I learned to tackle difficult problems and persevere until arriving at a solution. Additionally, I would like to thank my brother, Kenneth Patrick, for his support and mathematical backup.

I would like to thank past and present members of the Knight lab including, Dr. Julie DeZutter who was not only an incredible scientific help but also a wonderful friend, Anthony Forget who took the electron micrographs, undergraduate students Mike Meuse and J.P. Verderese who made mentoring a rewarding experience, and Dharia McGrew who helped me stay sane while finishing my thesis.

I would like to thank members of other labs in the Biochemistry department, including Dr. Kara Levine of the Carruthers lab for years of laughter and scientific advice and Robert Simler of the Matthews lab who helped me enormously with the CD analysis and made my last year of graduate school a specially memorable one.

Last, but certainly not least, I would like to thank my graduate advisor, Dr. Kendall Knight. Under Ken's mentorship I gained confidence in my scientific ability. Ken was always available and willing to discuss experimental design as well as to check my math. His excitement and dedication to scientific research was a key motivating factor in my graduate career. After working with Ken, I feel that I have a developed the skills necessary to succeed in scientific research.

Abstract

The regulation of protein function through oligomerization is a common theme in biological systems. In this work, I have focused on the effects of the oligomeric states of the human Rad52 protein on activities related to DNA binding. HsRad52, a member of the *RAD52* epistasis group, is thought to play an important and as yet undefined role in homologous recombination. HsRad52 preferentially binds to ssDNA over dsDNA and stimulates HsRad51-mediated strand exchange (Benson *et al.*, 1998). In either the presence or absence of DNA, HsRad52 has been observed to form both 10 nm ring-like structures as well as higher order oligomers consisting of multiple 10 nm rings (Van Dyck *et al.*, 1998; Van Dyck *et al.*, 1999). Earlier protein-protein interaction studies mapped the domain responsible for HsRad52 self-association in the N-terminus (residues 85-159) (Shen *et al.*, 1996). Data presented here identifies a novel self-association domain in the C-terminus of HsRad52 that is responsible for the formation of higher order oligomers.

Van Dyck *et al.* observed DNA ending binding complexes consisting of multiple rings (Van Dyck *et al.*, 1999). They proposed that these higher order oligomers may be functionally relevant. In this work, we demonstrate that DNA binding depends on neither ring shaped oligomers nor higher order oligomers but that activities of HsRad52 that require simultaneous interaction with more

than one DNA molecule depend on the formation of higher order oligomers consisting of multiple HsRad52 rings.

Early studies of HsRad52 proposed that the DNA binding domain resides in the highly conserved N-terminus of the protein (Park *et al.*, 1996). A series of studies using truncation mutants of HsRad52 have provided evidence that supports this hypothesis. For example, we demonstrated that a truncation mutant containing only the first 85 residues of the protein is still able to bind DNA (Lloyd, submitted 2002). In this study, we demonstrate that aromatic (Y65, F79 and Y81) and hydrophobic (L43, I52 and I66) residues within the N-terminus contribute to DNA binding by either directly contacting the DNA or by stabilizing the structure of the protein.

In summary, through the work presented in this dissertation, we have determined that the formation of 10 nm rings is mediated by a self-association domain in the N-terminus and that the formation of higher order oligomers consisting of multiple HsRad52 rings is mediated by an additional self-association domain in the C-terminus. We have correlated the oligomeric properties of HsRad52 with its biochemical functions related to DNA binding. Additionally, we have demonstrated that aromatic and hydrophobic residues contribute to DNA binding. Further studies will differentiate between the contribution of these residues to the DNA binding by stabilizing the overall structure of the protein versus making specific DNA contacts. Additional

studies will also address how the oligomeric state of HsRad52 contributes to its role in HsRad51-mediated strand exchange.

Table of Contents

List of Tables

List of Figures

List of Abbreviations

ATP	adenosine triphosphate
β–ME	β-mercaptoethanol
BSA	bovine serum albumin
CD	circular dichroism
ds	double stranded DNA
DSB	double strand break
DTT	dithiothreitol
EDTA	ethylenediaminetetraacetic acid
EM	electron microscopy
HhH	helix-haripin-helix motif
HR	homologous recombination
HsRad51	Human Rad51
HsRad52	Human Rad52
HsRPA	Human replication protein A
IPTG	iospropyl-β-D-thiogalactopyranoside
IR	ionizing radiation
MMS	Methyl methanesulfonate
MRE	mean residue ellipticity
NHEJ	non-homologous end joining
Ni-NTA	nickel nitrilotriacetic acid
NP-40	nonident P40

NTPs	nucleoside triphosphates
PEI	polyethylenimine
PMSF	phenylmethylsulfonyl fluoride
ScRad51	*S. cerevisiae* Rad51
ScRad52	*S. cerevisiae* Rad52
ScRPA	*S. cerevisiae* RPA
SDS	sodium dodecyl sulfate
SFM	scanning force microscopy
SI	strand invasion
SSA	single strand annealing
SSB	single stranded binding protein
SsDNA	single stranded DNA
STEM	scanning transmission electron microscopy
TBP	TATA binding protein

Chapter I

Introduction and Literature Review

Overview of Genomic Stability and Repair

The maintenance of genomic stability is crucial for the viability of all organisms. The integrity of the human genome is continuously threatened by both environmental factors, e.g. ionizing radiation and chemical mutagens, and errors that occur naturally during normal cellular processes such as DNA replication. All of these events result in various DNA lesions, including double-strand breaks (DSBs) which if left unrepaired will lead to chromosomal aberrations and further to hereditary diseases, cancer, or cell death. To maintain the integrity of the genome, organisms utilize a variety of DNA repair pathways.

In mammalian cells, DSBs are repaired via two main pathways, homologous recombinational repair (HR) or non-homologous end joining (NHEJ). NHEJ repairs the damaged chromosome in a non-conservative manner by rejoining the broken ends. While this can result in accurate repair, it most often results in the addition or deletion of nucleotides and is, therefore, error-prone (Baumann and West, 1998). Alternatively, HR is a conservative, error-free process that uses either a homologous chromosome, duplicated sequence or a sister chromatid as a template to repair the damaged DNA. HR can be further divided into strand invasion (SI), a conservative pathway, or single-strand

annealing (SSA), a semi-conservative repair pathway. Evidence to date identifies SI as the major pathway of HR in mammalian cells with SSA playing a minor role (Pastnik et al., 2001).

Biochemically, SI can be categorized into 4 distinct steps (1) initiation, (2) homologous pairing and DNA strand exchange (3) DNA heteroduplex extension (branch migration) and (4) resolution (Bianco et al., 1998). Figure 1 represents a generic model for SI. SI begins with the processing of the DSB by exonucleases to produce a free 3′ -ssDNA overhang. In the second step, a search for homologous DNA begins and the 3′ -terminal end is paired with homologous DNA to form an intermediate, a joint molecule. This step is mediated by the recombinase RecA in prokaryotes and the Rad51 homologues in eukaryotes. Once the joint molecule is formed, the displaced strand is paired with a complementary strand to form a second intermediate designated a Holliday junction. Proteins involved in branch migration then extend the Holliday junction(s). The final step in SI involves the cleavage of the Holliday junction by a resolvase to yield recombinant products. Like SI, SSA is also initiated with the processing of the DSB to yield free 3′ -terminal ends. The homologous complementary regions of ssDNA surrounding the break are aligned and annealed resulting in the deletion of the intervening sequences (Baumann and West, 1998).

The observation in *S. cerevisiae* that mitotic recombination events were rarely accompanied by crossover events led to the proposal of an alternative pathway for SI, termed the synthesis-dependent strand annealing pathway (SDSA) (Paques et al., 1999). The initiating steps in SDSA and SI are similar beginning with the 5′-to-3′ resection of the DSBs and subsequent invasion of a homologous DNA template by the 3′-ssDNA tails. The SDSA pathway differs from SI in that after the 3′-ssDNA tail invades the homologous DNA sequence, the newly synthesized DNA strands are displaced from the template and then annealed to one another eliminating the Holliday junction intermediate. Therefore in SDSA, DNA synthesis is a conservative, with the newly synthesized sequences in the same molecule, whereas in SI DNA synthesis is semi-conservative, with the newly synthesized sequences present in both the donor DNA template and recipient DNA molecule. What determines which pathway is used may depend on the type of recombination event required. For example during meiosis in which the exchange of genetic information between DNA molecules is important SI may be favored over SDSA. Further experiments need to be performed in order to determine the relative contributions of these pathways for DSB repair.

Figure 1. General Model of DSB repair.

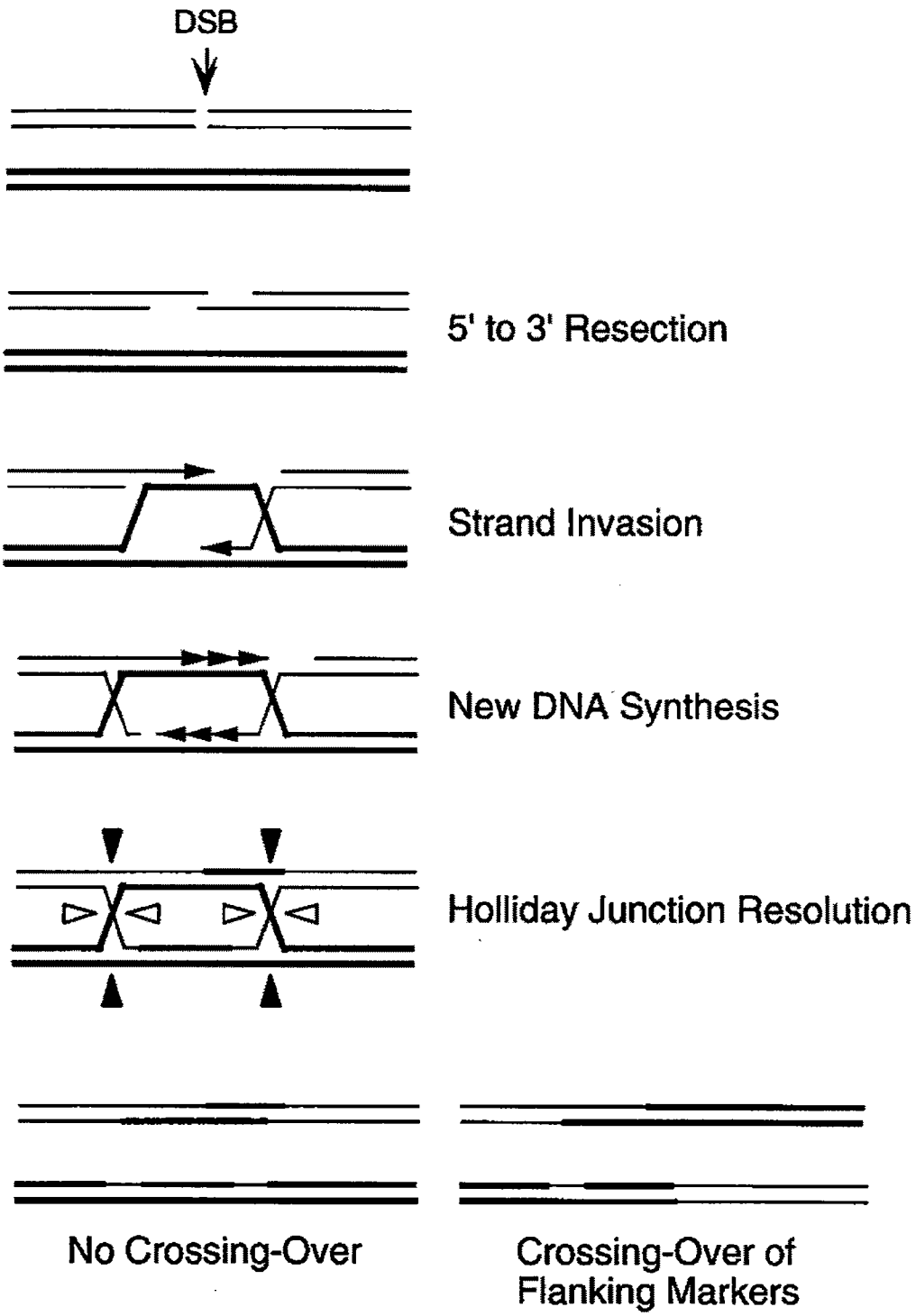

Figure 1. General model for DSB repair. DSB formation is followed by 5′ -to-3′ resection of the ends. The resulting 3′ ends are recombinogenic and can invade a homologous template, to initiate new DNA synthesis. Two HJs are formed and resolved independently by cutting the crossed (open arrowhead) or noncrossed (closed arrowhead) strands, resulting in crossover or noncrossover products. Figure is adapted from Paques *et al.* (1999) *Microbiol Mol Review* **63,** 349-404.

While earlier studies suggested that NHEJ is the predominant pathway for DSB repair in mammalian cells, new data supports a more significant role for HR. A number of studies designed to evaluate the types of repair at a defined DSB have provided data indicating that HR is responsible for a greater percentage of repair events than previously realized (Liang et al., 1998; Bishop and Schiestl, 2000; Johnson and Jasin, 2000; Thompson and Schild, 2001). Accumulating evidence that defects in HR are associated with tumorigenesis reinforces the importance of HR in the maintenance of genomic integrity (Thompson and Schild, 2001). Additionally, Takata *et al.* looked at the relative contribution of both pathways in DSB repair and showed that the NHEJ pathway plays an important role during G1-early S phase while the HR pathway seems to be preferred during late S -G2 phase (Takata et al., 1998). Therefore, the pathway which cells utilize to repair damaged DNA appears to be affected by the cell cycle.

HR in *S. cerevisiae*

Genetic Analysis of the *RAD52* Epistasis Group in *S. cerevisiae*

Knowledge about HR has largely come from studies in *S. cerevisiae*. In *S. cerevisiae* members of the *RAD52* epistasis group, including *RAD50-55, 57, XRS2* and *MRE11*, were originally identified as components of the HR pathway due to the increased sensitivity of mutants to ionizing radiation (IR) (Game and Mortimer, 1974). Strains that are mutated in *RAD50, MRE11* or *XRS2* show defects in DNA repair and meiotic recombination yet show normal levels of

mitotic recombination and mating-type switching. Analysis of the DNA intermediates in these strains indicates that the gene products of *RAD50, MRE11,* and *XRS2* are critical for the incision step during meiotic recombination (Shinohara and Ogawa, 1995). Additionally in strains that are mutated in *RAD50, MRE11,* and *XRS2*, the 5'-to-3' processing of the DSB ends in mitotic cells is delayed, suggesting that these gene products are also involved in the early stages of HR to process the DSBs to produce 3´ ssDNA tails (Shinohara and Ogawa, 1995). Strains mutated in *RAD51, RAD52, RAD54, RAD55,* or *RAD57* show defects in DNA repair and both mitotic and meiotic recombination (with the exception of *RAD54* that displays a partial defect in meiotic recombination). Analysis of the DNA intermediates in these strains shows the accumulation of unrepaired DSBs with processed 3´ ssDNA tails, suggesting that these gene products are involved in the search for homologous DNA and DNA pairing following the initial processing of DSBs (Shinohara et al., 1992; Shinohara and Ogawa, 1995; Sugawara et al., 1995). Mutant *rad52* strains display the most severe phenotype of all *RAD52* epistasis group members implying that Rad52 is an integral component of SI (Petes, 1991; Paques and Haber, 1999).

Based on the phenotypes of the mutant strains the model depicted in Figure 2 has been proposed for HR, specifically SI, in *S. cerevisiae* (Bianco et al., 1998). Early after a DSB has been introduced either by the endonuclease, Spo11, in meiotic cells or DNA damaging agents in mitotic cells, the heterotrimeric protein complex, Rad50/Mre11/Xrs2, is localized to the site of damage. This

complex is involved in the resection of DSBs resulting in the production of 3′ ssDNA tails. Unexpectedly, it has been demonstrated that Mre11 has a 3′-to-5′ exonculease activity and so the mechanism by which this complex participates in the resection of DSB ends remains to be elucidated (Paques et al., 1999). Once the 3′-ssDNA tails have been produced, multiple *RAD52* epistasis group proteins are recruited to the site of damage including, replication protein A (RPA), Rad51, Rad52, Rad54, Rad55, and Rad57. These proteins participate in the search for homologous DNA, strand exchange, Holliday junction formation and subsequently heteroduplex extension. The final step in SI is resolution of the Holliday junctions via nucleolytic cleavage. During SI, two Holliday junctions are formed which are resolved. While all of the components necessary for Holliday junction resolution remain to be identified, there is recent genetic evidence indicating that the Mus81 protein may be involved in this process (Haber and Heyer, 2001). The mechanistic details of Holliday junction resolution await the biochemical characterization of Mus81 as well as the identification of the other proteins involved. Processing of the Holliday junctions results in either spliced or patched products depending on the directionality of nucleolytic cleavage (Bianco et al., 1998). While the proteins of the *RAD52* epistasis group have been identified as being important for Holliday junction formation, the mechanism by which these junctions are resolved is unclear.

Genetic experiments in *S. cerevisiae* suggested that RPA, Rad51, Rad52, Rad55, and Rad57 proteins might be involved in the homologous pairing and

DNA strand exchange step of HR (Game and Mortimer, 1974; Petes, 1991). The results of cytological studies support this notion by demonstrating that a number of *RAD52* group proteins colocalize. For example, Rad52 is present in a number of subnuclear complexes with RPA and Rad51 (Gasior et al., 1998). Rad51 foci appear in cells at sites of DNA damage, most likely at the DSB and are thought to represent assemblages of protein oligomers (Gasior et al., 2001). Gasior *et al.* determined that in order for Rad51 foci to form at DSBs in meiotic cells, RPA, Rad52, Rad55 and Rad57 must be present (Gasior et al., 1998). A later study further defined the requirements for Rad51 foci formation by demonstrating that in irradiated mitotic cells Rad51 foci form in either the presence of the Rad52 protein or the Rad55 and Rad57 proteins, however in meiotic cells all the three proteins are necessary for Rad51 assembly (Gasior et al., 2001).

Figure 2. A model for Strand Invasion in *S. cerevisiae*.

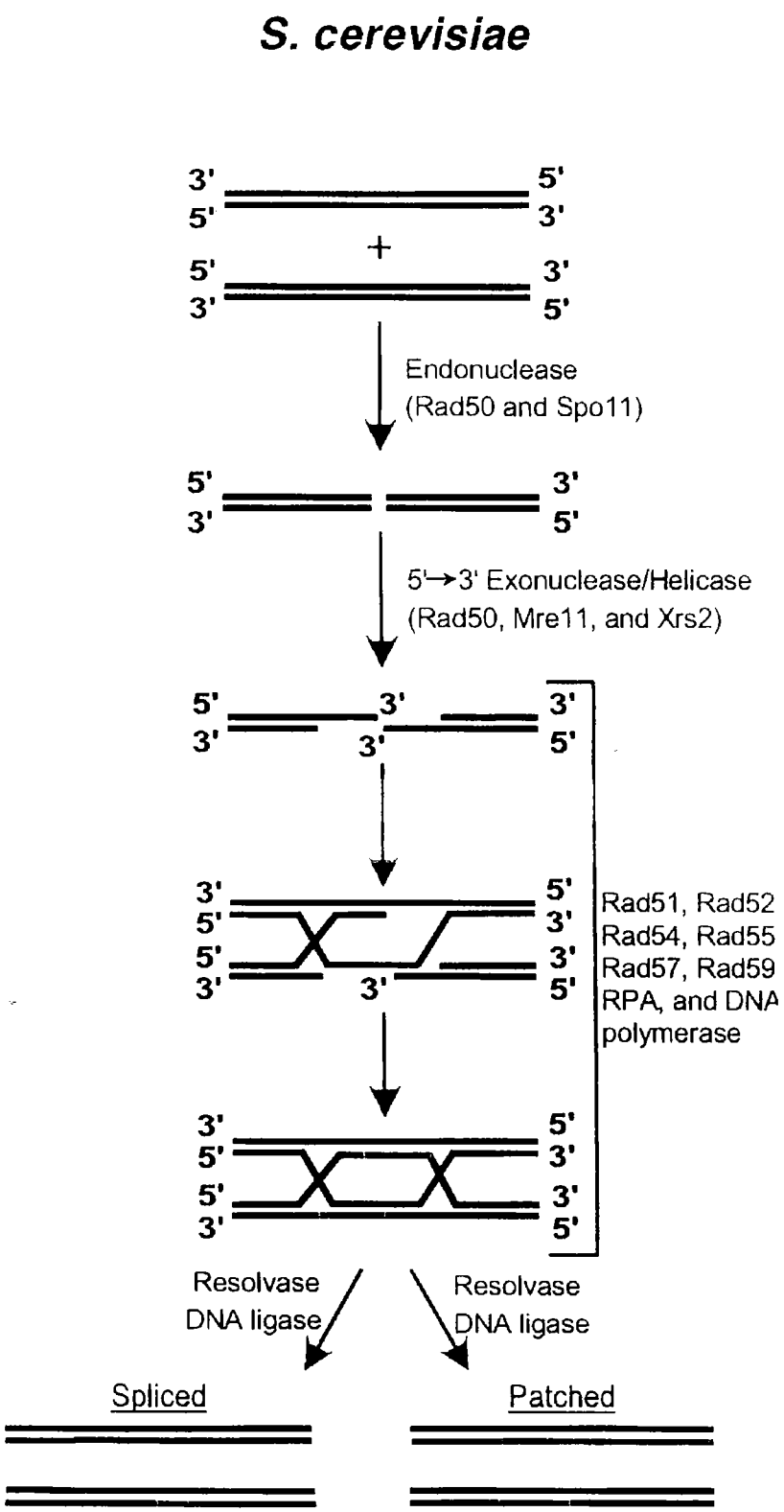

Figure 2. Biochemical model for HR in *S. cerevisiae*. Proteins involved in each step are indicated in parentheses. Nascent DNA synthesized by DNA polymerase is depicted by light blue lines. Adapted from Bianco *et al.* (Bianco et al. (1998) Frontiers in Bioscience **17**: 570-603.

Colocalization of a number of *RAD52* epistasis proteins suggested that the proteins might interact with one another during HR. By combining the results of both *in vivo* and *in vitro* experiments, the following interactions between *RAD52* epistasis group members were determined. Rad51 interacts with Rad52 (Shinohara et al., 1992; Milne and Weaver, 1993; Donovan et al., 1994; Hays et al., 1995), Rad54 (Clever et al., 1997; Petukhova et al., 1998), Rad55 (Hays et al., 1995; Johnson and Symington, 1995), and itself (Donovan et al., 1994). In addition to interacting with Rad51, Rad52 also interacts with RPA and itself (Boundy and Livingston, 1993; Hays et al., 1998). Finally, the Rad55 and Rad57 proteins have to been shown to interact to form a heterodimer (Hays et al., 1995; Johnson and Symington, 1995; Sung, 1997).

Biochemical properties of *RAD52* group proteins

The genetic, cytological, and protein-protein interaction studies suggest that *RAD52* group proteins colocalize and interact with one another, possibly forming a recombination complex. To investigate the mechanistic roles of the individual proteins in HR, the biochemical functions of each have been studied.

RPA, present in a number of DNA metabolic pathways including replication, recombination and repair, is the eukaryotic homologue of *E. coli*, SSB. RPA is a ssDNA binding protein that alleviates secondary structure in the DNA

and increases the ssDNA-dependent ATPase activity of Rad51 when phage ssDNA is used as a cofactor (Sugiyama et al., 1997). Additionally, Sung has shown that RPA potentiates Rad51-mediated strand exchange (Sung, 1994). Further studies have shown that the RPA potentiation of Rad51 mediated strand exchange is dependent upon the order of assembly of components on the ssDNA tail. Rad51-mediated strand exchange is efficient if Rad51 nucleates onto ssDNA prior to RPA. In contrast if RPA binds to the DNA prior to Rad51, RPA inhibits Rad51-mediated strand exchange, presumably by saturating all the ssDNA binding sites thereby implying that RPA must be displaced prior to Rad51 filamentation (Sung, 1997).

Rad51 is the eukaryotic homologue of *E. coli* RecA. The ScRad51 and EcRecA proteins share 30% sequence identity over a 207-amino acid core region which contains the ATP binding consensus sequences: the Walker A and Walker B boxes (Shinohara et al., 1992). DNA binding studies have determined that Rad51 binding to both ss- and dsDNA is dependent on the presence of ATP and Mg^{2+} (Namsaraev and Berg, 1998; Zaitseva et al., 1999). While Rad51 does not show a preference for either ss- or dsDNA, the dsDNA-Rad51 complexes were more stable than the ssDNA-Rad51 complexes (Zaitseva et al., 1999). Electron microscopy (EM) studies have shown Rad51 polymerizes onto ssDNA and dsDNA to form nucleoprotein filaments and that the ssDNA-Rad51 nucleoprotein filament is the active species in strand exchange (Ogawa et al., 1993; Sung and Robberson, 1995). Rad51 also possesses a ssDNA ATPase activity

that is stimulated by the presence of RPA (Sugiyama et al., 1997). Interestingly, SSB is able to substitute for RPA in the promotion of strand exchange by Rad51 (Sugiyama et al., 1997). This suggests that RPA exerts its effects through alleviating the secondary structure in the DNA rather than through a direct interaction with Rad51. Since RPA has a higher DNA binding affinity and faster binding kinetics than Rad51 (Gasior et al., 2001), RPA inhibits Rad51 mediated strand exchange by binding to the ssDNA prior to Rad51 and forcing Rad51 to bind dsDNA. Thus in order for strand exchange to occur, an additional component may be required to mediate the competition between Rad51 and RPA for ssDNA.

Rad52 is a prime candidate to fill the role of mediator. Based on the genetics, Rad52 is an essential protein for HR, yet no clear role for Rad52 has been elucidated. Rad52 binds to both ssDNA and dsDNA with a preference for ssDNA (Mortensen et al., 1996). Unlike Rad51, the interaction between ssDNA and Rad52 is not dependent on the presence of either ATP or Mg^{2+} (Mortensen et al., 1996; Shinohara et al., 1998). Rad52 binding to dsDNA is actually inhibited by Mg^{2+} (Shinohara et al., 1998). EM studies by Shinohara *et al.* show that Rad52 forms ring-like structures with a diameter of approximately 9±1 nm in both the absence and presence of ssDNA. In the presence of ssDNA, the Rad52 rings appear to coat the DNA by aligning themselves side by side but not forming filaments on the DNA in a manner analogous to Rad51 (Shinohara et al., 1998).

Rad52 is able to stimulate the annealing of complementary strands of DNA, a process further enhanced by the presence of RPA if the DNA substrate is plasmid length DNA (Mortensen et al., 1996; Shinohara et al., 1998; Sugiyama et al., 1998). RPA stimulates the annealing activity of Rad52 by eliminating secondary structure within the ssDNA substrate (Sugiyama et al., 1998). While SSB is able to substitute for RPA in the Rad51 mediated strand exchange reaction, SSB is not able to substitute for RPA in promoting Rad52 annealing activity (Sugiyama et al., 1998). This suggests that RPA stimulates annealing through a specific interaction with Rad52 in addition to removing secondary structure in the DNA.

In experiments where Rad51 is allowed to filament onto the ssDNA prior to introducing RPA, RPA enhances Rad51 mediated strand exchange (Sung, 1997). In contrast under conditions which more closely mimic the *in vivo* situations, e.g. simultaneous introduction of RPA, Rad51 and the DNA substrates, RPA diminishes Rad51 mediated strand exchange through competition for ssDNA binding sites (Sung, 1997). This paradox supports the notion that there may be an additional factor that mediates the competition between RPA and Rad51 for ssDNA binding sites. Studies have shown that neither Rad52 alone nor in combination with Rad51 stimulates strand exchange (Sung, 1997). However in the presence of RPA, Rad52 stimulates Rad51 mediated strand exchange. These studies provide evidence that Rad52 assists in the loading of Rad51 onto ssDNA by alleviating the inhibition caused by the assembly of RPA on DNA and thus stimulating Rad51 mediated strand

exchange. (Sung, 1997; New et al., 1998; Shinohara and Ogawa, 1998; Song and Sung, 2000). Therefore, Rad52 has been proposed to act as a molecular mediator that functionally links Rad51 and RPA (Song and Sung, 2000).

Biochemical experiments have provided evidence that the Rad55 and Rad57 proteins can also mediate strand exchange. Sequence comparison shows that Rad55 and Rad57 appear to be homologues of RecA/Rad51. These proteins form a stable heterodimer that shares biochemical properties with Rad51 such as ATPase activity and preferential binding of ssDNA over dsDNA (Hays et al., 1995; Sung, 1997). The Rad55-Rad57 heterodimer is not able to perform strand exchange itself, but like Rad52, it does stimulate strand exchange in the presence of RPA and Rad51 (Sung, 1997).

The amino acid sequence of the Rad54 protein shows significant homology to Swi2p/Snf2p (Emery et al., 1991). This sequence homology contains motifs proposed to identify a family of DNA binding proteins which function as helicases (Emery et al., 1991). As expected, ScRad54 possesses a dsDNA dependent ATPase activity and stimulates the rate of pairing between homologous ss- and supercoiled dsDNA (Petukhova et al., 1998). Further studies have demonstrated that Rad54 is able to loosen duplex DNA and that this activity is enhanced if Rad54 interacts with the Rad51 nucleoprotein filament (Van Komen et al., 1999; Mazin et al., 2000).

While early studies of HR focused on the SI pathway, recent work has shown that SSA, a semi-conservative HR pathway, may play a major role in repairing DSBs in yeast, when the DSB is flanked by homologous repeated sequences. Genetic studies have shown that unlike SI, SSA is not dependent upon *RAD51, RAD54, RAD55* and RAD57 (Ivanov et al., 1996). To date the genes identified as important in SSA are also components of other repair pathways including: excision repair genes, *RAD1* and *RAD10*, mismatch repair genes, *MSH2* and *MSH3*, and recombinational repair genes, *RAD52* and its homologue, *RAD59* (Ivanov and Haber, 1995; Sugawara et al., 1995; Bai and Symington, 1996; Saparbaev et al., 1996). Rad59, approximately half the length of Rad52, is homologous to the N-terminal region of Rad52 (Bai and Symington, 1996). Rad59 interacts with Rad52, binds ssDNA, possesses a single strand annealing activity and further stimulates the annealing activity of Rad52 (Petukhova et al., 1999; Davis and Symington, 2001). However Rad59 is not able to perform the annealing activity in the presence of RPA, to substitute for Rad52, nor participate in SI (Davis and Symington, 2001). It may be that the role of Rad59 in SSA is to potentiate the annealing activity of Rad52. The dependence of SSA on Rad52 helps to explain the severity of null *rad52* phenotypes.

The data from the combined biochemical experiments suggests that *RAD52* epistasis group proteins work together as a recombinational repair complex in HR. At this time, the temporal order in which these proteins assemble and disassemble at the site of DNA damage is not known. The

biochemical data support a model in which the components assemble at the site of damage to form a recombination complex instead of arriving at the site already assembled (Kowalczykowski, 2000). Identifying this order will further elucidate the mechanism by which these components repair DSBs.

HR in Vertebrates

Genetic Analysis of *RAD52* group proteins in vertebrates

Sequence analysis has helped identify the vertebrate homologues for *RAD52* epistasis group proteins. The number of gene products involved in HR in vertebrates is larger than in *S. cerevisiae*. To date, homologues have been identified for *RAD51* (Shinohara et al., 1993), *RAD52*(Muris et al., 1994; Shen et al., 1995), and *RAD54* (Kanaar et al., 1996) that share 68%, 30% and 48% identity with the *S. cerevisiae* protein, respectively. Five additional human genes, *RAD51B* (Albala et al., 1997; Rice et al., 1997; Cartwright et al., 1998), *RAD51C* (Dosanjh et al., 1998), *RAD51D* (Cartwright et al., 1998; Pittman et al., 1998), *XRCC2* (Cartwright et al., 1998; Liu et al., 1998), and *XRCC3* (Tebbs et al., 1995; Cartwright et al., 1998; Liu et al., 1998), which share 20-30 % sequence homology with *RAD51,* have been cloned. Alignment of the amino acid sequences reveals that the homology is restricted to specific regions of the proteins. For example, the ScRad51 and HsRad51 proteins are highly homologous in a core region of the protein which contains the Walker A and B motifs for ATP binding, whereas the N- and C-terminal regions of the proteins are less conserved (Shinohara et al., 1993). The ScRad52 and HsRad52 proteins share significant homology in the N-

terminal regions of the proteins (Muris et al., 1994; Shen et al., 1995) and the ScRad54 and HsRad54 proteins are most highly conserved in the DNA dependent ATPase domain (Kanaar et al., 1996). The *RAD51* paralogs are mostly conserved in the regions of the Walker A and B motifs for ATP binding.

The phenotypes of the vertebrate homologues show some intriguing differences when compared with the phenotypes in *S. cerevisiae*. Null *rad52* yeast strains display the most severe phenotype amongst *RAD52* epistasis group members. In striking contrast, null *rad52* vertebrate cells display only a mild phenotype. Neither *rad52*$^{-/-}$ mouse ES cells nor *rad52*$^{-/-}$ chicken DT40 cells are hypersensitive to DNA damaging agents and both show only a slight defect in targeted recombination (Rijkers et al., 1998; Yamaguchi-Iwai et al., 1998). Additionally, knockout mice of Rad52 are viable, fertile, and show no abnormalities in their immune system (Rijkers et al., 1998.). In *S. cerevisiae*, deletions of *RAD54* and *RAD51* are less sensitive to IR and have less severe effects on mitotic homologous recombination than deletion of *RAD52*. Knockout mice of *RAD54*, like knockout mice of *RAD52*, are viable (Kanaar et al., 1996). However, *rad54*$^{-/-}$ mouse ES cells and *rad54*$^{-/-}$ DT40 cells display an increased sensitivity to IR and the DNA damaging agent, MMS, and display a defect in targeted recombination (Kanaar et al., 1996; Bezzubova et al., 1997). Unlike knockout mice of *RAD52* and *RAD54*, knockout mice of *RAD51* are not viable (Lim and Hasty, 1996; Tsuzuki et al., 1996). Analogously, *RAD51*$^{-/-}$ DT40 cells transfected with a repressible *RAD51* transgene accumulate chromosomal

abnormalities and are hypersensitive to IR when transgene expression is turned off (Sonoda et al., 1998). Targeted disruption of *RAD51B, RAD51D* and *XRCC2* in mice result in embryonic lethality (Shu et al., 1999; Deans et al., 2000; Pittman and Schimenti, 2000). Analysis of DT40 cell lines deficient in each of the Rad51 paralogs shows that all cell lines have defects in targeted recombination (Takata et al., 2001). DT40 cells deficient in *RAD52* or *XRCC3* show slight defects in targeted recombination, but surprisingly DT40 cells conditionally deficient in both *RAD52* and *XRCC3* exhibit a lethal phenotype (Fujimori et al., 2001). These results show that Rad52 and the paralogs have overlapping but non-reciprocal roles in the maintenance of HR (Fujimori et al., 2001).

A number of cytological studies have elucidated the expression patterns and cellular localization of a number of *RAD52* epistasis group proteins. Both HsRad51 and HsRad52 share similar expression patterns. They are expressed in the lowest amounts during G_0/G_1 and reach a maximum expression level during G_2/M when DNA repair by HR is favored over NHEJ (Chen et al., 1997; Takata et al., 1998). In cells treated with ionizing radiation, HsRad51 colocalizes with HsRPA, HsRad52, and HsRad54 (Golub et al., 1998; Liu and Maizels, 2000; Tanaka et al., 2000). Additionally, HsRad52 colocalizes with HsRad50 (Liu and Maizels, 2000). Unlike in *S. cerevisiae*, HsRad51 focus formation is not dependent on the presence of HsRad52 (Gasior et al., 1998; Yamaguchi-Iwai et al., 1998). Rather, HsRad51 focus formation is dependent upon the presence of the five HsRad51 paralogs and HsRad54 (Bishop et al., 1998; Tan et al., 1999; Takata et al.,

2001). The lack of HsRad51 focus formation coupled with the defect in targeted recombination in DT40 cell lines deficient for each of the *RAD51* paralogs suggests the paralogs may facilitate the loading of HsRad51 onto ssDNA, a role similar to the one proposed for the ScRad55-ScRad57 heterodimer.

Biochemical Properties of *RAD52* Group Proteins

Protein-protein interaction studies have established that like the *RAD52* group proteins in *S. cerevisiae*, members of the vertebrate *RAD52* epistasis group interact with one another. HsRad51 interacts with HsRPA (Golub et al., 1998), HsRad52 (Shen et al., 1996), HsRad51C (Dosanjh et al., 1998), XRCC3 (Liu et al., 1998), and HsRad54 (Golub et al., 1997). HsRad52 in turn interacts with HsRad51 (Shen et al., 1996), HsRPA (Park et al., 1996), and itself (Shen et al., 1996; Kito et al., 1999). Interactions have been identified between the RAD51 paralogs as follows: HsRad51B with HsRad51C, HsRad51C with XRCC3, HsRad51C with HsRad51D, and HsRad51D with XRCC2 (Dosanjh et al., 1998; Liu et al., 1998; Braybrooke et al., 2000; Schild et al., 2000). Recently, it has been determined that the Rad51 paralogs interact with one another to form two discrete complexes. One complex, named BCDX2, is comprised of HsRad51B, HsRad51C, Rad51D, and XRCC2 and the other complex is comprised of HsRad51C and XRCC3 (Masson et al., 2001). The greater number of gene products involved in HR, along with the more intricate array of protein interactions among the *RAD52* group

proteins, is indicative of the complexity of HR in vertebrates.

The colocalization and physical interaction amongst members of the vertebrate *RAD52* epistasis group suggests that these human proteins may function together in a manner similar to their yeast counterparts. Biochemical studies investigating the mechanistic roles of the vertebrate proteins have revealed that not all biochemical properties are conserved between the yeast and human homologues, suggesting that the pathways themselves will differ mechanistically. DNA binding studies have determined that HsRad51 binds to both ss- and dsDNA with similar affinities (Benson et al., 1994; Baumann et al., 1996). Interestingly unlike ScRad51, HsRad51 binding to ssDNA is not dependent upon the presence of ATP (De Zutter and Knight, 1999). Analogous to its yeast homologue, the DNA binding of HsRad52 is not dependent on either Mg^{2+} or ATP (Benson et al., 1998; Van Dyck et al., 1998). HsRad52 binds preferentially to ssDNA over dsDNA (Benson et al., 1998; Van Dyck et al., 1998)

Like its yeast counterpart, HsRad52 is not able to mediate strand exchange itself but, unlike its yeast counterpart, it does stimulate Rad51 mediated strand exchange in the absence of HsRPA (Benson et al., 1998). The observed *in vitro* stimulation of HsRad51 by HsRad52 was optimal when HsRad52 was allowed to bind to the ssDNA substrate prior to the introduction of sub-stoichiometric amounts of HsRad51 relative to ssDNA (Benson et al., 1998). However, when stoichiometric amounts of HsRad51 were used, HsRad52 was found to inhibit

product formation (Baumann and West, 1999). The same study confirmed that competition between HsRad51 and HsRad52 for ssDNA provided a mechanism of inhibition (Baumann and West, 1999). Addition of stoichiometric amounts of HsRad52 relative to ssDNA resulted in HsRad51 binding to dsDNA, thereby inhibiting the reaction. Further experimentation demonstrated that the HsRad52 inhibition could be relieved by the presence of HsRPA (Baumann and West, 1999). It is possible that HsRPA displaces HsRad52 from the DNA thus enabling HsRad51 to load onto the ssDNA (Baumann and West, 1999). HsRPA alone is also able to stimulate HsRad51 mediated strand exchange, most likely through removal of secondary structure in the DNA, as in the yeast system (Baumann and West, 1997; Baumann and West, 1999). The mechanism by which HsRad52 stimulates HsRad51 mediated strand exchange is still unclear. HsRad52 could be recruiting HsRad51 to the ssDNA tails through its interaction with HsRad51 as suggested by Benson *et al.* (Benson et al., 1998). Alternatively, HsRad52 could induce structural changes in the DNA upon binding allowing HsRad51 to more readily filament onto the ssDNA as suggested by McIlwraith *et al.* (McIlwraith et al., 2000).

Adding to the complex relationship between HsRad51, HsRad52 and HsRPA, biochemical data collected on HsRad54 and the paralogs suggests that these proteins are also involved in the HsRad51-mediated strand exchange pathway. HsRad54, is a dsDNA dependent ATPase, binds to dsDNA and induces a topological change in the DNA (Swagemakers et al., 1998; Tan et al.,

1999). As is the case with HsRad52, the mechanism by which HsRad54 functions in HR remains unclear. Several roles for HsRad54 have been proposed. Among these HsRad54 may translocate along the DNA via ATP hydrolysis thereby providing processivity to HsRad51 mediated strand exchange and promoting heteroduplex extension (Swagemakers et al., 1998). Indirectly, HsRad54 may affect chromatin structure by displacing histones which might impair homologous pairing, thereby stimulating HR (Tan et al., 1999).

Initial biochemical characterization of the *RAD51* paralogs has revealed that the BCDX2 complex preferentially binds to ssDNA in a Mg^{2+} dependent manner and possesses ssDNA dependent ATPase activity, although at a reduced level compared to HsRad51 (Masson et al., 2001). The HsRad51C-XRCC3 complex also binds ssDNA in a Mg^{2+} dependent manner and in the absence of HsRad51, the HsRad51C-XRCC3 complex is capable of stimulating homologous pairing and strand exchange (Kurumizaka et al., 2001; Masson et al., 2001). Individual components of the BCDX2 complex possess biochemical properties as well. For example, the HsRad51D protein preferentially binds ssDNA and hydrolyzes ATP in a ssDNA dependent manner (Braybrooke et al., 2000). The HsRad51B-HsRad51C heterodimer preferentially binds ssDNA, hydrolyzes ATP, and stimulates HsRad51 mediated strand exchange with HsRPA andHsRad51 competing for ssDNA binding sites (Sigurdsson et al., 2001). Sigurdsson *et al.* have proposed that the HsRad51B-HsRad51C complex functions as a mediator of HsRad51 strand exchange analogous to the ScRad52 protein and ScRad55-

ScRad57 heterodimer. The role of the *RAD51* paralogs in HR may be to facilitate the polymerization of HsRad51 on ssDNA.

Oligomerization of *RAD52* Group Proteins

The use of EM has enabled the visualization of a number the *RAD52* group proteins, namely HsRad51, HsRad52, HsRad54 and the BDCX2 and HsRad51-XRCC3 complexes. Use of EM to monitor the structures of the proteins revealed that they form dynamic oligomeric structures that are affected by the presence of DNA and/or nucleotides.

EM studies of the HsRad51 protein have shown that, like ScRad51 protein, it forms nucleoprotein filaments on ssDNA as well as dsDNA and a HsRad51-ssDNA nucleoprotein filament is the active species in strand exchange (Benson et al., 1994). Scanning force microscopy (SFM) of HsRad54 and DNA revealed that in the absence of ATP, HsRad54 bound as several small complexes on each DNA substrate. Addition of ATP resulted in a drastic redistribution of HsRad54 as larger complexes less frequently dispersed on the DNA (Ristic et al., 2001). HsRad54, appeared to bind DNA as trimers and possibly hexamers (Ristic et al., 2001). The relevance of multiple DNA bound HsRad54 monomers to the facilitation of strand exchange has yet to be determined.

In the absence of DNA, the HsRad51C -XRCC3 complex forms mainly irregular structures although some ring-like structures containing central

cavities, similar to ScRad52 and HsRad52 (see below), could be observed (Masson et al., 2001). In the presence of ssDNA, the HsRad51C-XRCC3 complex or the BCDX2 complex form larger complexes which promote DNA aggregation, an effect similar to the that observed with HsRad52 (see below) (Van Dyck et al., 1998; Masson et al., 2001; Masson et al., 2001)

To date, the most extensive EM studies of *RAD52* group proteins have been done with the HsRad52 protein. HsRad52 forms ring-like structures that are 10 nm in diameter in the absence of DNA (Van Dyck et al., 1998). Using both conventional transmission electron microscopy and scanning transmission electron microscopy (STEM), Stasiak et al. suggested that the rings are composed of seven subunits (Stasiak et al., 2000). Three-dimensional reconstructions revealed that the rings contain a large central channel and that seven protrusions extend from the rings (Stasiak et al., 2000).

In the presence of ssDNA, individual HsRad52 rings are distributed equally among the DNA molecules and appear to form small clusters with a diameter of approximately 30 nm, although some 10 nm rings could still be observed (Van Dyck et al., 1998). The pattern of rings along the ssDNA was similar to that seen by Shinohara *et al.* with ScRad52 in the presence of ssDNA (Shinohara et al., 1998). In contrast when HsRad52 was visualized in the presence of dsDNA, much of the dsDNA remained unbound while other portions of the DNA were bound by multiple HsRad52 rings which formed small

protein aggregates (Van Dyck et al., 1998). Increasing the concentration of HsRad52 resulted in the formation of large aggregates (Van Dyck et al., 1998). In the presence of dsDNA with either 5´ - or 3´ -ssDNA tails, complexes of HsRad52 rings appeared to bind to the ends of the DNA (Van Dyck et al., 1999). These ring complexes were amorphous in shape and ranged from approximately 15-60 nm in diameter (Van Dyck et al., 1999). This observation led Van Dyck *et al.* to propose that HsRad52 prefers to bind the ends of DNA molecules and consequently facilitates the end-end interactions of DNA (Van Dyck et al., 1999). In support of their theory, Van Dyck *et al.* demonstrated that HsRad52 promotes ligation linearized dsDNA (Van Dyck et al., 1999). However, recent work contradicts the above findings and suggests instead that ScRad52 and HsRad52 do not have a clear preference for DNA ends [S.C. Kowalczykowski, personal communication].

Both HsRad52 and ScRad52 promote the annealing of complementary strands of DNA (Reddy et al., 1997; Parsons et al., 2000). EM studies designed to monitor the intermediates in this process provided images in which multiple HsRad52 rings can be seen on the ss-tails of DNA substrates as well as connecting pieces of complementary DNA (Van Dyck et al., 2001). These observations led Van Dyck *et al.* to propose that the HsRad52 rings are the active species in single strand annealing (Van Dyck et al., 2001).

At this time a number of aspects of HsRad52 structure and function remain unclear. For example, individual Rad52 rings form higher order oligomeric complexes but the functional significance of these complexes is not known. Additionally, the mode of DNA binding, i.e. specific protein domains and specific amino acid-DNA interactions are not known. To address these issues, we asked what were the determinants of HsRad52 self-association and which complexes of HsRad52 were functionally relevant. As discussed in Chapter 3, we have identified a novel self-association domain in the C-terminus of HsRad52 that mediates the formation of higher order complexes of HsRad52 containing multiple rings. In Chapter 4, we demonstrate that HsRad52 activities involving simultaneous interaction with more than one DNA molecule are dependent on the formation of oligomers consisting of multiple HsRad52 rings but that DNA binding by HsRad52 was dependent on neither ring shaped oligomers nor higher order oligomers. In Chapter 5, we investigated which residues in the highly conserved N-terminus of HsRad52 are critical for DNA binding and discovered that this activity was dependent on hydrophobic and aromatic residues.

Chapter II

Materials and Methods

Materials

Labeled NTPs were from NEN. Restriction enzymes, T4 DNA ligase and T4 polynucleotide kinase were from New England BioLabs. The QuickChange mutagenesis kit (including 10X reaction buffer, 100 mM dNTPs, Pfu Turbo and Dpn1), XL1 Blue Supercompetent cells and BL21 Codon Plus competent cells were from Stratagene. Superbroth and 2XYT media were purchased from Bio101, Inc. PMSF, benzamidine, lysozyme, PEI, n-octyl β-D-glucopyranoside, and imidazole were purchased from Sigma. IPTG and n-dodecylmaltoside were purchased from Anatrace, Inc., and NP-40 from Calbiochem. Kanamycin and guandine-HCl were purchased from VWR. Phosophocelluose resin was purchased from Whatman and Ni-NTA resin from Novagen and Qiagen. Q-Sepharose resin, the Superose 6 HR 10/30 gel filtration column, and the Superdex 200 HR 10/30 gel filtration column were purchased from Amersham Pharmacia Biotech/LKB. Protein concentrators with polyethersulfone membranes were purchased from VivaScience. Oligonucleotides were made using an ABI 392 DNA/RNA synthesizer.

Plasmids and DNA substrates

Wild-type and all mutant *HsRAD52* genes are carried on the pet28b plasmid (a gift from Dr. Gloria Borgstahl). Double-stranded ϕX174 DNA used in the ligation assay was purchased from New England Biolabs.

Buffers

T-buffer contains 20 mM Tris (pH 7.9) and 10 % glycerol. Q-buffer contains 20 mM Tris (pH 7.9), 10 % glycerol, 1 mM EDTA, 5 mM β-mercaptoethanol (βME) and 0.1 % n-dodecylmaltoside. DNA binding and DNA annealing buffers contain 20 mM triethanolamine-HCl (pH 7.5), 1 mM dithiothreitol (DTT), 1 mM $MgCl_2$ and 0.1 mg/ml BSA. DNA ligation buffer contains 50 mM Tris-HCl (pH 7.5), 10mM $MgCl_2$, 10 mM DTT and 25 μg/ml BSA. TBE buffer contains 45 mM Tris-borate and 1 mM EDTA, and TAE buffer contains 40 mM Tris-Acetate and 1 mM EDTA.

Mutagenesis

HsRad52 (1-212) and HsRad52 (1-85) were constructed using standard PCR techniques. Briefly, reactions included a top strand primer containing an NcoI restriction site (5′-GGA GAT ATA CCA TGG GGA TGT CTG GG-3′), a bottom strand primer containing an XhoI restriction site (5′-CGA ACA TTC TCG AGT CCC ATG TTC GGT CGG CAG CTG TTG TAT CTT GC-3′ for 1-212, or 5′-CGA CCA TTC TCG AGT CCT GCC CAG CCA TTG TAA CCA AAC ATC TC-3′ for 1-85), 50 ng of template DNA, 1X reaction buffer (Stratagene), 0.2 mM of each

NTP and Pfu turbo. The thermocycler program was set as follows: 1 minute at 95 °C/1 minute at 65 °C/1 minute at 72 °C for 30 cycles and an additional 5 minutes at 72 °C. PCR products were digested with NcoI and XhoI, ligated into NcoI/XhoI digested pet28b and transformed into XL1 Blue supercompetent cells. Mutations were confirmed by DNA sequence analysis of plasmid DNA from individual colonies and confirmed mutants were transformed into BL21(DE3) Codon Plus cells for purification.

Alanine scanning mutagenesis was performed using the QuickChange Mutagenesis kit from Stratagene. Briefly, primers, template DNA, dNTP mix, 1 X reaction buffer, and Pfu Turbo were incubated at 95 °C for 1 minute followed by 26 cycles at 95 °C for 30 seconds, 55 °C for 1 minute, and 68 °C for 15 minutes. PCR reactions were digested for 2 hours with Dpn1 and transformed into XL1 Blue Supercompetent cells. Mutations were confirmed by DNA sequence analysis of plasmid DNA from individual colonies and confirmed mutants were transformed into BL21(DE3) Codon Plus cells for purification.

Wild type HsRad52 Purification (Fig. 3)

Cultures of transformed BL21(DE3) Codon Plus *E. coli* (Stratagene) were grown at 37 °C in 10.8 liters of Superbroth and induced for 3 hrs. with 3 mM IPTG. Wild-type *RAD52* cells were resuspended in T-buffer /500 mM NaCl/0.5% NP-40/5 mM imidazole. Protease inhibitors (1mM phenylmethylsulfonyl fluoride (PMSF) and 10 mM benzamidine) were used

throughout the purification. Cells were lysed with 0.2 mg/ml lysozyme on ice followed by sonication. The lysate was clarified by centrifugation at 12,000 rpm for 90 minutes. Polyethyleneimine (PEI) was added to this supernatant (final concentration = 0.1%) followed by centrifugation at 18,500 rpm for 30 minutes. The supernatant was then applied to a phosphocellulose column (20 mls) equilibrated in T-buffer/500 mM NaCl/0.5% NP-40/5 mM imidazole, and the column was washed with 4 volumes of the same buffer. Protein was eluted with T-buffer/750 mM NaCl/0.5% NP-40/5 mM imidazole. Salt was reduced to 500 mM NaCl with T-buffer/0.5% NP-40/5 mM imidazole and the protein mixed with 5 mls of Ni-NTA (Qiagen) resin. A column was poured and washed with 10 volumes of T-buffer/1 M NaCl/0.5% NP-40/25 mM imidazole followed by 10 volumes of T-buffer/1 M NaCl/0.5% NP-40/50 mM imidazole and protein was eluted with 5 volumes of T-buffer/500 mM NaCl/500 mM imidazole/0.1% n-dodecylmaltoside. The sample was dialyzed against T-buffer/100mM NaCl/1mM EDTA/5 mM βME/0.1% NP40 and mixed with 1 ml of Q-Sepharose resin. This column was washed with 10 volumes of T-buffer/100 mM NaCl/1 mM EDTA/0.1% NP-40. Protein was eluted with 2 mls of T-buffer/300 mM NaCl/1 mM EDTA. We and other groups have found that the Q-Sepharose column is useful for removal of nucleases. The protein was dialyzed and stored in of T-buffer/200 mM NaCl/ 1 mM EDTA.

Figure 3. wild type HsRad52 purification

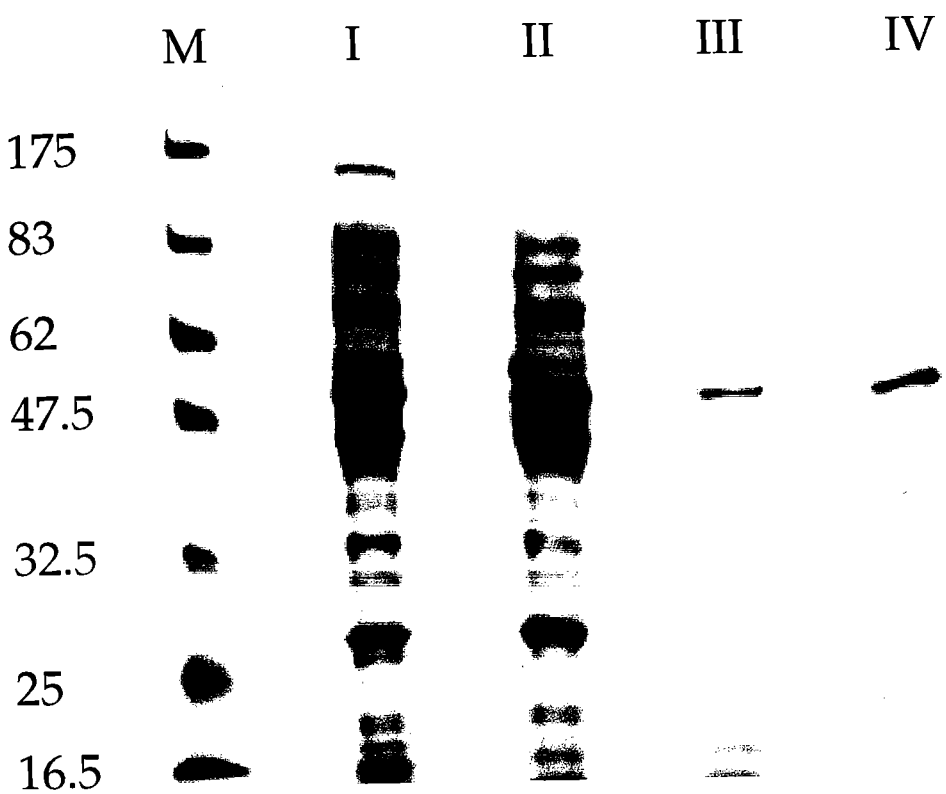

Figure 3. Purification of wild type HsRad52. SDS gel showing purity at different stages in the procedure as described in Materials and Methods. M=molecular weight markers; I=crude extract; II=PEI supernatant; III=fractions eluted from phosphocellulose; IV=fractions eluted from Ni – NTA column.

HsRad52 (1-212) Purification

Purification of HsRad52 (1-212) was the same as for the wild type protein through the PEI step. The PEI supernatant was diluted with T-buffer/0.5% NP-40/5 mM imidazole and applied to a phosphocellulose column equilibrated in T-buffer/200 mM NaCl/0.5% NP-40, 5 mM imidazole. The column was washed with 4 volumes each of T-buffer/200 mM NaCl/0.5% NP-40/5 mM imidazole and T-buffer/300 mM NaCl/0.5% NP-40/5 mM imidazole. Protein was eluted with 3 volumes of T-buffer/500 mM NaCl/0.5% NP-40/5 mM imidazole. The eluant was mixed with 5 mls of Ni-NTA resin (Qiagen) equilibrated in T-buffer/500 mM NaCl/0.5% NP-40/5 mM imidazole. The column was washed with 10 volumes each of T-buffer/1 M NaCl/0.5% NP-40/25 mM imidazole and T-buffer/1 M NaCl/0.5% NP-40/50 mM imidazole. Protein was eluted with 5 column volumes of T-buffer/500 mM NaCl/0.1% n-dodecylmaltoside/500 mM imidazole. The protein was dialyzed and stored in a buffer containing T-buffer/0.1% NP-40/200 mM $(NH_4)_2SO_4$.

HsRad52 (1-85) Purification

Cells expressing HsRad52 (1-85) were resuspended in 0.25 M Tris/25% sucrose. Samples were lysed with 0.2 mg/ml lysozyme followed by sonication. The lysate was then centrifuged at 12,000 rpm for 90 minutes. The cellular membrane was resuspended in 200 mls of 20 mM Tris (pH 7.9)/6 M guanidine-HCl/4 mM n-octyl β-D-glucopyranoside/200 mM $(NH_4)_2SO_4$ followed by centrifugation at 18,500 rpm for 30 minutes. PEI was added to

0.1% followed by centrifugation at 18,500 rpm for 30 minutes. This supernatant was applied to a phosphocelluose column equilibrated with 20 mM Tris (pH 7.9)/6 M guanidine-HCl/4 mM octylglucoside/200 mM $(NH_4)_2SO_4$. The column flow through was then applied to a 5 ml Ni column (Novagen). The protein was renatured by washing the column with 20 volumes of 20 mM Tris (pH 7.9)/100 mM $(NH_4)_2SO_4$. The column was washed with 5 volumes each of T-buffer/400 mM $(NH_4)_2SO_4$ and T-buffer/600 mM $(NH_4)_2SO_4$. The protein was eluted with 4 volumes of T-buffer/200 mM $(NH_4)_2SO_4$/0.1% n-dodecylmaltoside/50 mM EDTA. Protein samples were concentrated using VivaSpin concentrators.

Alanine Mutant Purification

Transformed cultures of BL21 (DE3) Codon Plus were grown in 1/2 X Superbroth (1.8L) containing 50 ug/ml kanamycin and induced with 3 mM isopropyl-1-thio-B-D-galactopyranoside. Cells were resuspended in T-buffer/500mM NaCl/0.5% nP-40/5 mM imidazole. Protease inhibitors (1 mM PMSF and 10 mM benzamidine) were used throughout purification. Cells were lysed with 0.2mg/ml lysozyme on ice followed by sonication. The lysate was clarified by centrifugation at 12,000 rpm for 90 minutes. 0.1% PEI was added to this supernatant followed by centrifugation at 18,500 rpm for 30 minutes. This supernatant was then applied to a 10 ml phosphocellulose column equilibrated in T-buffer/ 500 mM NaCl/0.5% NP-40/5 mM imidazole. The column was

washed in that buffer and the protein was eluted with T-buffer/750 mM M NaCl/0.5% NP-40/5 mM imidazole. The protein was diluted to 500 mM NaCl with T-buffer/0.5% NP-40/ 5 mM imidazole and mixed with 5 mls Ni-NTA resin equilibrated in T-buffer/ 500 mM NaCl/0.5% NP-40/5 mM imidazole. The column was washed with 10 column volumes T-buffer/1 M NaCl, 0.5% NP-40/25 mM imidazole, T-buffer/ 1 M NaCl/0.5% NP-40/50 mM imidazole and eluted with 5 column volumes of T-buffer /500 mM NaCl/500 mM imidazole/ 0.1% n-dodecylmaltoside. The sample was then dialyzed against a buffer consisting of Q-buffer/100 mM NaCl/0.1% NP40 and stored in that buffer.

Alanine mutants used for CD experiments were purified as described except the proteins were stored in Q-buffer/200mM NaCl/0.1% n-dodecylmaltoside.

HsRad52(1-192) and HsRad52(218-418) Purification

The HsRad52(1-192) and the HsRad52(218-418) proteins were provided by our collaborator Dr. Gloria Borgstahl from the University of Toledo.

ssDNA Binding Assay

Reactions (20 µl) for wild type HsRad52 and HsRad52 (1-192) contained 20 mM triethanolamine-HCl (pH 7.5,) 1 mM DTT, 1mM $MgCl_2$, 0.1 mg/ml BSA, 2 nM 5′ -end labeled 95 base oligonucleotide (concentration in bases), and

the indicated amounts of protein. The oligonucleotide sequence is as follows: 5′ -AGA CGA TAG CGA AGG CGT AGC AGA AAC TAA CGA AGA TTT TGG CGG TGG TCT GAA CGA CAT CTT TGA GGC GCA GAA AAT CGA GTG GCA CTA ATA AG –3′. Reactions (25 µl) for wild type HsRad52, HsRad52 (1-212), HsRad52 (1-85) and the alanine mutants contained 20 mM triethanolamine-HCl (pH 7.5,) 1 mM DTT, 1mM $MgCl_2$, 0.1 mg/ml BSA, 100 nM 5′-end labeled 54 base oligonucleotide (concentration in bases), and the indicated amounts of protein. The oligonucleotide sequence is as follows: 5′-GGC GGA GGC CAG AAG GTG TGC TAC ATT GCG GCT GCT CGG GTA ATT AAT CTG GCC –3′. Reactions were incubated at 37 °C for 15 minutes followed by the addition of glutaraldehyde to 0.2% and continued incubation at 22 °C for 15 min. Glycerol was added to a final concentration of 1.6% (w/v) and reactions were loaded onto a 0.8% agarose gel and electrophoresed at 100 mV in 0.5 X TBE buffer with 15 mM $MgCl_2$. Gels were analyzed using a Molecular Imager FX and QuantityOne software (Bio-Rad). The 54-base and 95-base oligonucleotides used in the gel-shift assays were made using an ABI 392 DNA/RNA synthesizer.

Stimulation of DNA Annealing

Reactions (20 µl) contained 20 mM triethanolamine-HCl (pH 7.5), 1 mM DTT, 1 mM $MgCl_2$, 0.1 mg/ml BSA, 50 nM 5′- end-labeled 54 base oligonucleotide (concentration in bases), and the indicated amounts of protein.

The oligonucleotide is the same as that used in the gel shift assays (see above). Reactions were incubated at 37 °C for 15 minutes, a 105 base oligonucleotide containing a sequence complementary to the initial 54 base oligonucleotide was added to a final concentration of 50 nM (in bases) and incubation was continued for 10 minutes. The sequence of the 105 base oligonucleotide is as follows: 5'- GGC CAG ATT AAT TAC CCG AGC AGC CGC AAT GTA GCA CAC CTT CTG GCC TCC GCC GAT ATC GAC AAC CTG CTG TGC TCC CAG GAT ACG GGC GAG TTA GCT TGA ACG 3'. SDS and proteinase K were added to final concentrations of 0.5% and 0.5 mg/ml, respectively, and incubation was continued at 37 °C for 15 minutes. Products were analyzed by electrophoresis on a 10% polyacrylamide gel using 1 x TBE. Gels were analyzed using a Molecular Imager FX and QuantityOne software (Bio-Rad).

Stimulation of DNA Ligation

Proteins were incubated with 20 μM XhoI-digested, linearized ϕX174 dsDNA (concentration of base pairs) in 20 mM triethanolamine-HCl (pH 7.5) for 15 minutes at 37 °C. To this reaction 2 μl of 10X buffer (500 mM Tris-HCl, pH 7.5, 100 mM $MgCl_2$, 100 mM DTT, 10 mM ATP, 250 mg/ml BSA) were added followed by ligase (40 units), and the incubation was continued for an additional 2 hours. SDS and proteinase K were added as in the annealing reaction and incubation was continued at 37 °C for 15 minutes. Products were resolved on a 0.7% agarose gel using 1 x TAE buffer and visualized by staining with ethidium bromide.

Electron Microscopy

Proteins were prepared for EM by diluting wild-type or mutant Rad52 to 2 μM in a buffer containing 20 mM Tris-Hcl (pH 7.5), 5% glycerol, 5 mM βME, 0.1 mM EDTA, and 100 mM KCl. Samples were spread onto thin carbon films on holey carbon grids (400 mesh), stained with 1% uranyl acetate, and visualized by transmission electron microscopy using a Philips CM10 microscope.

Determining the Oligomeric State of HsRad52 Proteins by Gel Filtration

Wild type HsRad52 (1.5 mg/ml) was loaded onto a Superose 6 HR 10/30 gel filtration column equilibrated in T-buffer/200 mM NaCl/1 mM EDTA. The 1-212 and 1-85 proteins (2.0 mg/ml) were loaded onto a Superose 6 column equilibrated in T-buffer/200 mM $NH_4(SO_4)_2$/1 mM EDTA. Samples of HsRad52 (218-418) at 1.2 mg/ml were loaded onto a Superdex 200 HR 10/30 gel filtration column equilibrated in a buffer containing 20 mM MES pH 6.0/10% glycerol/400 mM NaCl/100 mM KCl/1 mM EDTA/ 5 mM βME. Analysis was performed using a BioLogic chromatography system (Bio-Rad) with an in-line UV detector.

Scanning Transmission Electron Microscopy

Analyses were carried out at the Brookhaven National Laboratory using unstained, unshadowed freeze-dried samples. Protein samples (0.1 mg/ml) were applied to a thin carbon film supported by a thick holey film on titanium

grids and freeze-dried overnight. The microscope operates at 40 kV. Operation of the STEM and data analyses were performed as described previously (Wall et al., 1998).

Circular Dichroism

Far UV experiments were performed on a JASCO J – 810 spectrometer with an attached thermoelectric cell holder. Wavelength scans for wild type HsRad52 and alanine mutants were performed at a concentration of 5 or 10 μM in a 0.1 cm pathlength cell. CD spectra were collected from 280 to 200 nm using a continuous scanning mode with a data pitch of 0.5 nm, an averaging time of two seconds, and a bandwith of 2 nm. All samples were equilibrated to 25°C in Q - buffer/ 200 mM NaCl/ 0.1% n – dodecylmaltoside. Mean residue ellipticity (MRE) was calculated as follows:

$$[\Theta]_{MRE} = \frac{\Theta}{10 \times pathlength(cm) \times concentration(M) \times \#residues}$$

Chapter III

Human Rad52 Exhibits Two Modes of Self-Association

Introduction

The importance of specific protein-protein interactions in the catalysis of homologous recombination was first suggested by studies demonstrating specific contacts and functional interactions between ScRad52 and ScRad51 (Milne and Weaver, 1993; Hays et al., 1995; Johnson and Symington, 1995; Sung, 1997; New et al., 1998; Shinohara and Ogawa, 1998), which catalyzes homologous pairing and strand exchange, and replication factor A (RPA) (Shinohara et al., 1998; Sugiyama et al., 1998; Petukhova et al., 1999), a heterotrimeric single-stranded DNA binding protein (Wold, 1997).

Studies of the equivalent human proteins have identified similar interactions between the HsRad52, HsRad51, and HsRPA proteins (Park et al., 1996; Shen et al., 1996; Benson et al., 1998; Golub et al., 1998; Van Dyck et al., 1998; Baumann and West, 1999). Based on a series of protein-protein interaction assays (Shen et al., 1996; Shen et al., 1996; Benson et al., 1998) and DNA binding studies [unpublished, cited in Park, 1996 #4], a domain map of HsRad52 was proposed by Park *et al.* (Park et al., 1996). (Fig. 4) The determinants of self-

association were proposed to exist exclusively within a region defined by residues 65–165, a result supported by studies of several isoforms of HsRad52 (Kito et al., 1999). Electron microscopy (EM) studies of ScRad52 and HsRad52 have revealed formation of ring-shaped structures (9 –13 nm in diameter), as well as higher order oligomers (Shinohara et al., 1998; Van Dyck et al., 1998; Van Dyck et al., 1999). Stasiak et al. (Stasiak et al., 2000) performed image analyses of negatively stained electron micrographs and determined that the 10-nm HsRad52 rings are composed of seven subunits. Scanning transmission electron microscopy (STEM) analysis indicated a mean mass of 330 ± 59 kDa supporting a heptameric ring-shaped HsRad52 structure (Stasiak et al., 2000). Recent studies show that HsRad52 binds to double-stranded DNA ends as an aggregated complex (Van Dyck et al., 1999). These end-binding complexes were amorphous in shape and ranged in size from 15 to 60 nm. Within these complexes, HsRad52 rings were observed occasionally. Binding of HsRad52 to the DNA ends promoted end-to-end associations between DNA molecules and stimulated ligation of both cohesive and blunt DNA ends (Van Dyck et al., 1999).

Therefore, given that the formation of both ring-shaped oligomers and aggregates of these rings seem relevant to HsRad52 function, we sought to investigate further the self-association properties of the HsRad52 protein. We performed a series of analyses comparing full-length HsRad52 (1–418) with two different mutant HsRad52 proteins: (i) a 1–192 mutant that spans the N-terminal portion and includes the entire proposed DNA binding and self-association

domains and (ii) a 218–418 mutant that spans the C-terminal portion of HsRad52 that includes the proposed HsRPA- and HsRad51-binding domains (Fig. 4). In contrast to previous studies, our results show that there are experimentally separable determinants for two different modes of self-association by HsRad52, one in the N-terminal portion and one in the C-terminal portion of the protein.

Figure 4. Schematic diagram of wild type HsRad52 and deletion mutants.

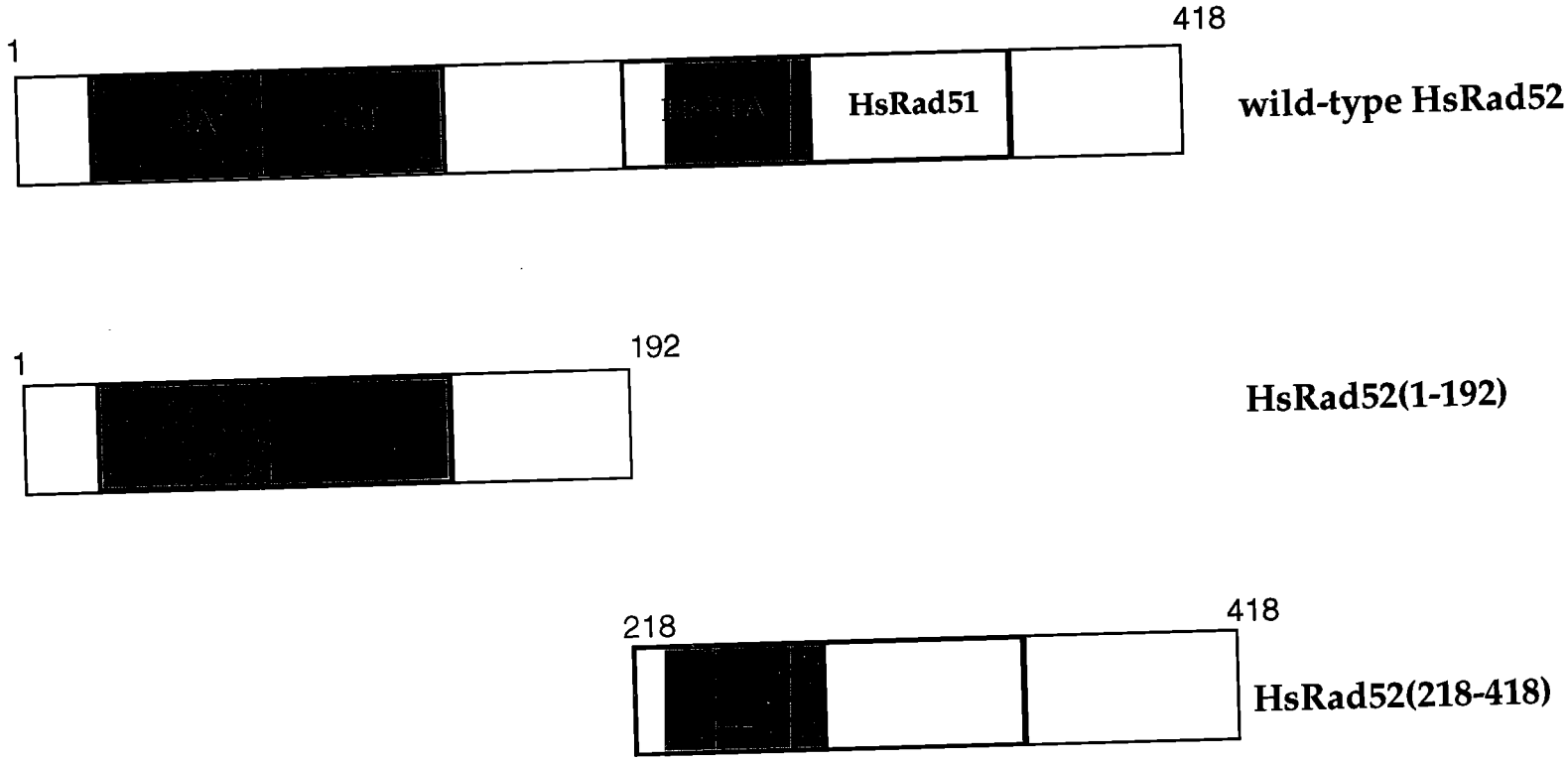

Figure 4. Schematic diagram of wild-type HsRad52 and deletion mutants. The beginning and ending residue numbers of each mutant are indicated along with domain structure. The following domains and residue numbers were defined by Park *et al.* (Park *et al.*, 1996): DNA binding - 39-80; self-association - 85-159; HsRPA binding – 221-280; HsRad51 binding – 290-330.

Results

Oligomeric Characteristics of RAD52 Proteins

EM analyses of wild type HsRad52 and HsRad52 (1–192) show that both proteins form ring-shaped structures (Fig. 5). The average diameter of these particles, measured across the surface with the central pore, is 10 ± 1 nm, consistent with previous reports (Shinohara et al., 1998; Van Dyck et al., 1998; Stasiak et al., 2000). Wild type HsRad52 also forms higher order aggregates that contain multiple rings. For HsRad52 (1–192) the majority of protein forms ring-shaped oligomers, and no aggregates were seen (Figure 5). Even at increased concentrations (6 and 10 μM) HsRad52 (1–192) shows no larger aggregates (data not shown). Higher magnifications reveal "protrusions" extending from the 10-nm rings formed by wild type HsRad52 that are missing in the 1–192 protein (see arrows in Figure 5, B and D). These protrusions likely correspond to those modeled by Stasiak *et al.* (Stasiak et al., 2000), and our data show that they are part of the C-terminal portion of HsRad52.

Figure 5. Electron micrographs

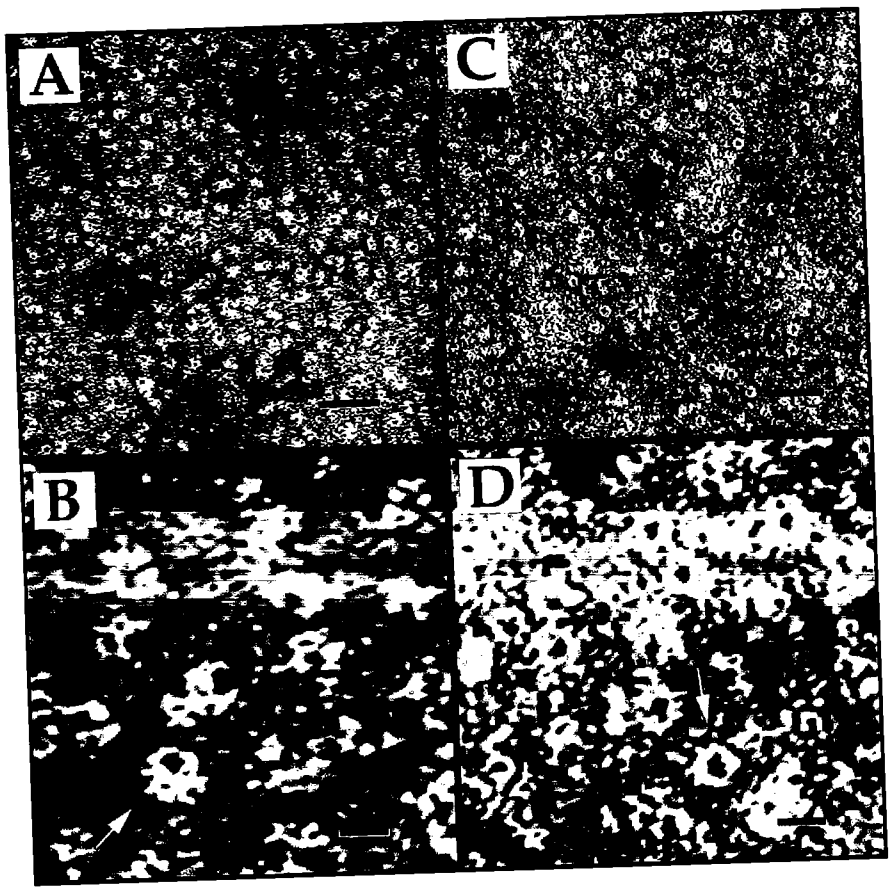

Figure 5. Negative stained electron micrographs of wild type HsRad52 and HsRad52 (1-192) protein. Proteins (4.0 μM) were prepared as described in **Materials and Methods** (Chapter II). The majority of protein for both wild type HsRad52 (*A* and *B*) and HsRad52 (1-192) (*C* and *D*) forms 10 nm diameter ring-shaped oligomers. Larger particles of wild type HsRad52 in *A* are not formed by HsRad52 (1-192). Higher magnifications of both proteins reveal that the protrusions observed on the 10 nm rings of wild type HsRad52 are missing in the HsRad52 (1-192) rings (*arrows* in *B* and *D*). Black bars = 0.5μm in *A* and *C* and 0.01 μm in *B* and *D*.

STEM analyses of wild type HsRad52 (2 μM) showed particle sizes ranging from 175 to 625 kDa with a mass average of 298 ± 69 kDa (n = 309; Fig. 6). Given a molecular mass of 48 kDa for the His-tagged HsRad52 protein, this range corresponds to particles that contain from 4 to 13 subunits with an average of six subunits. Similar analyses of the 1–192 protein showed particle sizes ranging from 100 to 350 kDa with a mass average of 227 ± 30 kDa (n = 277; Fig. 6B). For a monomer molecular mass of 23 kDa, this range corresponds to particles that contain from 4 to 15 subunits with an average of 10 subunits. Resolution of the ring-shaped oligomers in the electron micrographs was not high enough to count individual subunits, but our STEM data are consistent with previous work in which oligomeric rings of wild type HsRad52 were determined to be heptameric (Stasiak et al., 2000).

The above analyses indicate at least two modes of HsRad52 self-association that are experimentally separable, (i) formation of ring-shaped oligomers and (ii) formation of larger aggregates. Because the latter seems to depend largely on the presence of residues C-terminal to position 192, we performed a number of assays to test for self-association on a mutant HsRad52 protein containing only residues 218–418. Initial EM studies showed no distinct structural characteristics for this protein (data not shown), but STEM analysis revealed particle sizes ranging from 75 to 275 kDa (Fig. 6C) with a mass average of 153 ± 40 kDa (n = 119; Fig. 7C). Given a monomer molecular mass of 39 kDa, the particle composition ranges from two to seven subunits with an

average of four subunits. Gel filtration shows a homogeneous peak corresponding to a molecular mass of 166 kDa (Fig. 7) and therefore to a particle containing approximately four subunits. The data from the gel filtration and STEM analysis indicate that the C-terminal portion of HsRad52 (residues 218–418) contains determinants of protein self-association that are distinct from those required to form 10-nm rings.

Figure 6. STEM histograms.

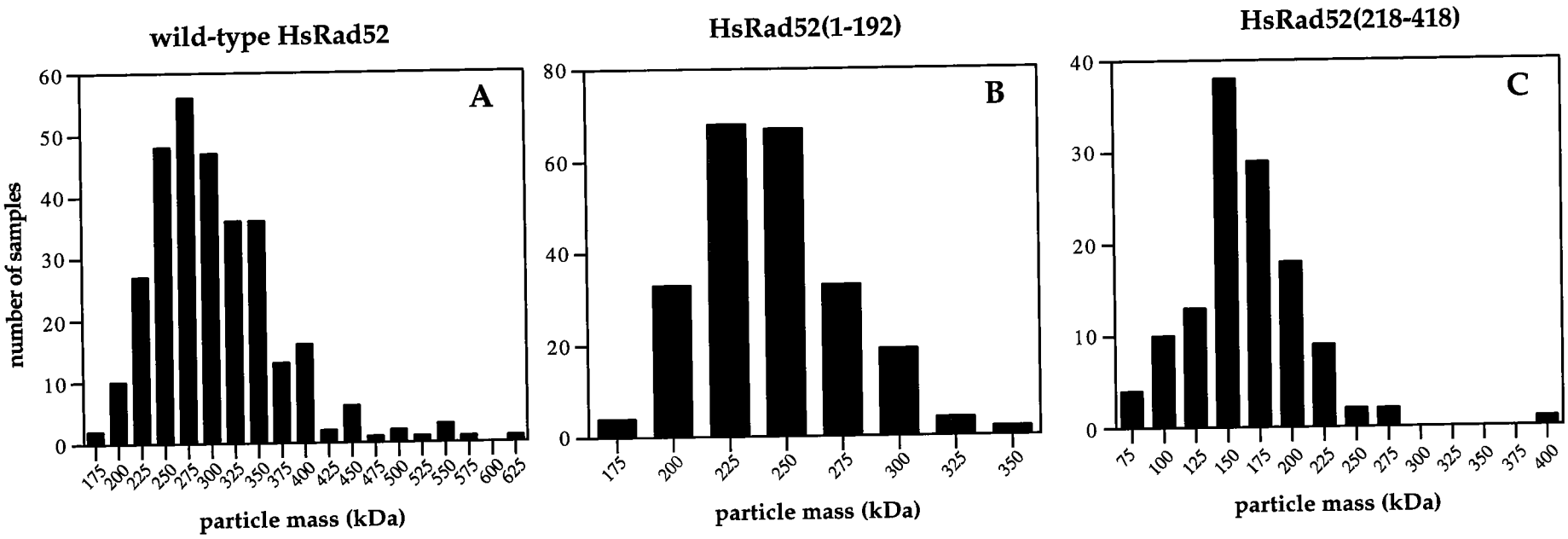

Figure 6. STEM histograms. STEM mass analyses were performed as described in **Materials and Methods** (Chapter II). Histograms include pooled data from several separate analyses (eight for wild type HsRad52, six for HsRad52 (1-192), and five for HsRad52 (218-218). Average mass values were as follows: *A*, wild type HsRad52 298 ± 69 kDa (n = 309); *B*, HsRad52 (1-192) 227 ± 30 kDa (n= 277); *C*. HsRad52 (218-418) 153 ± 40 kDa (n= 119).

Figure 7. Gel filtration of HsRad52(218-418).

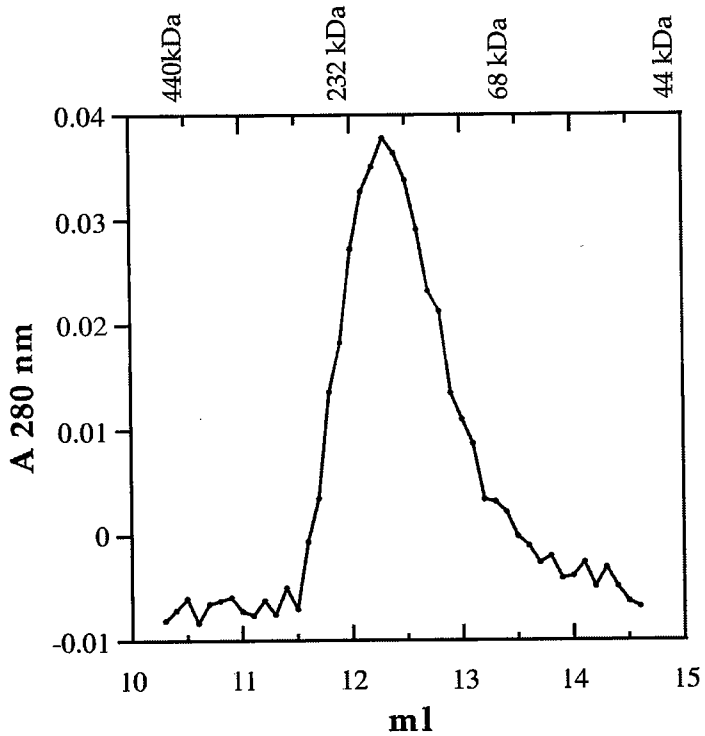

Figure 7. Gel Filtration profile of the HsRad52 (218-418) protein. The mutant protein (1.2 mg/ml, 35.8 μM) was loaded onto a Superdex 200 HR 10/30 gel filtration column, and elution of the protein was followed at A 280nm. The indicated elution volumes of standards (ferritin, *440 kDa*, 61.0 Å; catalase, *232 kDa*, 52.2 Å; BSA, *68 kDa*, 35.5 Å; ovalbumin, 44 *kDa*, 30.5 Å) were an average of four runs.

DNA Binding

Binding of wild type HsRad52 and HsRad52 (1–192) to single-stranded DNA was analyzed by gel shift assays. The gels in Figure 8 are representative of five different experiments, each of which gave similar results. In each case, analysis of unbound and bound DNA (including that in the gel well) gave rise to a $K_{D(app)}$ of 35 and 25 nM for wild type HsRad52 and HsRad52 (1–192), respectively. This slight enhancement in binding affinity was observed consistently for HsRad52 (1–192). With wild type HsRad52 a significant portion of bound DNA remained in the gel well, a result that likely reflects the ability of the wild-type protein to form greater amounts of self-aggregates than the 1–192 mutant protein (see below). Additionally, 100% of the DNA (2 nM total nucleotides) was bound by the 1–192 protein at 40–60 nM protein in the titration profile, whereas 100% binding by wild type HsRad52 consistently required greater than 100 nM protein. Assays using the HsRad52 (218–418) mutant protein showed no DNA binding up to 2.0 μM protein (data not shown). These results show that the DNA binding domain of HsRad52 is contained within the N-terminal portion of the protein and that removal of the C-terminal 227 residues results in a slight enhancement of DNA binding.

Figure 8. Gel shift DNA binding assays

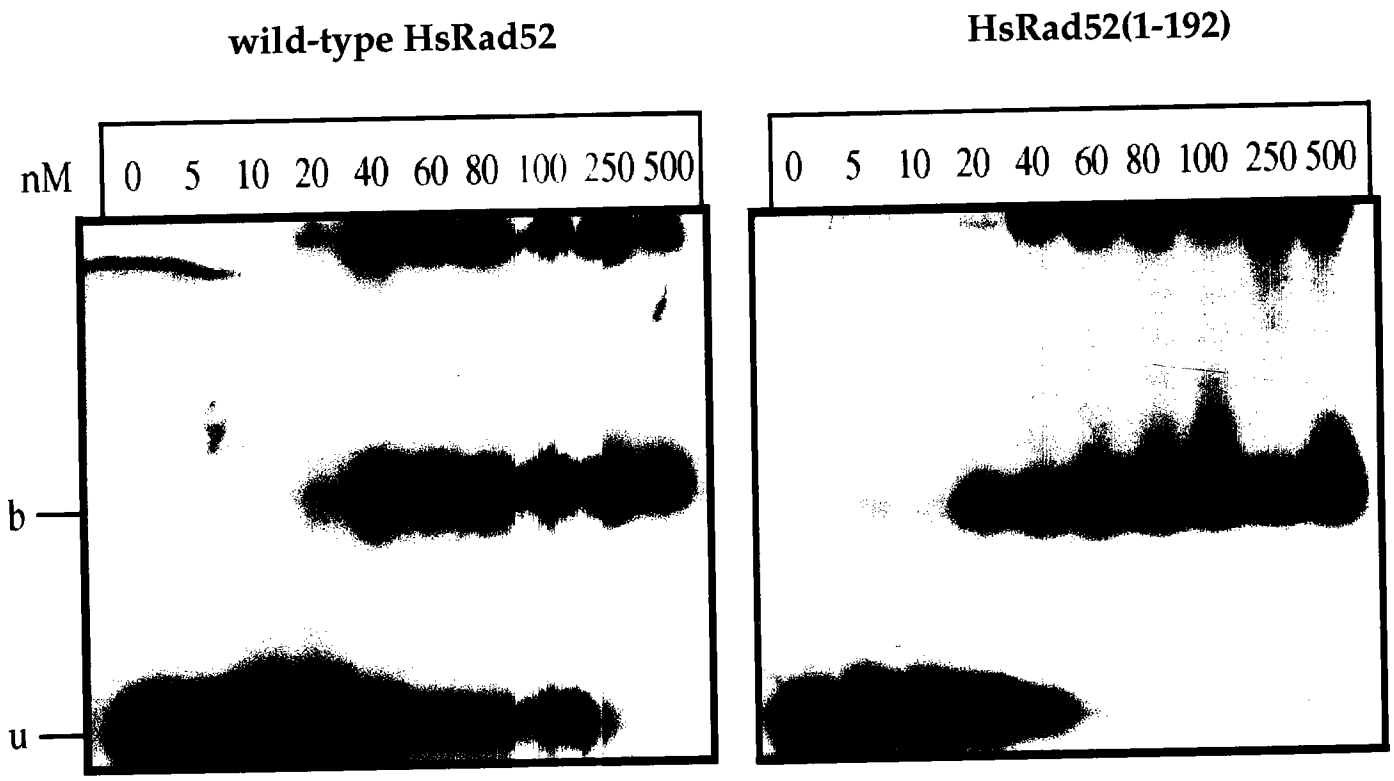

Figure 8. Gel shift DNA binding assays. Indicated concentrations of either wild type HsRad52 or HsRad52 (1-192) were incubated with a 5´ end-labeled 95 base oligonucleotide followed by cross- linking with glutaraldehyde as described in **Materials and Methods** (Chapter II). Reactions were electrophoresed on a 0.8% agarose gel. Radioactive material at the *top* of the gel represents protein-DNA complex trapped in the gel well. *u*, unbound DNA; *b*, protein-DNA complex

Discussion

Previous studies have shown that HsRad52 exists in a number of oligomeric states ranging from rings with a 10 nm diameter to larger complexes with diameters of greater than 30 nm (Shinohara et al., 1998; Van Dyck et al., 1998; Van Dyck et al., 1999; Stasiak et al., 2000). Recent observations indicate a direct role for these higher order protein-protein interactions in promoting DNA end-joining (Van Dyck et al., 1999). We therefore sought to investigate the self-association properties of HsRad52 utilizing an array of biophysical techniques.

In our EM studies of wild type HsRad52 and HsRad52 (1–192), we observed ring structures with an average diameter of 10 ± 1 nm as has been reported previously (Shinohara et al., 1998; Van Dyck et al., 1998; Van Dyck et al., 1999; Stasiak et al., 2000). Additionally, and as seen previously (Van Dyck et al., 1998; Van Dyck et al., 1999; Stasiak et al., 2000), we observed protrusions extending from wild type HsRad52 rings as well as a population of distinct larger particles. However, neither the protrusions nor the larger particles were observed with HsRad52 (1–192). This suggests that residues within the C - terminal portion of the protein (residues 193–418) make up these protrusions and carry determinants for higher order HsRad52 self-association. Our collaborators performed dynamic light scattering (DLS) analysis of wild type HsRad52 and the two mutant proteins. This analysis provided additional and complementary

evidence for two distinct modes of HsRad52 self-association. DLS analysis of wild type HsRad52 shows a multimodal profile that likely corresponds to the 10 nm ring-shaped oligomers and the larger aggregates observed by EM. In contrast, both HsRad52 (1–192) and HsRad52 (218–418) show a monomodal DLS profile indicating the presence of a single population of structures. The HsRad52 (1–192) R_H is consistent with a ring structure and the HsRad52 (-218–418) R_H indicates a complex composed of three subunits. This self-association of HsRad52 (218–418) was confirmed by size-exclusion chromatography and STEM. To ensure that the self-association of HsRad52 (218-418) determined by our biophysical methods was due to specific interaction, our collaborators performed functional assays with this mutant to ensure the truncated protein maintained the native fold. Previous studies mapped residues 221-280 as the domain in HsRad52 that interacts with RPA, therefore we tested the ability of HsRad52 (218-418) as well as wild type HsRad52 to bind to RPA using an immunoassay. Both proteins exhibit a similar affinity for RPA.

The ability of HsRad52 (218–418) to self-associate was unexpected. Previous studies have suggested that residues 65–165 define the exclusive self-association domain in the HsRad52 protein (Shen et al., 1996). Shen *et al.* (Shen et al., 1996) found that although N-terminal fragments of the protein self-associated in two-hybrid screens and affinity chromatography assays, fragments containing various portions of the C terminus, e.g. 287–418 or 166–418, did not. In contrast to these results, we find that HsRad52 (218–418) is able to self-associate.

Although our EM analysis revealed no distinct oligomeric structures for HsRad52 (218–418), three different methods (STEM, gel filtration, and DLS) showed that this mutant formed oligomeric particles containing 3–4 subunits. These data for HsRad52 (218–418), coupled with the inability of HsRad52 (1–192) to form structures larger than the 10 nm rings, indicate that residues within the C-terminal region of the protein make important contributions to HsRad52 self-association. Thus, the C-terminal region of HsRad52 contains a novel self-association domain distinct from that previously identified within residues 65–165 (Shen et al., 1996).

Importantly, functional analyses of both the 1–192 and 218–418 mutant proteins show that each maintains an expected activity. Both the wild type HsRad52 and the HsRad52 (1–192)proteins, which form ring-shaped oligomers, bound single-stranded DNA with similar affinities. This is consistent with previous studies that mapped the DNA binding domain of HsRad52 to residues 39–80 [unpublished, cited in Park, 1996 #4]. The elevated affinity of HsRad52 (1–192) for single-stranded DNA was noted for a similar ScRad52 construct (Mortensen et al., 1996). Also as expected, HsRad52 (218–418) showed a specific interaction with RPA. Again, this is consistent with previous studies that mapped the RPA interaction domain to residues 221–280 in Rad52 (Park et al., 1996). The fact that both mutant proteins showed the expected functions demonstrates that they very likely maintain native structure, thereby supporting

the relevance of differences observed in their oligomeric characteristics compared with wild type HsRad52.

In summary, our data support a model in which the self-association domain within the N-terminal region of HsRad52 (residues 1–192) promotes the formation of ring-shaped oligomers that are functional for DNA binding, whereas the C-terminal domain (residues 218–418) mediates higher order self-association events. Additionally, the protrusions extending from the 10 nm ring structure of wild type HsRad52, originally modeled by Stasiak *et al.* (Stasiak et al., 2000) and seen clearly in our electron micrographs, are dependent upon the C-terminal region of the protein. Given the likely importance of higher order self-association to the ability of HsRad52 to promote end-to-end joining of DNA breaks (Van Dyck et al., 1999), these protrusions seem to mediate a critically important aspect of HsRad52 function. Further studies of various mutant HsRad52 proteins will clarify the contribution made by the different aspects of self-association toward the overall function of this important DNA repair protein.

Chapter IV

Correlation of Biochemical Properties with the Oligomeric State of the Human Rad52 Protein

Introduction

The human Rad52 protein (HsRad52) shares many similarities with yeast Rad52 regarding both its structure and function in homologous recombination. In either the absence or presence of DNA, Rad52 forms ring-shaped oligomers, approximately 10 nm in diameter, as well as higher order complexes of these rings (Shinohara et al., 1998; Van Dyck et al., 1998; Van Dyck et al., 1999; Stasiak et al., 2000; Ranatunga et al., 2001). Rad52 binds to both single- and double-strand DNA (Mortensen et al., 1996; Reddy et al., 1997; Shinohara et al., 1998; Sugiyama et al., 1998; Van Dyck et al., 1998; Kito et al., 1999; Van Dyck et al., 1999; Kagawa et al., 2001) stimulates annealing of complementary DNA strands (Mortensen et al., 1996; Reddy et al., 1997; Shinohara et al., 1998; Sugiyama et al., 1998; Kagawa et al., 2001; Van Dyck et al., 2001) and promotes ligation of both cohesive and blunt end fragments (Van Dyck et al., 1999). Rad52 also interacts specifically with the Rad51 strand exchange enzyme (Milne and Weaver, 1993; Shen et al., 1996) as well as the single-strand DNA binding protein, RPA (Park et al., 1996; Hays et al., 1998). Biochemical studies support the idea that Rad52 is a

recombination mediator in that it optimizes catalysis of strand exchange by the Rad51 protein (Sung, 1997; Benson et al., 1998; New et al., 1998; Shinohara and Ogawa, 1998; Song and Sung, 2000).

Park *et al.* (Park et al., 1996) proposed a domain map for HsRad52 that included specific regions for self-association (residues 85 – 159) as well as interactions with the 34 kDa subunit of HsRPA (residues 221 – 280) and HsRad51 (residues 290 – 330). This map has been modified by our identification of a C-terminal self-association domain that mediates formation of higher order oligomerization of Rad52 rings (Ranatunga et al., 2001). Regarding the possible functional relevance of these higher order oligomers, Van Dyck *et al.* (Van Dyck et al., 1999) observed DNA end binding complexes consisting of multiple rings of HsRad52. In yeast, distinct Rad52 foci that undoubtedly contain multiple protein rings form under conditions that result in DSBs, e.g. during meiosis and in S phase mitotic cells and following exposure to γ-irradiation (Lisby et al., 2001). Also, co-localization of *RAD52* group proteins, including Rad51, Rad52 and Rad54, is observed following DNA damage in mammalian cells (Liu et al., 1999; Raderschall et al., 1999; Liu and Maizels, 2000; Essers et al., 2002). Therefore, it appears that the ability of Rad52 to form higher order oligomeric complexes may be important to its function in promoting homologous recombination, and it has been suggested that such complexes may be required as an early step in the efficient catalysis of DNA repair via homologous recombination (Lisby et al., 2001). Given the domain structure of the HsRad52 protein it may be that higher

order oligomers of the protein are used in promoting complex formation among repair proteins and DNA through simultaneous interaction with multiple components. Additionally, the higher order oligomers may be important for optimization of a fundamental biochemical function of Rad52, e.g., events related directly to DNA binding. Therefore, in this work we asked if the ability of HsRad52 to perform various activities related directly to DNA binding are affected by the protein's oligomeric state. Using two truncation mutants, HsRad52 (1-212) and HsRad52 (1-85) which block formation of higher order oligomers and the 10 nm ring structure, respectively, we show that DNA binding depends on neither ring shaped oligomers nor higher order oligomers but that formation of oligomers consisting of multiple Rad52 rings is important for activities involving simultaneous interaction with more than one DNA molecule.

Results

Oligomeric Characteristics of wild type HsRad52 and mutant Proteins

Electron micrographs of wild type HsRad52 and HsRad52 (1-212) show that both proteins form ring-shaped oligomers with an average diameter of 10 ± 1 nm (Fig. 9). Higher magnifications show that wild type HsRad52 forms higher-order oligomeric structures that are never seen with the 1-212 mutant (Fig. 9, panels B and D). For example, the arrow in Figure 9B indicates a side by-side

association of three 10 nm rings. Related structures are frequently observed with wild type HsRad52 but not with the 1-212 protein. The observation of higher-order oligomers for wild type HsRad52 is consistent with previous studies (Shinohara et al., 1998; Van Dyck et al., 1998; Van Dyck et al., 1999; Stasiak et al., 2000; Ranatunga et al., 2001). Also, the lack of higher order oligomers for the 1-212 mutant is consistent with our previous identification of a new self-association domain in the C-terminal half of the protein that is responsible for the oligomerization of the 10 nm rings (Ranatunga et al., 2001). Electron microscopic analysis of HsRad52 (1-85) revealed no observable structures (not shown), indicating that this protein does not form ring-shaped structures like the wild type and 1-212 mutant proteins.

Figure 9. Electron micrographs of wild type HsRad52 and HsRad52 (1-212).

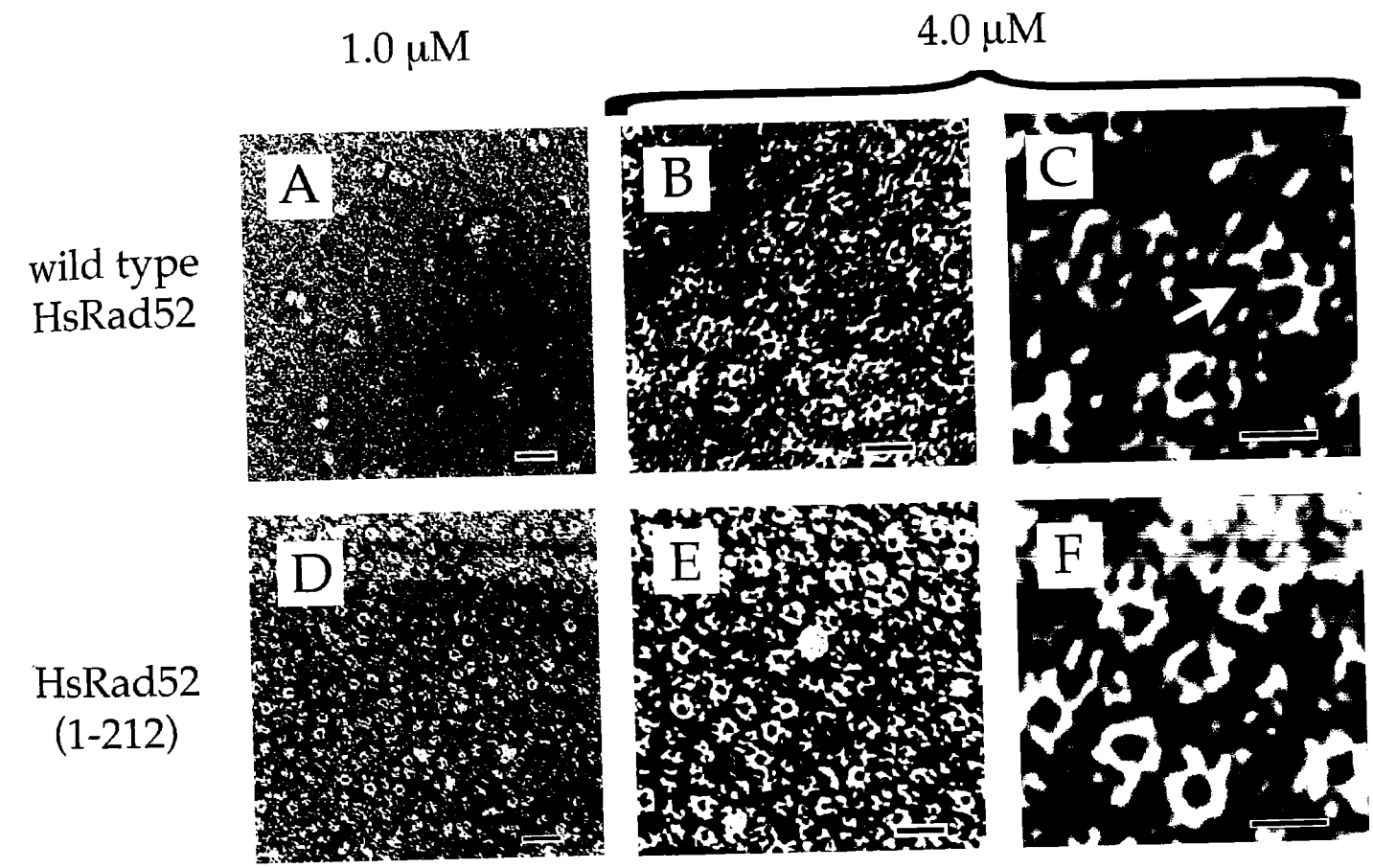

Figure 9. Negative stained electron micrographs of wild type HsRad52 and HsRad52 (1-212). Proteins (1.0 μM in *A* and *D*; 4.0 μM in *B*,*C*,*E*, and *F*) were prepared as described in **Materials and Methods** (Chapter II). Clearly defined ring-shaped oligomers (≈10 nm in diameter) are seen for both proteins. Wild type HsRad52 (*A* - *C*) also shows higher order oligomers and specific interactions between rings whereas the 1-212 mutant does not (*D* - *F*). *Black bars* = 0.03 μm in *A* and *D*, 0.02 μm in *B* and *E*, and 0.01 μm in *C* and *F*.

Gel filtration was used to address the oligomeric distribution of the proteins. Using a Superose 6 column wild type HsRad52 shows a peak that begins at approximately 10 ml and trails to approximately 16 ml, with a distinct center at 11 ml (Fig. 10). This corresponds to a particle with a Stoke's radius of 111 Å. Given a molecular weight of 48 kDa for the His-tagged HsRad52 protein this corresponds to particles containing 20 monomers. The 1-212 mutant shows a homogeneous peak centered at 16.5 ml, which correlates to a particle with a Stokes' radius of 49 Å. Given a molecular weight of 23 kDa this corresponds to a particle containing approximately 10 subunits, a result consistent with our observations by electron microscopy of only 10 nm ring oligomers for this mutant. A similar gel filtration result has been observed for the $HsRad52_{1-237}$ mutant protein (Kagawa et al., 2001). In contrast to both wild type HsRad52 and the 1-212 mutant, the 1-85 mutant shows a very broad profile beginning at the column void (8 ml) and continuing to approximately 21 ml, with a distinct peak centered at 18.5 ml, which corresponds to a particle with a Stoke's radius of 26 Å. Given a molecular weight of 10 kDa this peak corresponds to a particle containing approximately 3 monomers. Therefore, it appears that the 1-85 mutant self-associates in both a non-specific and specific manner (see **Discussion**). Of course, the mobility of these proteins on a gel filtration column is dictated by the Stoke's radius of the particle, not the precise particle mass, and this assay is intended as a relative size estimate of these three proteins.

Figure 10. Gel filtration profiles.

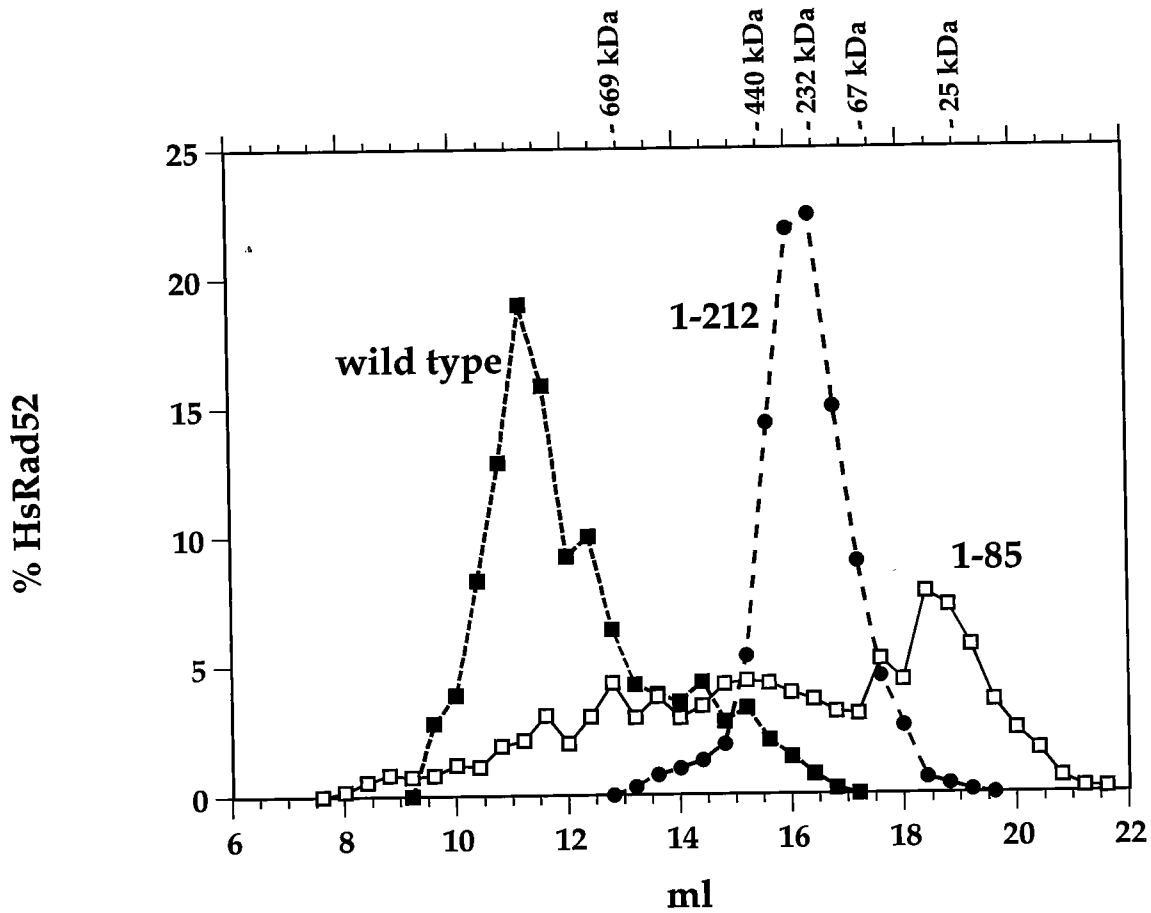

Figure 10. Gel filtration profiles of wild type HsRad52, HsRad52 (1-212), and HsRad52 (1-85). Proteins were loaded onto a Superose 6 HR 10/30 gel filtration column and protein elution was followed at A_{280nm}. The indicated elution volume of standards (thyroglobulin, *650 kDa*, 85.0 Å; ferritin, *440 kDa*, 61.0 Å; catalase, *232 kDa*, 52.2 Å; bovine serum albumin, *67 kDa*, 35.5 Å; chrymotrypsinogen, *25 kDa*, 20.9 Å) is an average of three runs.

ssDNA Binding

To compare the ssDNA binding properties of wild type HsRad52, HsRad52 (1-212) and HsRad52 (1-85), gel mobility shift assays were performed. The gels in Figure 11 are representative of 5 different experiments, each of which gave similar results. The apparent difference in the intensity of the three gels results from different exposure times. Scans reveal a similar radioactive content in all lanes. K_{Dapp} was estimated from the protein concentration that gives rise to 50% of the labeled ssDNA being in the bound state, including protein-DNA complexes trapped in the gel well. Wild-type HsRad52 binds with a $K_{Dapp} \approx 8$ nM and the 1-212 mutant binds with a $K_{Dapp} \approx 5$ nM. Interestingly, despite the fact that the 1-85 mutant forms no ring shaped particles that contain from 40 to 6 monomers, with the peak center corresponding to oligomers, it still shows a reasonably high affinity for ssDNA ($K_{Dapp} \approx 50$ nM). At higher protein concentrations wild-type HsRad52 (120 nM) and the 1-85 mutant (80 nM) result in a majority of the ssDNA being trapped in the gel wells. In contrast, at the same higher concentrations, e.g. 60 and 120 nM, although the 1-212 protein does result in smearing of the band representing the protein-DNA complex (B), it does not result in any significant trapping of DNA in the gel wells. This likely reflects the fact that the 1-212 protein does not form higher order oligomers, whereas wild type HsRad52 forms specific higher order oligomers and the 1-85 mutant protein

may aggregate in a non-specific manner as shown by the gel filtration (see **Discussion**). Together these results demonstrate that the N-terminal 85 residues of HsRad52 are sufficient for specific binding to ssDNA and that this function of HsRad52 does not require formation of ring-shaped oligomers.

Figure 11. Gel shift DNA binding assays.

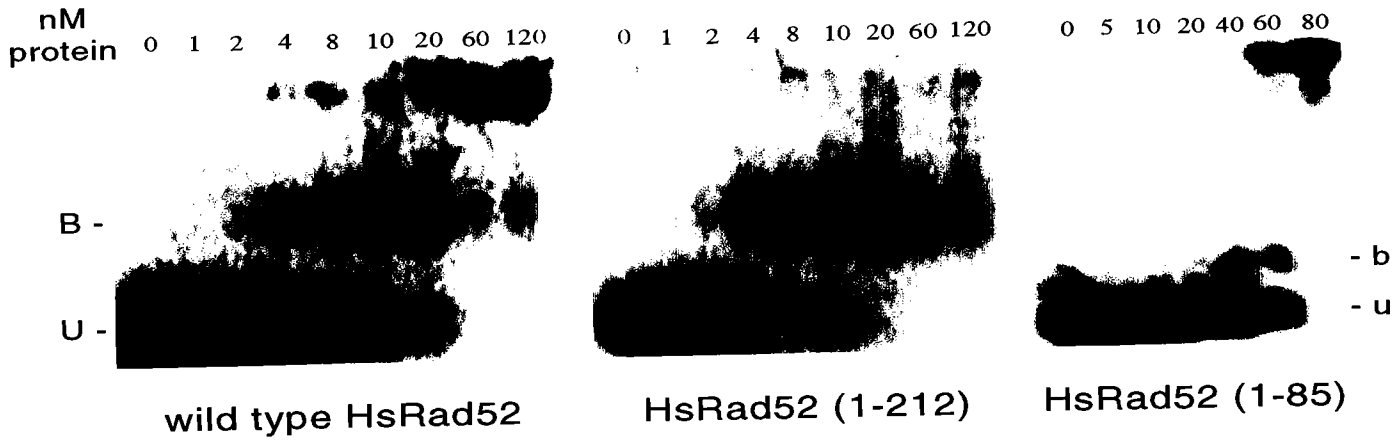

Figure 11. Gel shift DNA binding assays. Indicated concentrations of wild type HsRad52, HsRad52 (1-212) or HsRad52 (1-85) were incubated with a 5′ end-labeled 54 base oligonucleotide followed by cross-linking with glutaraldehyde as described in **Materials and Methods** (Chapter II). Reactions were electrophoresed on a 0.8% agarose gel. Radioactive material at the top of the gel represents protein-DNA complexes trapped in the gel well. U = unbound DNA; B = protein-DNA complexes for wild type and the 1-212 protein; b = protein-DNA complexes for the 1 – 85 mutant protein.

DNA Strand Annealing

Both the yeast and human Rad52 proteins promote annealing of complementary strands of DNA (Mortensen et al., 1996; Reddy et al., 1997; Shinohara et al., 1998; Sugiyama et al., 1998; Kagawa et al., 2001; Van Dyck et al., 2001). To address the functional oligomeric form of HsRad52 required for this activity, we performed the following strand annealing assay using wild type HsRad52, HsRad52 (1-212) and HsRad52 (1-85). A 5'-end labeled oligonucleotide (54 bases) was incubated with increasing concentrations of each protein followed by addition of a 105 base oligonucleotide with 54 bases complementary to the initial oligonucleotide. The data in Figures 12A and 12B show that at 1 nM, wild type HsRad52 performs strand annealing very efficiently, with 76% of the labeled oligonucleotide in the double-strand form compared to 10% spontaneous annealing. With increasing protein concentration the annealing efficiency decreases, and we find that at 50 nM protein the efficiency has dropped to 47%. A similar protein concentration-dependent decrease in annealing efficiency has been observed by Van Dyck *et al.* (Van Dyck et al., 2001) for wild type HsRad52. In contrast, increasing the concentration of the 1-212 mutant protein over the same range, from 1 to 50 nM, results in a steady increase in the efficiency of strand annealing, from 31 – 57%. Despite the fact that the ssDNA binding affinity is equivalent or slightly better than wild type HsRad52, the efficiency of annealing by the 1-212 protein is significantly less. The 1-85 mutant protein also promotes strand annealing, but at a much lower efficiency than both the wild

type and 1-212 proteins. Over a range of protein concentrations from 25-200 nM the efficiency of annealing shows a steady increase from 26-42%. As for ssDNA binding, these results indicate that formation of ring-shaped oligomers is not necessary for strand annealing activity by HsRad52. However, optimal annealing efficiency requires higher order complexes of HsRad52 rings.

Figure 12. HsRad52 mediated DNA strand annealing.

A

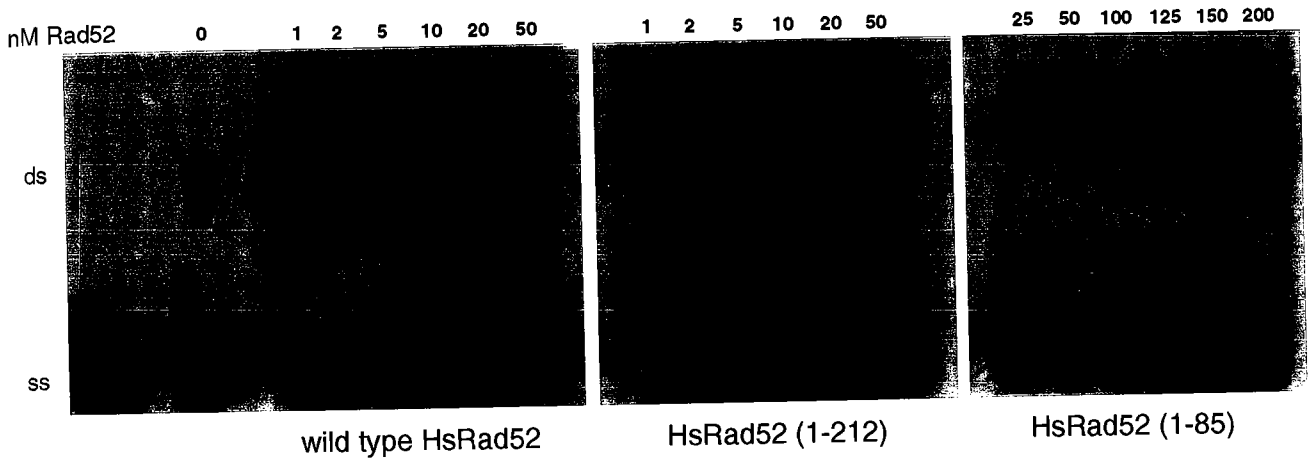

B

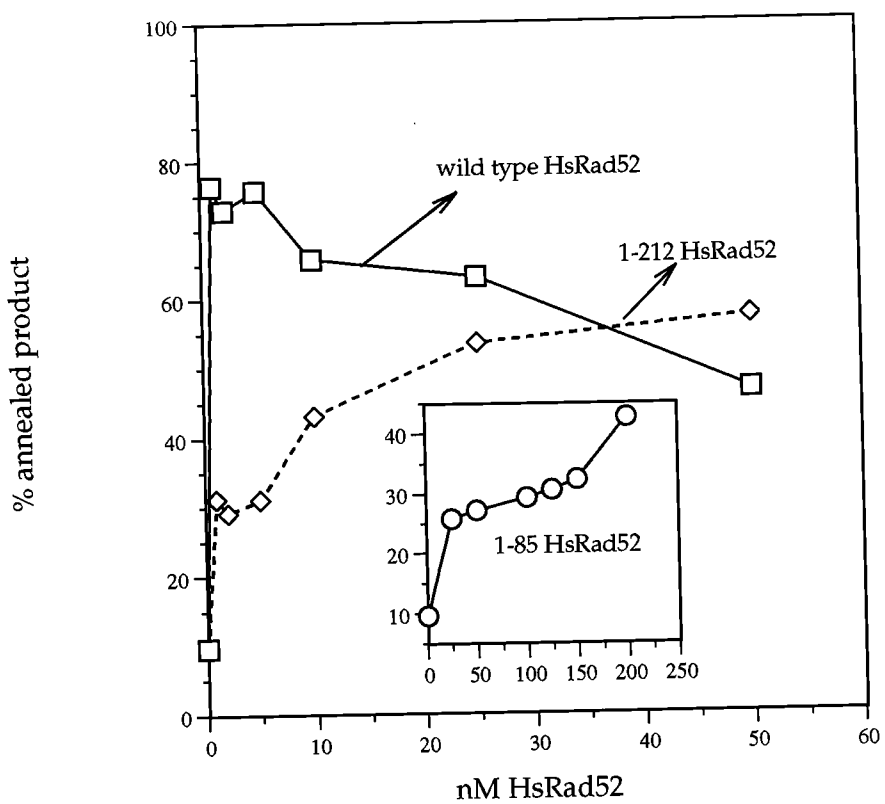

Figure 12. HsRad52 – mediated DNA strand annealing. Indicated concentrations of wild type HsRad52, HsRad52 (1-212) or HsRad52 (1-85) were incubated with a 5′ end-labeled 54 base oligonucleotide followed by addition of a 105 base oligonucleotide with 54 complementary bases as described in **Materials and Methods** (Chapter II). *A* – reactions were electrophoresed on a 10% non-denaturing polyacrylamide gel. *ss* = single-stranded 54 base labeled oligonucleotide; *ds* = double-stranded annealed product. *B* – graphical representation of data in *A*.

DNA Ligation

Wild type HsRad52 has been shown to increase the efficiency of DNA ligation (Van Dyck et al., 1999). To determine the oligomeric requirements for this activity we tested each protein for its ability to promote DNA ligation. Addition of ligase to dsDNA that had not been incubated with HsRad52 resulted in approximately 15% of the linear dsDNA appearing as linear dimers and < 0.5% as multimers (Fig. 13). Preincubation of the linear dsDNA with increasing concentrations of wild type HsRad52 (from 1–6 μM) before addition of ligase resulted in a modest increase in the amount of linear dimers and a significant increase in the amount of multimeric ligation products. In the presence of 1 μM HsRad52 the addition of ligase resulted in approximately 15% of the linear dsDNA appearing as dimers and 37% as multimers, and with 6 μM HsRad52 this increased to 21% dimers and 54% multimers. When the DNA is preincubated with the 1-212 protein a similar small increase in the amount of linear dimers over the control appears at higher protein concentrations (20% linear dimers with 6 μM protein). However, in contrast to wild type HsRad52 only a very small percentage of the ligation products are multimeric (≈ 13%), and this is observed only at the highest protein concentration used. When the DNA is preincubated with 1-85 protein, no increase in the amount of ligation product is observed. These data suggest that formation of higher order oligomers by the 10 nm HsRad52 rings is important for the promotion of DNA end-joining. These results do not necessarily imply that HsRad52 binds specifically to DNA ends, thereby

promoting DNA ligation. Rather they are most simply interpreted as an increase in the local concentration of DNA ends that occurs only when the protein can form higher order oligomers of the 10 nm rings.

Figure 13. HsRad52 promotes ligation of DNA ends.

A.

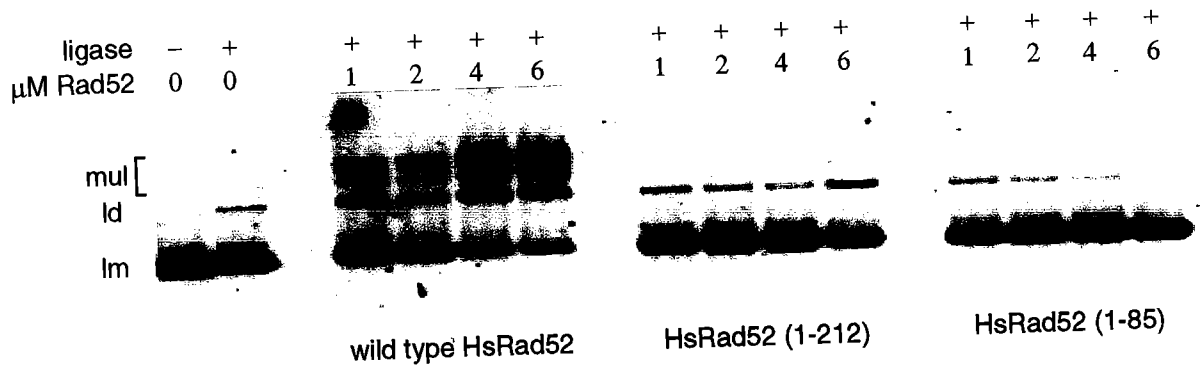

B.

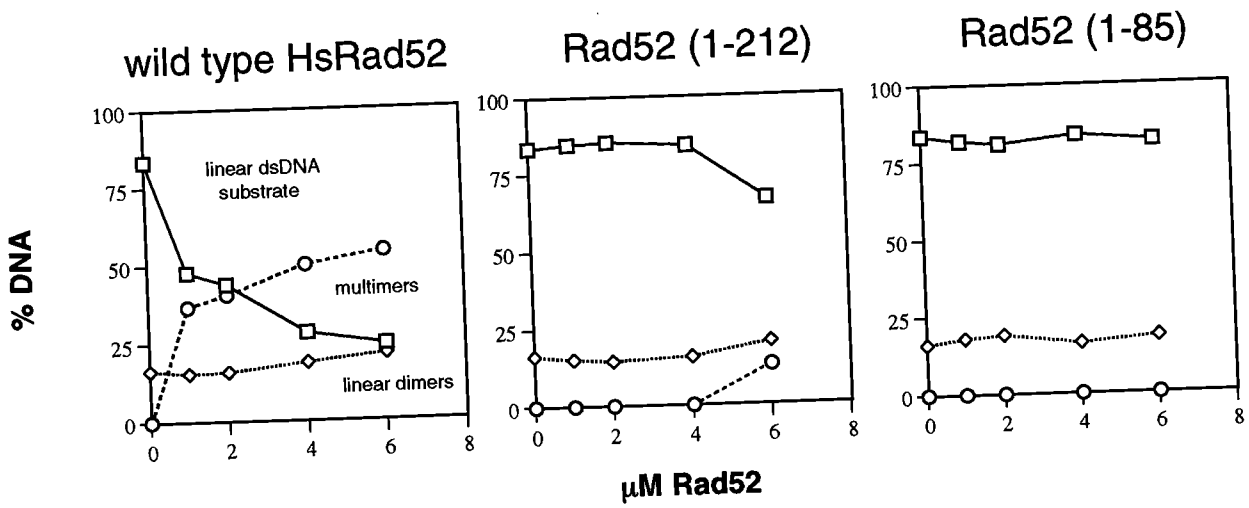

Figure 13. HsRad52 promotes ligation of DNA ends. Indicated concentrations of wild type HsRad52, HsRad52 (1-212) or HsRad52 (1-85) were incubated with XhoI digested ϕX174 dsDNA followed by addition of T4 DNA ligase as described in **Materials and Methods** (Chapter II). *A* – reactions were electrophoresed on a 0.7 % agarose gel. *lm* = linear monomeric double-stranded DNA; *ld* = linear dimers of double-stranded DNA; *mul* = linear, multimeric double-stranded DNA. *B* – graphical representation of data in *A*.

Discussion

Both the yeast and human Rad52 proteins exist in heterogeneous oligomeric states including ring-shaped multimers approximately 10 nm in diameter as well as higher order associations of these ringed structures (Shinohara et al., 1998; Van Dyck et al., 1998; Van Dyck et al., 1999; Stasiak et al., 2000; Ranatunga et al., 2001). However, the functional relevance of these different oligomeric states has not been studied. In this work we sought to correlate the oligomeric properties of the HsRad52 protein with its biochemical functions related to DNA binding that are fundamental to its role in homologous recombination. We find that while neither the higher order oligomers nor the ring-shaped structures are necessary for inherent DNA binding, both are required to efficiently promote the interaction of more than one DNA molecule.

Using both electron microscopy and gel filtration we find that the 1-212 mutant protein exists in a homogeneous oligomeric state relative to wild type HsRad52 and the 1-85 mutant. Its ring-shaped appearance and size are consistent with our previous studies of a 1-192 mutant protein (Ranatunga et al., 2001). Importantly, the rings do not interact in any way to form higher order oligomeric complexes. In contrast, electron micrographs of wild type HsRad52 show clearly that the protein rings form distinct side-to-side interactions that give rise to higher order complexes and the existence of these complexes in solution is

supported by the gel filtration results (Fig. 10). For the 1-85 mutant protein, although we see no distinct structures of any kind in electron micrographs, the broad trail from 8–16 ml in the gel filtration profile (Fig. 10) suggests that the protein aggregates in a non-specific manner. It may be that a surface that is sequestered in the full length 418 residue wild type protein is now exposed to solvent in the 1-85 protein and promotes non-specific self-association. The distinct peak at 18.5 ml, which approximates a complex containing 3 subunits, also suggests some specific interaction between the 1-85 subunits.

Our gel shift assays show the single-stranded DNA binding affinities of the wild type and 1-212 proteins to be similar, ≈ 8 nM and 5 nM, respectively. However, an important difference is that the 1-212 protein shows no protein-DNA networks that get trapped in the gel well as does wild type HsRad52. This undoubtedly is due to the fact that the 1-212 protein lacks the C-terminal self-association domain and is therefore no longer able to form higher order complexes of Rad52 rings. Although the single-stranded DNA binding affinity of the 1-85 mutant protein is ≈10-fold lower than the wild type and 1-212 proteins, it still shows formation of specific protein-DNA complexes (*b* in Fig. 11) with a reasonably strong affinity (≈ 50 nM). Like the 1-212 protein, the 1-85 protein is also missing the C-terminal self-association domain. Therefore, the non-specific aggregation suggested by gel filtration is likely responsible for the protein-DNA complexes trapped in the gel well. Our previous data show that another

truncation mutant protein, HsRad52 (218-418), maintains native protein structure but does not bind single-stranded DNA even at concentrations up to 2.0 μM (Ranatunga et al., 2001). Together, these data show that most if not all the determinants for single-stranded DNA binding lie within the N-terminal 85 residues of HsRad52, and that effective DNA binding is accomplished without formation of ring-shaped or higher order oligomers.

Interestingly, the three proteins show significant differences in their abilities to promote strand annealing and DNA ligation. At low concentrations, 1–5 nM, wild type HsRad52 increases the level of strand annealing dramatically above background. At concentrations greater than 5 nM there is an inhibition of double strand product formation. Therefore, it appears that the ability of wild type HsRad52 rings to form higher order oligomers contributes both to the increased efficiency of strand annealing at lower protein concentration as well as the inhibition of annealing at higher protein concentrations. In contrast, despite the fact that the DNA binding affinity of the 1-212 protein is equivalent to or slightly better than wild type Rad52, its ability to promote strand annealing is significantly less at low protein concentrations and shows no inhibition as the protein concentration increases, rather it shows a steady increase in annealing efficiency. The 1-85 protein also shows a protein concentration-dependent increase in annealing efficiency but requires higher amounts of protein to achieve an overall less percent of double strand product, in correspondence with its lower ssDNA binding affinity. An even greater discrepancy between the

activities of the three proteins is seen in the DNA ligation assay. Over the same range of protein concentration, from 1-6 μM, wild type Rad52 shows a steady increase in the amount of ligation product whereas the 1-212 and 1-85 proteins show little, if any, product formation. For example, at 6 μM wild type protein 54% of the total DNA is in the form of linear multimers, whereas with the 1-212 and 1-85 proteins there is 13% and 0% multimer formation, respectively.

Our data supports a model in which activities of Rad52 that involve binding to multiple DNA substrates require the ability of Rad52 to form higher order oligomeric complexes consisting of at least several Rad52 heptamer rings. However, are these in vitro activities relevant to *in vivo* Rad52 function? In fact, Lisby et al. (Lisby et al., 2001) have proposed that higher order Rad52 oligomers serve an important function in initiating recombinational DNA repair. Based on the small number of Rad52 foci formed relative to the expected number of DSBs following exposure to a particular dose of γ-rays, as well as *in vitro* data showing that multiple Rad52 rings bind to DNA (Shinohara et al., 1998; Van Dyck et al., 1998; Van Dyck et al., 1999) they proposed that aggregates of Rad52 serve to attract multiple lesions for repair within one locus, thereby serving as centers of recombinational repair. Our data are consistent with this idea. We have shown that efficient Rad52-mediated strand annealing and DNA ligation correlates with the ability to form higher order oligomers. This undoubtedly results from the ability to interact effectively with multiple pieces of DNA, an activity that may reflect an important *in vivo* function. Additionally, mammalian Rad52 group

proteins, including Rad51, Rad52 and Rad54, co-localize following DNA damage (Liu et al., 1999; Raderschall et al., 1999; Liu and Maizels, 2000; Essers et al., 2002) and specific protein-protein interactions between Rad52 and Rad51 contribute to optimal Rad51-mediated strand exchange activity (Song and Sung, 2000). Therefore, binding of Rad52 to single- and double-stranded DNA, as well as to Rad51 and RPA, may promote and/or stabilize the joint molecules that initiate the recombination pathway. Further investigation of the DNA binding properties of Rad52, as well as its ability to interact simultaneously with several components of a repair complex, e.g. single- and double-stranded DNA, Rad51 and RPA, will be important in establishing the biochemical mechanism by which Rad52 functions to mediate homologous recombinational DNA repair.

Chapter V

Essential Residues for DNA Binding in Human Rad52

Introduction

Among members of the *ScRAD52* epistasis group, *rad52* mutants display the most severe phenotypes indicating an integral role for this protein in HR. The human homologue of *RAD52*, which shares 30% identity and 58% similarity with the ScRad52, was identified through sequence analysis (Muris et al., 1994; Shen et al., 1995). Many of the biochemical properties and structural characteristics of ScRad52 have been conserved in HsRad52. For example, the yeast and human proteins both bind ss- and dsDNA (Mortensen et al., 1996; Reddy et al., 1997; Benson et al., 1998; Shinohara et al., 1998; Van Dyck et al., 1998), anneal complementary strands of DNA (Mortensen et al., 1996; Reddy et al., 1997; Shinohara et al., 1998; Sugiyama et al., 1998; Parsons et al., 2000; Van Dyck et al., 2001) and in conjunction with RPA stimulate Rad51 mediated strand exchange (Sung, 1997; Benson et al., 1998; New et al., 1998; Shinohara and Ogawa, 1998; Baumann and West, 1999; McIlwraith et al., 2000; Song and Sung, 2000). Structurally, electron microscopy studies have shown that both proteins self-associate to form ring – like structures (9-13 nm in diameter), as well as higher order aggregates, and both proteins appear to bind DNA either as a single

ring or as a complex of rings (Shinohara et al., 1998; Van Dyck et al., 1998; Van Dyck et al., 1999).

Comparison of the sequences of the yeast and human proteins revealed that the N–termini are highly conserved (65 -75% identical) whereas the C–termini are only minimally conserved (6-7% identical) (Park et al., 1996). Protein – protein interaction studies have identified specific contacts between ScRad52, ScRad51, (Shinohara et al., 1992; Milne and Weaver, 1993) and ScRPA (Hays et al., 1998) as well as between HsRad52, HsRad51 (Shen et al., 1996) and HsRPA (Park et al., 1996) and have mapped the RPA and Rad51 interaction domains to residues within the highly divergent C–terminus (Milne and Weaver, 1993; Park et al., 1996; Shen et al., 1996; Hays et al., 1998). We have also identified a self – association domain in the C–terminus that mediates the higher order oligomerization of HsRad52 rings (Ranatunga et al., 2001). Thus, it appears that a primary function of the C–terminal domain of Rad52 is to mediate a species – specific interaction between Rad51, Rad52 and RPA in addition to promoting the higher order oligomerization of Rad52 rings.

Mortensen *et al.* identified a DNA binding domain spanning residues 34-169 in the N–terminus of ScRad52 (Mortensen et al., 1996). The ScRad52 and HsRad52 proteins are highly conserved in the N–terminus suggesting that the DNA binding domain in the human protein also lies in the N–terminus. Park *et al.* proposed that the DNA binding domain for HsRad52 is located between

residues 39-80 (unpublished, cited in Park *et al.*, 1996). A series of studies using truncation mutants of HsRad52 has provided evidence that supports this hypothesis. Kito *et al.* demonstrated that a naturally occurring isoform of HsRad52, containing only the first 94 residues retains DNA binding ability (Kito et al., 1999). Two N–terminal ring forming truncation mutants, HsRad52 (1-192) and HsRad52 (1-237), have also been shown to bind DNA (Kagawa et al., 2001; Ranatunga et al., 2001). Additionally, we have recently demonstrated that a truncation mutant containing only the first 85 residues of the protein is still able to bind DNA (Lloyd *et al.*, 2002 submitted). Collectively, these studies suggest that the DNA binding domain in HsRad52 is located between residues 39–85. In the following study we have used an alanine scanning mutagenesis procedure to identify residues in the N–terminal region of HsRad52 that are critical for binding to ssDNA.

To identify specific areas within the proposed DNA binding domain (residues 39-80) that are critical for this function, we created 16 mutants by changing two to three consecutive amino acids to alanine between residues 37 –81. Current studies in the lab are analyzing the effect of mutations through residue 85.

Results

ssDNA Binding of Alanine Block Mutants

The effects of these alanine mutations on DNA binding are assayed by gel shift analysis. The gels in Figure 14 are representative of 5 different experiments, each of which gave similar results. The apparent difference in the intensity of the gels is a result of different exposure times. Scans reveal a similar radioactive content in all lanes. To assess the DNA binding activities of the mutants, % DNA bound at each protein concentration by the mutants is compared to the % DNA bound by wild type HsRad52 at each concentration. For the purpose of categorizing mutants in this study, we have defined wild type **(wt)** binding as 100% DNA bound at a protein concentration of 20 nM and higher. Mutants exhibiting **wt** binding include 40-42A, 61-62A, 63-64A, and 67-69A. Two categories of mutants that exhibit reduced DNA binding are defined: 1. "***r***" includes those that show a less severe reduction in DNA binding, defined as 100% DNA bound at protein concentrations ≤ 100 nM and, 2. "***R***" includes those that show a severe reduction in DNA binding defined as less than 100% DNA bound at the highest protein concentration (100 nM). Mutants that exhibit ***r*** binding include 46-48 and 58-60. Mutants that exhibit ***R*** binding include 37-39A, 49-51A, 55-57A, 70-72A and 73-75A. Finally, mutants 43-45A, 52-54A, 65-66A, 76-78A, and 79-81A are classified as dead **(D)** since these mutants have lost the

ability to bind DNA even at the highest protein concentrations used in this assay (100 nM).

Figure 14. ssDNA binding gel shift assays of wild type HsRad52 and alanine block mutants.

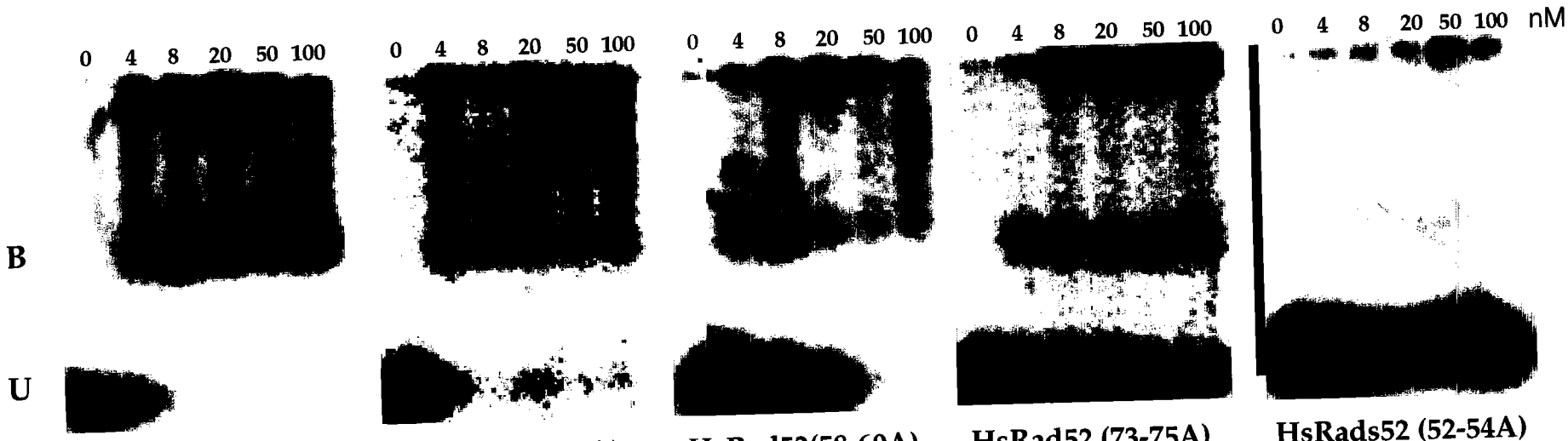

wt
100% DNA bound at 20 nM

r
100% DNA bound at < 100 nM

R
< 100% DNA bound at 100 nM

D
no DNA binding at 100 nM

Figure 14. Gel shift assays of the alanine block mutants. Indicated concentrations of wild type HsRad52 or the alanine block mutants were incubated with a 5′ end-labeled 54 base oligonucleotide followed by cross-linking with glutaraldehyde as described in **Materials and Methods** (Chapter II). Reactions were electrophoresed on a 0.7% agarose gel. Radioactive material at the top of the gel represents protein-DNA complexes trapped in the gel well. U= unbound DNA; B=specific protein-DNA complexes.

Table I. ssDNA Binding of Alanine Block Mutants.

Mutations	Alanine Substitutions	DNA Binding
37-39	QAI	R
40-42	QKA	wt
43-45	LRQ	D
46-48	RLG	r
49-51	PEY	R
52-54	ISS	D
55-57	RMA	R
58-60	GGG	r
61-62	QK	wt
63-64	VC	wt
65-66	YI	D
67-69	EGH	wt
70-72	RVI	R
73-75	NLA	R
76-78	NEM	D
79-81	FGY	D

wt = 100% DNA bound at 20 nM protein; ***r*** = 100% DNA bound at ≤ 100 nM protein ; ***R*** = less than 100% DNA bound at 100nM protein; **D** = no DNA binding at protein 100 nM.

ssDNA Binding of Alanine Point Mutants

Following initial screening of the sixteen alanine block mutants, point mutants were created at individual positions for the five dead alanine block mutants to determine the contribution to DNA affinity made by each residue. The gels in Figure 15 are representative of 3 different experiments, each of which gave similar results. The classification system applied to alanine block mutants is applied to the point mutants. Unexpectedly, the majority of these point mutants display **wt** binding. Point mutants L43A and I52A displayed slight reductions in binding and the I66A mutant exhibited a significant reduction in DNA binding. Only 3 alanine point mutations (Y65A, F79A, and Y81A) abolished HsRad52 DNA binding activity. The results from the DNA binding assays suggest that hydrophobic residues, especially the aromatic tyrosines at positions 65 and 81 and phenylalanine at position 79 are critical for mediating the interaction of HsRad52 with DNA. From the above analyses of both block and point mutants, it is clear that charged residues in this region do not contribute significantly to DNA binding.

Figure 15. Gel shift assays of alanine point mutants.

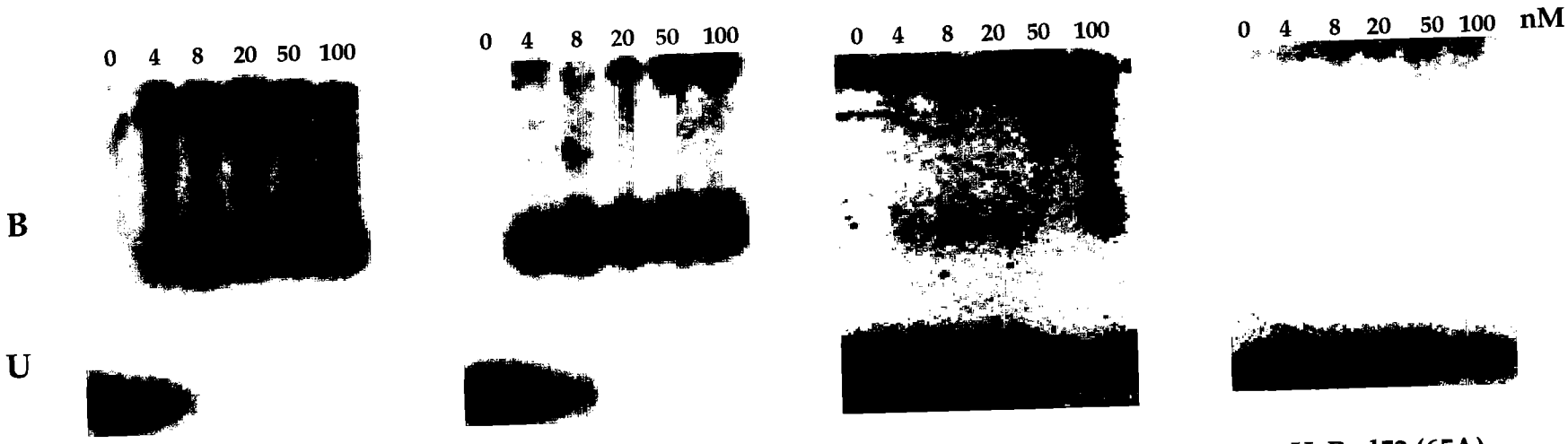

wild type HsRad52

HsRad52 (53A)

wt
100% DNA
bound at
20 nM

HsRad52 (43A)

R
< 100% DNA
bound at
100 nM

HsRad52 (65A)

D
no DNA binding
at 100 nM

Figure 15. Gel shift assays of the alanine point mutants. Indicated concentrations of wild type HsRad52 or the alanine point mutants were incubated with a 5′ end-labeled 54 base oligonucleotide followed by cross-linking with glutaraldehyde as described in **Materials and Methods** (Chapter II). Reactions were electrophoresed on a 0.7% agarose gel. Radioactive material at the top of the gel represents protein-DNA complexes trapped in the gel well. U=unbound DNA; B=specific protein-DNA complex.

Table II. ssDNA Binding of Alanine Point Mutants.

Mutation	Alanine Substitution	DNA Binding
43	L	R
44	R	Wt
45	Q	Wt
52	I	R
53	S	Wt
54	S	Wt
65	Y	D
66	I	R
76	N	Wt
77	E	Wt
78	M	Wt
79	F	D
80	G	Wt
81	Y	D

wt = 100% DNA bound at 20 nM protein; ***r*** = 100% DNA bound at ≤ 100 nM protein; ***R*** = less than 100% DNA bound at 100nM protein; **D** = no DNA binding at 100 nM protein.

Structural Analysis of the Alanine Block Mutants and wild type HsRad52

DNA binding could be affected by a disruption in either the local or global structure induced by alanine substitutions. Hence, far-UV circular dichroism (CD) spectra were collected to assess the secondary structure content of wild type and dead alanine block mutants of HsRad52. By comparing these CD spectra, a loss of DNA binding due to structural changes can be differentiated from a loss due to the removal of essential residues for DNA-protein interaction. The CD spectrum for wild type HsRad52 features a dual minima at 222 and 208 nm, characteristic of α -helical structure. The 52-54A block mutant displays a nearly identical spectrum to that of wild type, indicating that there were no significant structural changes. By contrast, the 65-66A block mutant exhibits a substantial decrease in mean residue ellipticity (MRE), a measure of the secondary structural content, signifying a disruption in the secondary structure. CD spectra for 43-45A, 76-78A and 79-81A block mutants show an increase in the MRE, implying that these block mutations induced the formation of additional secondary structure. This is best illustrated in the 79-81A block mutant which demonstrates an increase in MRE of approximately 60%. CD spectra of the dead alanine point mutants Y65A, F79A, and Y81A are currently being collected.

Figure 16. CD spectra of alanine block mutants.

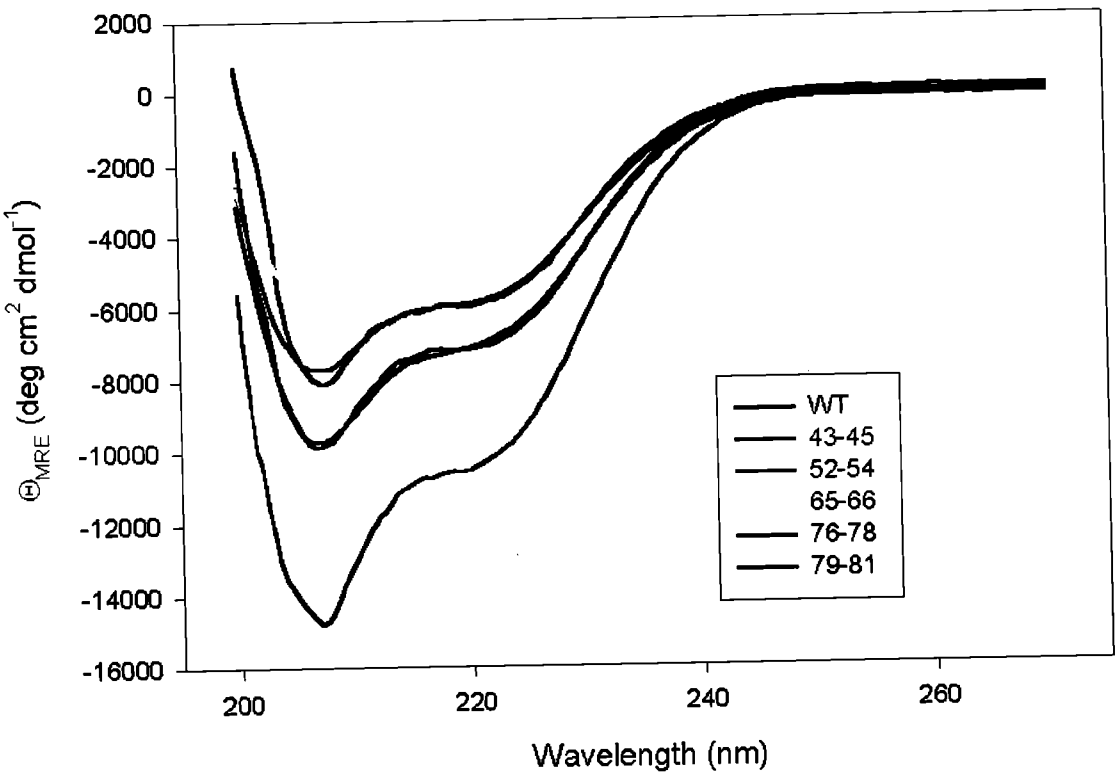

Figure 16. CD spectra of the alanine block mutants. CD spectra for wild type and alanine block mutants. CD spectra for all proteins except 79-81A were measured at protein concentrations of 10 μM. CD spectrum for 79-81A was measured at a protein concentration of 5 μM.

Discussion

The first 85 residues of HsRad52 are 75% identical to ScRad52 (Park et al., 1996). Two classic ScRa52 mutants, *rad52–1* and *rad52 –2*, carry substitutions in the N-terminus, suggesting that an important function of Rad52 is located in that region (Adzuma et al., 1984; Boundy and Livingston, 1993). The *rad52-1* mutant displays a null phenotype resulting from an alanine 90 → valine substitution (Adzuma et al., 1984). The *rad52-2* mutant carries a single proline 64 → leucine substitution and displays severe defects in DSB repair and sporulation, yet exhibits elevated levels of mitotic recombination (Boundy and Livingston, 1993). Mortensen *et al.* mapped the DNA binding domain of ScRad52 to the N–terminus spanning residues 34 through 169 (Mortensen et al., 1996). Studies by a number of groups have implied that the DNA binding domain of HsRad52 is also contained within the N–terminus (Park et al., 1996; Kito et al., 1999; Kagawa et al., 2001; Ranatunga et al., 2001). Furthermore, we have recently shown that an N-terminal truncation mutant of HsRad52, consisting of only the first 85 residues, maintains DNA binding activity (Lloyd, submitted 2002). In the present study alanine scanning mutagenesis was used to identify residues in this region that are critical for DNA binding. First, five alanine block mutants were identified that no longer bind DNA. Subsequently, the contribution to DNA binding made by each residue within these 5 block mutants was determined.

The results of our studies show that a combination of hydrophobic and uncharged polar residues, especially aromatic residues, appeared to be important for DNA binding. Alanine substitution at Y65, F79 and Y81 had the greatest impact on DNA binding, as evidenced by the inability of these mutants to bind ssDNA. These aromatic residues may participate in stacking interactions with DNA bases. Aromatic residues have been shown to stabilize the interaction between HsRPA and ssDNA through phenylalanine –base stacking (Bochkarev et al., 1997). Similar stacking interactions between aromatic residues and bases have been observed for the TATA binding protein (TBP) (Juo et al., 1996). Alanine substitutions at L43 and I52 resulted in moderate defects in DNA binding while an alanine substitution at I66 resulted in a significant reduction. These hydrophobic and aromatic residues may exert their effect on DNA binding by directly contacting the DNA or by stabilizing the structure of the DNA binding domain. Based on our analysis of the block alanine mutants, only 2 (R55 and R70) of the 7 basic residues (K41, R44, R46, R55, K62, H69, and R70) in the proposed DNA binding domain may have an effect on DNA binding. Current studies are addressing the relative contribution of R55 and R70 to DNA binding by analyzing alanine point mutants at these positions.

The structural integrity of the alanine block mutants was probed by CD to determine the secondary structural content of the mutants. For 3 of the "dead" alanine block mutants (43-45A, 52-54A and 76-78A) point mutations were created at each position, and each of the single mutants retained either wt DNA binding

activities or displayed only minimally reduced binding. This showed that none of these 9 residues are critical for DNA binding, but suggested instead that a structural alteration in the block mutants might account for the loss of DNA binding. The CD spectra of 43-45A, 76-78A and 79-81A show an increase in MRE implying that the alanine mutations produced a change in the secondary structure, most likely by inducing the formation of additional α-helical structure. This is not surprising as the introduction of 2-3 consecutive alanines, an amino acid with the greatest propensity to form α-helices, could result in an increase in secondary structure which may alter the native conformation of the DNA binding domain. Additionally, proteins with aromatic amino acids in close proximity often display a positive signal in their CD spectrum provided by exciton coupling between the two residues (Kuwajima et al., 1991). This could be the case for these mutants with an increased MRE, especially the 79-81A mutant in which F79 and Y81 have both been removed. The CD spectrum of 52-54A was similar to wild type indicating that there was no meaningful change to the secondary structure of the protein. However, while the alanine substitutions may not have altered the secondary structure of the protein, it is possible that the tertiary structure of the protein was perturbed. The CD spectrum of 65-66A displays a decrease in MRE, signifying a disruption of the secondary structure. Collectively, the CD studies suggest that structural perturbations may contribute to the loss of DNA binding observed with the alanine block mutants. Current CD studies of the dead alanine point mutations, Y65A, F79A, and Y81A, will clarify if the aromatic residues at these positions contact the DNA.

Utilizing computational sequence analysis and secondary structure predictions, Iyer *et al.* proposed that HsRad52 contains a helix-hairpin-helix (HhH) DNA binding motif in the N-terminus of HsRad52 (Fig. 17) (Iyer et al., 2002). This motif occurs in a number of non-sequence specific DNA binding proteins including, HsRad51, endonuclease III, and DNA polymerase β (Thayer et al., 1995; Doherty et al., 1996; Shao and Grishin, 2000). The HhH motif is characterized by two anti-parallel α-helices connected by a hairpin loop. Crystal structures of rat DNA polymerase β and *E. coli* endonuclease III have revealed that the residues within the hairpin loop are stabilized by the α-helices (Pelletier et al., 1994; Thayer et al., 1995). Thayer *et al.* has proposed that the central residues of the hairpin in the HhH motif bind DNA through hydrophobic interactions with the bases in the grooves (Thayer et al., 1995). However, the co-crystal structure of the rat pol β structure demonstrates that residues which border the loop and within the α-helix backbone form hydrogen bonds with the phosphate backbone of the DNA. These apparent discrepancies illustrate that there may not be rules which determine specific protein-DNA contacts made by these proteins like there are for helix-turn-helix DNA binding proteins. As shown in Figure 17, the HhH motif in HsRad52 is predicted to begin at residue G68 and continue through Q90. Mutants, HsY65A, HsF79A and HsY81A, identified in our study as making significant contributions to DNA binding are located in this area, supporting the prediction that residues within the HhH motif mediate the interaction between HsRad52 and DNA.

Figure 17. Sequence alignment of Rad52 proteins.

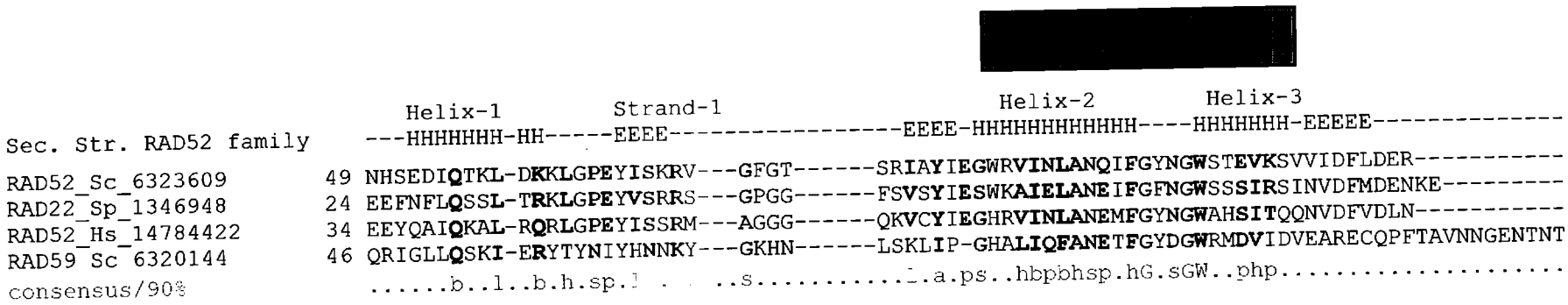

Figure 17. Sequence alignment of RAD52 proteins. Proteins are denoted with their gene names, species abbreviation and gi numbers. The coloring reflects the consensus at 90% conservation. The consensus abbreviations and coloring scheme are as follows: h: hydrophobic residues (L,I,Y,F,M,W,A,C,V), l: aliphatic (L,I,A,V) and a: aromatic (F,Y,W,H) residues shaded yellow; o: alcohol (S,T), colored blue, c: charged (K,E,R,D,H) residues, +: basic (K,R,H) residues, -: acidic (D,E) residues, and p: polar (S,T,E,C,D,R,K,H,N,Q) residues colored purple; s: small (S,A,C,G,D,N,P,V,T) and; b: big (L,I,F,M,W,Y,E,R,K,Q) residues shaded gray. Secondary structure assignments are as follows: H: Helix, E: Extended (Strand). Species abbreviations are as follows: Sc: *Saccharomyces cerevisiae*, Sp: *Schizosaccharomyces pombe*, Hs: *Homo Sapiens*. Figure is adapted from Iyer *et al.* (2002) *BMC Genomics* **3**, 1471-1428.

In a recent mutagenesis study by Mortensen *et al.*, alanine point mutations were systematically introduced at all positions in the N–terminus of ScRad52 with the exception of acidic residues. This study genetically distinguished residues important for various functions of ScRad52. Alanine substitutions at ScN91 and ScF94 conferred null phenotypes, suggesting that these residues are essential for Rad52 function. These residues correspond to the human positions, N76 and F79. In contrast to the yeast study we find that an alanine substitution at HsN76 had no effect on DNA binding. However in agreement with the yeast results, the alanine substitution at HsF79 completely inhibited DNA binding. Other mutants identified by Mortensen *et al.* include ScY66A, ScR70A, ScW84A, ScR85A, ScY96A. Alanine substitutions at these positions resulted in a slight sensitivity to γ-rays and displayed either wild type or increased rates of heteroallelic recombination. The corresponding mutations in HsRad52, HsY51A, HsR55A, HsH69A, HsR70A, and HsY81A, exhibit varied effects on DNA binding. Alanine block mutants 55-57A and 70-72A exhibited reduced DNA binding activities, therefore alanine substitutions at HsR55 and HsR70 may have an effect on DNA binding. Mutants ScY66A, ScR70A, and ScP64L are in a region of ScRad52 that is predicted to be mainly unstructured (see Fig. 17) (Boundy and Livingston, 1993). These yeast mutants correspond to residues (HsY51, HsR55, and HsP49) contained within alanine block mutants that exhibited reduced DNA binding activities. The location of these residues in the mainly unstructured protein region suggests that these mutations may have disrupted the conformation of the proteins, resulting in their less drastic phenotypes. Mutants,

ScR85A and ScY96A, which resulted in a slight sensitivity to γ-rays and either wild type or increased rates of heteroallelic recombination, and mutants ScN91A and ScF94A, which resulted in null phenotypes, are in a region of ScRad52 proposed to be mainly α-helical and which contain the HhH motif (Fig. 17). Point mutants in our screen that lost DNA binding, Y65A, F79A and Y81A, were located in the corresponding region of the HsRad52. Interestingly, the above comparison of conserved residues reveals that only the effects of the HsF79→A /ScF94→A mutations show similar importance, emphasizing the functional significance of this residue. While it is difficult to compare the effects of mutations at conserved residues in the yeast and human proteins based on the yeast phenotypes and our biochemical studies of HsRad52, one similarity is clear. In both studies, alanine substitutions at charged residues did not produce dramatic effects. The alanine substitutions at hydrophobic and aromatic residues had varied effects between the two proteins. DNA binding studies of the yeast mutants identified in the study by Mortensen *et al.* will facilitate these comparisons. Our data supports a model in which the primary contacts between HsRad52 and DNA are stacking interactions between DNA bases and the aromatic residues Y65, F79 and Y81. Less critical, yet significant interactions may also occur between L43, I52, I66, R55 and R70 with DNA. Studies that are currently in progress will assist in differentiating between an effect of mutations on the overall structure of the DNA binding domain versus a direct effect on the specific protein-DNA contacts.

Chapter VI

Conclusions and Future Directions

Regulation of protein function through oligomerization is a common theme in biological systems, and contributes significantly to the control of all cellular metabolic pathways. The process of homologous genetic recombination is a critical pathway in all organisms for the maintenance of genomic integrity and repair of DNA damage. During the last decade most of the components of this pathway in mammalian cells have been identified, thereby setting the stage for a detailed biochemical understanding of both the regulation and catalysis of homologous recombination. In the work presented here we have demonstrated a very complex relationship between the oligomeric state and functions of the HsRad52 protein. HsRad52 is a 418 amino acid polypeptide that exists in solution as a heterogeneous mix of oligomers. Its fundamental oligomeric state is a 10 nm diameter ring composed of approximately 7 subunits. Additionally, these rings form higher order associations that are at this point not well defined in terms of their size and the number of subunits.

Earlier protein – protein interaction studies identified a domain in the N–terminus of HsRad52, spanning residues 85 – 159, that was proposed to be exclusively responsible for mediating the self–association of HsRad52. However, through the use of truncation mutants, we identified an additional novel self –

association domain in the C–terminus of HsRad52. We generated a model in which the N–terminal self–association domain of HsRad52 promotes the formation of ring–shaped oligomers, and the C–terminal self–association domain promotes higher order self – association events, i.e., the oligomerization of HsRad52 rings. While we have distinguished between the self–association domains responsible for ring formation versus ring oligomerization, the identification of another self-association domain raises some questions. For example, what regulates the formation of higher order complexes by the 10 nm rings? Since the C–terminus of HsRad52 also contains the HsRPA and HsRad51 interaction domains, does the interaction of HsRad52 with either of these proteins affect the oligomerization?

We have asked if the ability of HsRad52 to perform various functions related directly to DNA binding was affected by the oligomeric state of the protein. By using truncation mutants which blocked formation of the 10 nm ring structure and the higher order ring oligomers, 1-85 and 1-212 respectively, we demonstrated that DNA binding by HsRad52 depends on neither ring formation nor higher order ring oligomerization. However, formation of oligomers consisting of multiple HsRad52 rings is important for activities that require simultaneous interaction with more than one piece of DNA. These activities include annealing of complementary DNA strands and promoting the end-to-end interactions between DNA molecules. Our work uncovered some intriguing subtleties between optimal activity and oligomeric state. For example, the wild

type HsRad52 protein was significantly more efficient at stimulating annealing than either of the truncation mutants. Wild type HsRad52 was the most efficient at promoting end-to-end interactions between DNA molecules, suggesting that this function of HsRad52 is not solely dependent on the ability of HsRad52 to bind DNA but also on the ability of HsRad52 rings to interact with each other. While the exact *in vivo* function of the higher order ring complexes remains to be determined, our studies demonstrate that optimal activity of HsRad52 depends on the ability of the rings to oligomerize supporting a hypothesis in which the higher order complexes of rings are functionally relevant *in vivo*.

Currently, it remains unclear how the DNA interacts with the HsRad52 rings. Using image reconstruction of negatively stained electron micrographs, Stasiak *et al.* generated the following model of HsRad52 rings (Fig. 18) (Stasiak et al., 2000). The ring, ~130 Å in diameter, contains 7 subunits which are joined together at one end to generate a funnel-shaped opening. Each subunit is separated from its neighbor at the opposite end of the channel to give rise to seven protrusions. The central channel is ~60 Å in diameter at the top of the funnel and ~ 40 Å at the narrowest point. This model suggests that two modes of binding are likely; either the DNA can wrap around the outside of the ring or the DNA can pass through the central channel. Since activities that HsRad52 mediates, such as annealing and ligation, rely on the ease with which multiple DNA molecules can simultaneously interact with HsRad52 and with another DNA molecule, this suggests that the DNA interacts with residues on the outer

Figure 18. Surface views of the 3D reconstruction of HsRad52 rings.

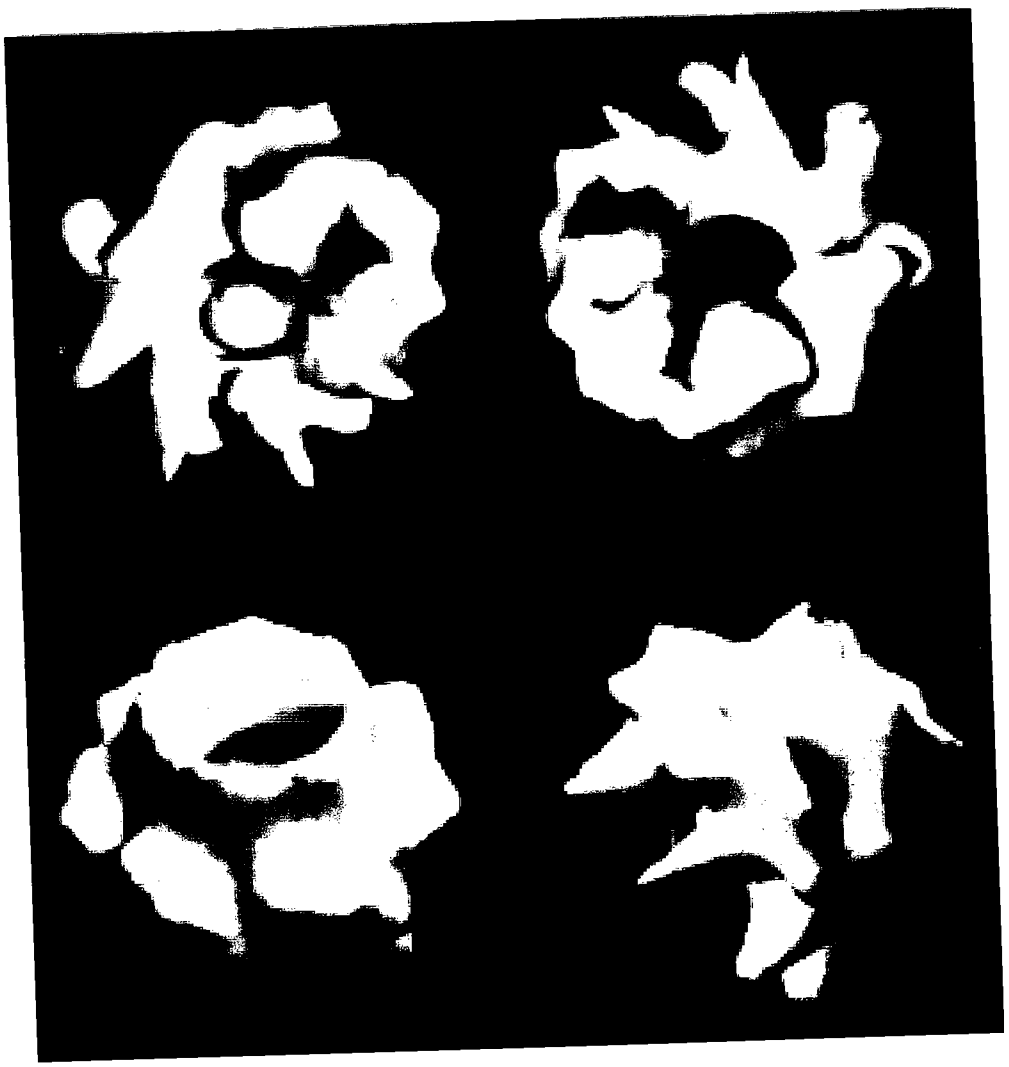

Stasiak *et al.* (2000) *Curr Biol* **10**, 337-340.

Figure 18. Surface views of the 3D reconstruction of heptameric HsRad52 rings. The surface has been chosen so as to enclose the expected molecular volume. Figure adapted from Stasiak *et al.* (2000) *Curr Biol.* **10**, 337-340.

surface of the rings. Confirmation of this theory awaits a crystal structure of HsRad52 in the presence of DNA. Another question that is prompted by the current HsRad52 DNA binding studies is how many of subunits per HsRad52 ring contact the DNA? Results from our annealing studies imply that multiple pieces of DNA interact with each HsRad52 ring, but a stoichiometry has not been determined.

Park *et al.* proposed that the DNA binding domain of HsRad52 is contained in the highly conserved N – terminus spanning residues 39 – 80 (unpublished, cited in Park *et al.*, 1996). We have identified three aromatic residues, Y65, F79 and Y81, within this region that inhibit DNA binding activity when mutated to alanine. Computational sequence analysis of HsRad52 has mapped a helix-hairpin-helix motif, commonly found in a number of non-sequence specific DNA binding proteins, spanning residues 68-90 (Iyer et al., 2002). Residues within the HhH motif have been proposed to directly contact DNA (Thayer et al., 1995). The residues which we identified as affecting DNA binding are located either within or just before this region. One possibility is that the aromatic residues Y65, F79 and Y81 contribute to DNA binding through stacking interactions with DNA bases. The participation of aromatic residues in stacking interactions with DNA bases has been observed for a number of proteins including HsRPA and TBP (Juo et al., 1996; Bochkarev et al., 1997). Crystal structures of these protein-DNA complexes have revealed that the stacking interactions between the aromatic residues and the DNA result in

bending of the DNA (Juo et al., 1996; Bochkarev et al., 1997). Mutations at residues L43, I52, and I66 result in a reduction in DNA binding, suggesting that these residues make minor contributions. These hydrophobic residues may exert their effects on DNA binding through stabilization of the protein structure and/or through making less critical contacts with the DNA. Studies are in progress to investigate the potential effect of alanine mutations at Y65, F79 and Y81 on HsRad52 structure by examining the secondary structural content of the point mutants Y65A, F79A and Y81. If the secondary structural content of the point mutants does not differ significantly from wild type HsRad52, this suggests that these residues directly contact the DNA. Additionally, we are continuing to study the DNA binding properties of residues beyond 81, with special attention to the aromatic residues, within the HhH motif.

Recently, a similar alanine scanning mutagenesis screen of the highly conserved N-terminus of ScRad52 was reported (Mortensen et al., 2002). The yeast screen genetically distinguished residues critical for various functions of ScRad52. Despite the conservation of residues between the proteins, the effects of mutations at conserved residues varied between yeast and human Rad52. The one similarity in both studies was the minimal contribution made by charged residues to ScRad52 function and HsRad52 DNA binding. While the effects of alanine substitutions at hydrophobic and aromatic residues varied between the proteins, data from both studies suggests a role for both hydrophobic and aromatic residues in mediating the functions of Rad52. The differences in these

studies also underscore the idea that while these proteins may be highly conserved in sequence, mostly in the N-terminus, the functional determinants in each appear to be quite different.

Collectively, our studies have demonstrated that there are two separable domains that mediate self-association, one in the N–terminus that mediates the formation of 10 nm rings and one in the C-terminus that mediates formation of ring complexes. We were able to correlate the oligomeric properties of the HsRad52 protein with its biochemical functions related to DNA binding. We further characterized the DNA binding of HsRad52 by illustrating that aromatic residues in the DNA binding domain of the HsRad52 rings may be participating in stacking interactions with the DNA bases. We also suggest that hydrophobic residues may also be contributing to DNA binding by either making less significant contacts with DNA or by stabilizing the overall structure of the protein.

While HsRad52 has been shown to stimulate HsRad51-mediated strand exchange in both the absence and presence of HsRPA, the role of HsRad52 in HR remains unclear. With the elucidation of the importance of HsRad52 self-association for optimal activity along with implications of aromatic residues participating in DNA binding, we propose the model depicted in Figure 19 for HsRad52 in DSB repair. Once a double strand break has been introduced, the break will be resected by the exonucleases to produce 3′ overhanging ssDNA

tails (**step I**). HsRPA binds to the newly resected DNA and alleviates secondary structure within the DNA (**step II**). HsRad52 is recruited to the resected DNA, perhaps by virtue of its affinity for both ssDNA and HsRPA (**step III**). Our studies have shown that HsRad52 activities related to DNA binding are optimal when the protein is able to oligomerize into ring complexes. An equilibrium likely exists *in vivo* between the 10 nm rings and the ring complexes, enabling HsRad52 to bind ssDNA either as a ring or in a complex of rings.

Prior to HsRad51 polymerization onto ssDNA, HsRPA is likely to be displaced. In yeast, Sugiyama *et al.* have recently demonstrated that ScRad52 and ScRPA are able to bind to ssDNA simultaneously and that displacement of ScRPA is dependent upon ScRad51 and ScRad52 (Sugiyama and Kowalczykowski, 2002). It has yet to be determined if HsRPA and HsRad52 bind ssDNA simultaneously, and by what mechanism HsRPA is displaced. How HsRad51 is loaded onto ssDNA is also unclear. It has been demonstrated that ScRad52 targets ScRad51 to ssDNA via complex formation between the two proteins (Song and Sung, 2000). Analogously, a role for HsRad52 in facilitating the loading of HsRad51 onto ssDNA has been proposed (Benson et al., 1998). Our DNA binding data now suggests a biochemical explanation for this function. If HsRad52 binds DNA through base stacking interactions with aromatic residues, this may result in a conformational change in DNA such that the polyphosphate DNA backbone is made optimally available for binding by

Figure 19. HsRad52 in DSB Repair.

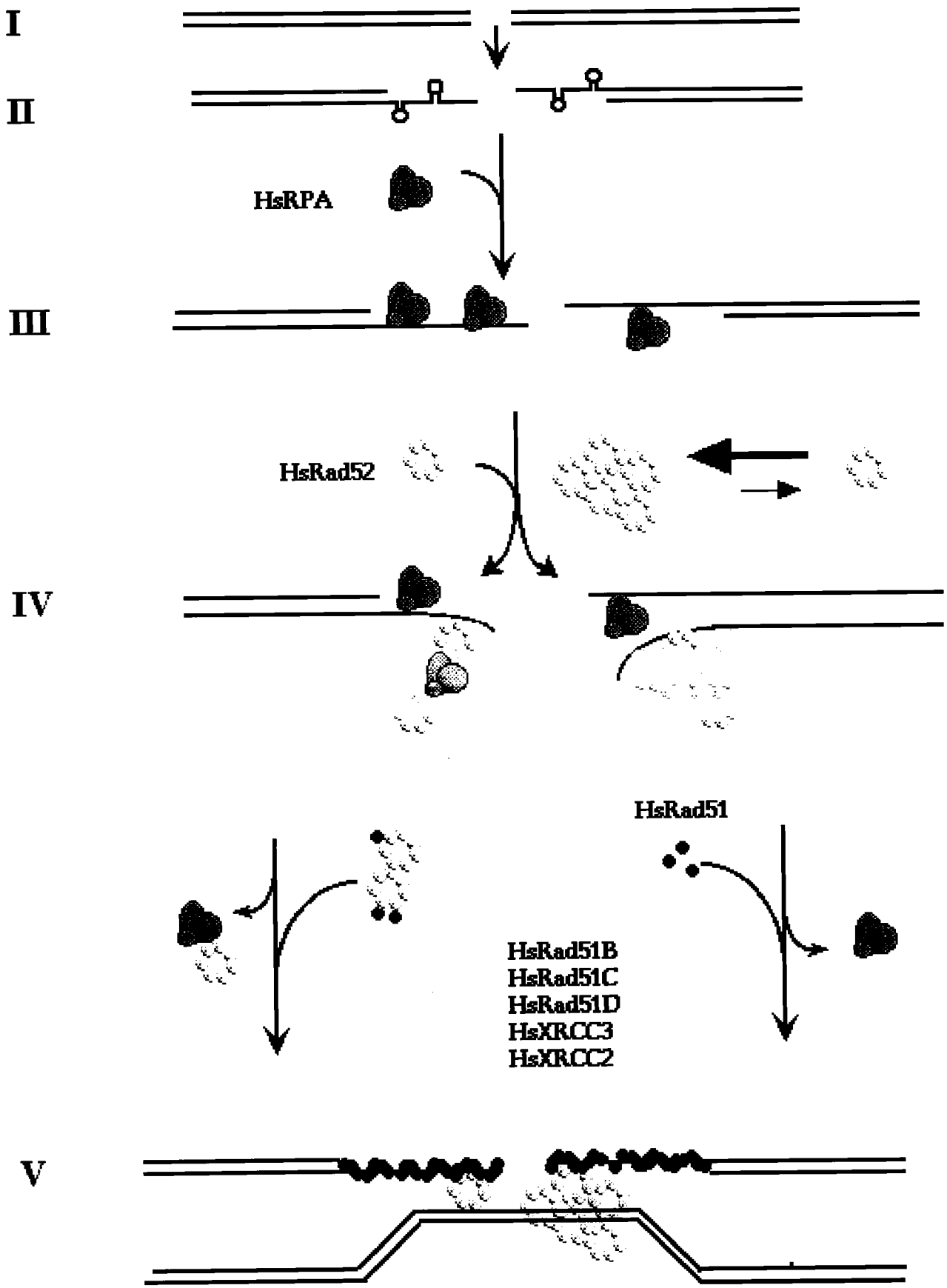

HsRad51. The RecA protein has been shown to interact exclusively with the backbone of ssDNA resulting in an extension of the DNA length and thereby allowing bases to find their Watson-Crick partners within the dsDNA substrate during strand exchange. It is very likely, although yet to be specifically demonstrated, that HsRad51 also binds exclusively to the backbone of ssDNA. Therefore, HsRad52 may help load HsRad51 by altering the conformation of the DNA upon binding allowing HsRad51 to more easily and quickly load onto the ssDNA (**step IV**). A role for the HsRad51 paralogs in helping to load HsRad51 onto ssDNA has also been proposed. Most likely, efficient loading of HsRad51 onto ssDNA is a combination of HsRad52 binding and inducing a structural change in the DNA, and the paralogs also assisting in someway to direct HsRad51 to this site.

Van Dyck *et al.* demonstrated that HsRad52 is able to simultaneously bind to ss- and dsDNA and that HsRad52 and HsRad51 are able to bind ssDNA simultaneously (Van Dyck et al., 1998). It is possible that once HsRad51 has polymerized onto ssDNA, HsRad52 may help in the search for homologous DNA by stabilizing joint molecule formation the simultaneous interactions with the HsRad51 nucleoprotein filament and the homologous dsDNA substrate (**step V**). Recent studies also suggest that ScRPA plays a direct role in strand exchange by removing the displaced strand from the complex thus further stabilizing the joint molecule (Eggler et al., 2002). Therefore, ScRPA appears to be required at steps prior to and after joint molecule formation. A similar scenario may occur in

the human system. For instance once HsRPA is displaced from the invading ssDNA it may bind HsRad52 and thereby remain near the site of damage so that it can participate in stabilizing the newly formed joint molecule through interactions with the displaced strand.

Data from cytological studies in yeast suggest that the ScRad52 foci represent "centers of recombinational repair capable of processing several lesions" (Lisby et al., 2001). Based on the data from our biochemical studies, we propose a similar role for HsRad52, that of a stabilizing factor. This role for HsRad52 takes advantage of its ability to form higher-order oligomeric structures that promote coincident interactions with other recombination proteins and DNA. HsRad52 may stimulate HsRad51-mediated recombination by binding the components in this pathway and anchoring them in one central location thus facilitating the interactions required for efficient strand exchange. Future studies will include biochemical experiments to look at the temporal order in which the different components of this pathway accumulate as the DSB. Additionally, these studies will investigate the effect of different HsRad52 mutants, i.e. mutants with defects in DNA binding or specific protein-protein interactions, on the efficiency of HsRad51 mediated-strand exchange.

References

Adzuma, K., T. Ogawa and H. Ogawa (1984). "Primary structure of the RAD52 gene in Saccharomyces cerevisiae." *Mol Cell Biol* **4**(12): 2735-44.

Albala, J. S., M. P. Thelen, C. Prange, W. Fan, M. Christensen, L. H. Thompson and G. G. Lennon (1997). "Identification of a novel human RAD51 homolog, RAD51B." *Genomics* **46**(3): 476-9.

Bai, Y. and L. S. Symington (1996). "A Rad52 homolog is required for RAD51-independent mitotic recombination in Saccharomyces cerevisiae." *Genes Dev* **10**(16): 2025-37.

Baumann, P., F. E. Benson and S. C. West (1996). "Human Rad51 protein promotes ATP-dependent homologous pairing and strand transfer reactions in vitro." *Cell* **87**(4): 757-66.

Baumann, P. and S. C. West (1997). "The human Rad51 protein: polarity of strand transfer and stimulation by hRP-A." *Embo J* **16**(17): 5198-206.

Baumann, P. and S. C. West (1998). "Role of the human RAD51 protein in homologous recombination and double- stranded-break repair." *Trends Biochem Sci* **23**(7): 247-51.

Baumann, P. and S. C. West (1999). "Heteroduplex formation by human Rad51 protein: effects of DNA end- structure, hRP-A and hRad52." *J Mol Biol* **291**(2): 363-74.

Benson, F. E., P. Baumann and S. C. West (1998). "Synergistic actions of Rad51 and Rad52 in recombination and DNA repair." *Nature* **391**(6665): 401-4.

Benson, F. E., A. Stasiak and S. C. West (1994). "Purification and characterization of the human Rad51 protein, an analogue of E. coli RecA." *Embo J* **13**(23): 5764-71.

Bezzubova, O., A. Silbergleit, Y. Yamaguchi-Iwai, S. Takeda and J. M. Buerstedde (1997). "Reduced X-ray resistance and homologous recombination frequencies in a RAD54-/- mutant of the chicken DT40 cell line." *Cell* **89**(2): 185-93.

Bianco, P. R., R. B. Tracy and S. C. Kowalczykowski (1998). "DNA Strand Exchange Proteins: A Biochemical and Physical Comparisoin." *Frontiers in Bioscience* **17**: d570-603.

Bishop, A. J. and R. H. Schiestl (2000). "Homologous recombination as a mechanism for genome rearrangements: environmental and genetic effects." *Hum Mol Genet* **9**(16): 2427-334.

Bishop, D. K., U. Ear, A. Bhattacharyya, C. Calderone, M. Beckett, R. R. Weichselbaum and A. Shinohara (1998). "Xrcc3 is required for assembly of Rad51 complexes in vivo." *J Biol Chem* **273**(34): 21482-8.

Bochkarev, A., R. A. Pfuetzner, A. M. Edwards and L. Frappier (1997). "Structure of the single-stranded-DNA-binding domain of replication protein A bound to DNA." *Nature* **385**(6612): 176-81.

Boundy, M. K. and D. M. Livingston (1993). "A *Saccharomyces cerevisiae* RAD52 allele expressing a C-terminal truncation protein: activities and intragenic complementation of missense mutations." *Genetics* **133**: 39-49.

Braybrooke, J. P., K. G. Spink, J. Thacker and I. D. Hickson (2000). "The RAD51 family member, RAD51L3, is a DNA-stimulated ATPase that forms a complex with XRCC2." *J Biol Chem* **275**(37): 29100-6.

Cartwright, R., A. M. Dunn, P. J. Simpson, C. E. Tambini and J. Thacker (1998). "Isolation of novel human and mouse genes of the recA/RAD51 recombination-repair gene family." *Nucleic Acids Res* **26**(7): 1653-9.

Cartwright, R., C. E. Tambini, P. J. Simpson and J. Thacker (1998). "The XRCC2 DNA repair gene from human and mouse encodes a novel member of the recA/RAD51 family." *Nucleic Acids Res* **26**(13): 3084-9.

Chen, F., A. Nastasi, Z. Shen, M. Brenneman, H. Crissman and D. J. Chen (1997). "Cell cycle-dependent protein expression of mammalian homologs of yeast DNA double-strand break repair genes Rad51 and Rad52." *Mutat Res* **384**(3): 205-11.

Clever, B., H. Interthal, J. Schmuckli-Maurer, J. King, M. Sigrist and W. D. Heyer (1997). "Recombinational repair in yeast: functional interactions between Rad51 and Rad54 proteins." *Embo J* **16**(9): 2535-44.

Davis, A. P. and L. S. Symington (2001). "The yeast recombinational repair protein Rad59 interacts with Rad52 and stimulates single-strand annealing." *Genetics* **159**(2): 515-25.

De Zutter, J. K. and K. L. Knight (1999). "The hRad51 and RecA proteins show significant differences in cooperative binding to single-stranded DNA." *J Mol Biol* **293**(4): 769-80.

Deans, B., C. S. Griffin, M. Maconochie and J. Thacker (2000). "Xrcc2 is required for genetic stability, embryonic neurogenesis and viability in mice." *Embo J* **19**(24): 6675-85.

Doherty, A. J., L. C. Serpell and C. P. Ponting (1996). "The helix-hairpin-helix DNA-binding motif: a structural basis for non- sequence-specific recognition of DNA." *Nucleic Acids Res* **24**(13): 2488-97.

Donovan, J. W., G. T. Milne and D. T. Weaver (1994). "Homotypic and heterotypic protein associations control Rad51 function in double-strand break repair." *Genes Dev* **8**(21): 2552-62.

Dosanjh, M. K., D. W. Collins, W. Fan, G. G. Lennon, J. S. Albala, Z. Shen and D. Schild (1998). "Isolation and characterization of RAD51C, a new human member of the RAD51 family of related genes." *Nucleic Acids Res* **26**(5): 1179-84.

Eggler, A. L., R. B. Inman and M. M. Cox (2002). "The Rad51-dependent pairing of long DNA substrates is stabilized by replication protein A." *J Biol Chem* **6**: 6.

Emery, H. S., D. Schild, D. E. Kellogg and R. K. Mortimer (1991). "Sequence of RAD54, a Saccharomyces cerevisiae gene involved in recombination and repair." *Gene* **104**(1): 103-6.

Essers, J., A. B. Houtsmuller, L. van Veelen, C. Paulusma, A. L. Nigg, A. Pastink, W. Vermeulen, J. H. Hoeijmakers and R. Kanaar (2002). "Nuclear dynamics of RAD52 group homologous recombination proteins in response to DNA damage." *Embo J* **21**(8): 2030-7.

Fujimori, A., S. Tachiiri, E. Sonoda, L. H. Thompson, P. K. Dhar, M. Hiraoka, S. Takeda, Y. Zhang, M. Reth and M. Takata (2001). "Rad52 partially substitutes for the Rad51 paralog XRCC3 in maintaining chromosomal integrity in vertebrate cells." *Embo J* **20**(19): 5513-20.

Game, J. C. and R. K. Mortimer (1974). "A genetic study of x-ray sensitive mutants in yeast." *Mutat Res* **24**(3): 281-92.

Gasior, S. L., H. Olivares, U. Ear, D. M. Hari, R. Weichselbaum and D. K. Bishop (2001). "Assembly of RecA-like recombinases: distinct roles for mediator proteins in mitosis and meiosis." *Proc Natl Acad Sci U S A* **98**(15): 8411-8.

Gasior, S. L., A. K. Wong, Y. Kora, A. Shinohara and D. K. Bishop (1998). "Rad52 associates with RPA and functions with rad55 and rad57 to assemble meiotic recombination complexes." *Genes Dev* **12**(14): 2208-21.

Golub, E. I., R. C. Gupta, T. Haaf, M. S. Wold and C. M. Radding (1998). "Interaction of human rad51 recombination protein with single-stranded DNA binding protein, RPA." *Nucleic Acids Res* **26**(23): 5388-93.

Golub, E. I., O. V. Kovalenko, R. C. Gupta, D. C. Ward and C. M. Radding (1997). "Interaction of human recombination proteins Rad51 and Rad54." *Nucleic Acids Res* **25**(20): 4106-10.

Haber, J.E. and W.D. Heyer (2001). "The Fuss about Mus81." *Cell* **107**: 551-554.

Hays, S. L., A. A. Firmenich and P. Berg (1995). "Complex formation in yeast double-strand break repair: participation of Rad51, Rad52, Rad55, and Rad57 proteins." *Proc Natl Acad Sci U S A* **92**(15): 6925-9.

Hays, S. L., A. A. Firmenich, P. Massey, R. Banerjee and P. Berg (1998). "Studies of the interaction between Rad52 protein and the yeast single- stranded DNA binding protein RPA." *Mol Cell Biol* **18**(7): 4400-6.

Ivanov, E. L. and J. E. Haber (1995). "RAD1 and RAD10, but not other excision repair genes, are required for double-strand break-induced recombination in Saccharomyces cerevisiae." *Mol Cell Biol* **15**(4): 2245-51.

Ivanov, E. L., N. Sugawara, J. Fishman-Lobell and J. E. Haber (1996). "Genetic requirements for the single-strand annealing pathway of double- strand break repair in Saccharomyces cerevisiae." *Genetics* **142**(3): 693-704.

Iyer, L. M., E. V. Koonin and L. Aravind (2002). "Classification and evolutionary history of the single-strand annealing proteins, RecT, Redbeta, ERF and RAD52." *BMC Genomics* **3**(1): 8.

Johnson, R. D. and M. Jasin (2000). "Sister chromatid gene conversion is a prominent double-strand break repair pathway in mammalian cells." *Embo J* **19**(13): 3398-407.

Johnson, R. D. and L. S. Symington (1995). "Functional differences and interactions among the putative RecA homologs Rad51, Rad55, and Rad57." *Mol Cell Biol* **15**(9): 4843-50.

Juo, Z. S., T. K. Chiu, P. M. Leiberman, I. Baikalov, A. J. Berk and R. E. Dickerson (1996). "How proteins recognize the TATA box." *J Mol Biol* **261**(2): 239-54.

Kagawa, W., H. Kurumizaka, S. Ikawa, S. Yokoyama and T. Shibata (2001). "Homologous pairing promoted by the human Rad52 protein." *J Biol Chem* **276**(37): 35201-8.

Kanaar, R., C. Troelstra, S. M. Swagemakers, J. Essers, B. Smit, J. H. Franssen, A. Pastink, O. Y. Bezzubova, J. M. Buerstedde, B. Clever, W. D. Heyer and J. H. Hoeijmakers (1996). "Human and mouse homologs of the Saccharomyces

cerevisiae RAD54 DNA repair gene: evidence for functional conservation." *Curr Biol* **6**(7): 828-38.

Kito, K., H. Wada, E. T. Yeh and T. Kamitani (1999). "Identification of novel isoforms of human RAD52." *Biochimica et Biophysica Acta* **1489**: 303-314.

Kowalczykowski, S. C. (2000). "Some assembly required." *Nat Struct Biol* **7**(12): 1087-9.

Kurumizaka, H., S. Ikawa, M. Nakada, K. Eda, W. Kagawa, M. Takata, S. Takeda, S. Yokoyama and T. Shibata (2001). "Homologous-pairing activity of the human DNA-repair proteins Xrcc3.Rad51C." *Proc Natl Acad Sci U S A* **98**(10): 5538-43.

Kuwajima, K., E. P. Garvey, B. E. Finn, C. R. Matthews and S. Sugai (1991). "Transient intermediates in the folding of dihydrofolate reductase as detected by far-ultraviolet circular dichroism spectroscopy." *Biochemistry* **30**(31): 7693-703.

Liang, F., M. Han, P. J. Romanienko and M. Jasin (1998). "Homology-directed repair is a major double-strand break repair pathway in mammalian cells." *Proc Natl Acad Sci U S A* **95**(9): 5172-7.

Lim, D. S. and P. Hasty (1996). "A mutation in mouse rad51 results in an early embryonic lethal that is suppressed by a mutation in p53." *Mol Cell Biol* **16**(12): 7133-43.

Lisby, M., R. Rothstein and U. H. Mortensen (2001). "Rad52 forms DNA repair and recombination centers during S phase." *Proc Natl Acad Sci U S A* **98**(15): 8276-82.

Liu, N., J. E. Lamerdin, R. S. Tebbs, D. Schild, J. D. Tucker, M. R. Shen, K. W. Brookman, M. J. Siciliano, C. A. Walter, W. Fan, L. S. Narayana, Z. Q. Zhou, A. W. Adamson, K. J. Sorensen, D. J. Chen, N. J. Jones and L. H. Thompson (1998). "XRCC2 and XRCC3, new human Rad51-family members, promote chromosome stability and protect against DNA cross-links and other damages." *Mol Cell* **1**(6): 783-93.

Liu, Y., M. Li, E. Y. Lee and N. Maizels (1999). "Localization and dynamic relocalization of mammalian Rad52 during the cell cycle and in response to DNA damage." *Curr Biol* **9**(17): 975-8.

Liu, Y. and N. Maizels (2000). "Coordinated response of mammalian Rad51 and Rad52 to DNA damage." *EMBO Rep* **1**(1): 85-90.

Masson, J. Y., A. Z. Stasiak, A. Stasiak, F. E. Benson and S. C. West (2001). "Complex formation by the human RAD51C and XRCC3 recombination repair proteins." *Proc Natl Acad Sci U S A* **98**(15): 8440-6.

Masson, J. Y., M. C. Tarsounas, A. Z. Stasiak, A. Stasiak, R. Shah, M. J. McIlwraith, F. E. Benson and S. C. West (2001). "Identification and purification of two distinct complexes containing the five RAD51 paralogs." *Genes Dev* **15**(24): 3296-307.

Mazin, A. V., C. J. Bornarth, J. A. Solinger, W. D. Heyer and S. C. Kowalczykowski (2000). "Rad54 protein is targeted to pairing loci by the Rad51 nucleoprotein filament." *Mol Cell* **6**(3): 583-92.

McIlwraith, M. J., E. Van Dyck, J. Y. Masson, A. Z. Stasiak, A. Stasiak and S. C. West (2000). "Reconstitution of the strand invasion step of double-strand break repair using human Rad51 Rad52 and RPA proteins." *J Mol Biol* **304**(2): 151-64.

Milne, G. T. and D. T. Weaver (1993). "Dominant negative alleles of RAD52 reveal a DNA repair/recombination complex including Rad51 and Rad52." *Genes Dev* **7**(9): 1755-65.

Mortensen, U. H., C. Bendixen, I. Sunjevaric and R. Rothstein (1996). "DNA strand annealing is promoted by the yeast Rad52 protein." *Proc Natl Acad Sci U S A* **93**(20): 10729-34.

Muris, D. F., O. Bezzubova, J. M. Buerstedde, K. Vreeken, A. S. Balajee, C. J. Osgood, C. Troelstra, J. H. Hoeijmakers, K. Ostermann, H. Schmidt and et al. (1994). "Cloning of human and mouse genes homologous to RAD52, a yeast gene involved in DNA repair and recombination." *Mutat Res* **315**(3): 295-305.

Namsaraev, E. A. and P. Berg (1998). "Binding of Rad51p to DNA. Interaction of Rad51p with single- and double- stranded DNA." *J Biol Chem* **273**(11): 6177-82.

New, J. H., T. Sugiyama, E. Zaitseva and S. C. Kowalczykowski (1998). "Rad52 protein stimulates DNA strand exchange by Rad51 and replication protein A." *Nature* **391**(6665): 407-10.

Ogawa, T., A. Shinohara, A. Nabetani, T. Ikeya, X. Yu, E. H. Egelman and H. Ogawa (1993). "RecA-like recombination proteins in eukaryotes: functions and structures of RAD51 genes." *Cold Spring Harb Symp Quant Biol* **58**: 567-76.

Paques, F. and J. E. Haber (1999). "Multiple pathways of recombination induced by double-strand breaks in Saccharomyces cerevisiae." *Microbiol Mol Biol Rev* **63**(2): 349-404.

Park, M. S., D. L. Ludwig, E. Stigger and S. H. Lee (1996). "Physical interaction between human RAD52 and RPA is required for homologous recombination in mammalian cells." *J Biol Chem* **271**(31): 18996-9000.

Parsons, C. A., P. Baumann, E. Van Dyck and S. C. West (2000). "Precise binding of single-stranded DNA termini by human RAD52 protein." *Embo J* **19**(15): 4175-81.

Pastnik, A., J. Eeken and P. Lohman (2001). "Genomic Integrity and the repair of double-strand DNA breaks." *Mutation Research* **480-481**: 37-50.

Pelletier, H., M. R. Sawaya, A. Kumar, S. H. Wilson and J. Kraut (1994). "Structures of ternary complexes of rat DNA polymerase beta, a DNA template-primer, and ddCTP." *Science* **264**(5167): 1891-903.

Petes, T. D., Malone,R.E>, and Symington, L.S. (1991). Recombination in Yeast. *In The Molecular and Cellular Biology of the Yeast Saccharomyces*, pp 406-522. Cold Spring Harbor Laboratory Press, New York.

Petukhova, G., S. Stratton and P. Sung (1998). "Catalysis of homologous DNA pairing by yeast Rad51 and Rad54 proteins." *Nature* **393**(6680): 91-4.

Petukhova, G., S. A. Stratton and P. Sung (1999). "Single strand DNA binding and annealing activities in the yeast recombination factor Rad59." *J Biol Chem* **274**(48): 33839-42.

Petukhova, G., S. Van Komen, S. Vergano, H. Klein and P. Sung (1999). "Yeast Rad54 promotes Rad51-dependent homologous DNA pairing via ATP hydrolysis-driven change in DNA double helix conformation." *J Biol Chem* **274**(41): 29453-62.

Pittman, D. L. and J. C. Schimenti (2000). "Midgestation lethality in mice deficient for the RecA-related gene, Rad51d/Rad51l3." *Genesis* **26**(3): 167-73.

Pittman, D. L., L. R. Weinberg and J. C. Schimenti (1998). "Identification, characterization, and genetic mapping of Rad51d, a new mouse and human RAD51/RecA-related gene." *Genomics* **49**(1): 103-11.

Raderschall, E., E. I. Golub and T. Haaf (1999). "Nuclear foci of mammalian recombination proteins are located at single- stranded DNA regions formed after DNA damage." *Proc Natl Acad Sci U S A* **96**(5): 1921-6.

Ranatunga, W., D. Jackson, J. A. Lloyd, A. L. Forget, K. L. Knight and G. E. Borgstahl (2001). "Human RAD52 exhibits two modes of self-association." *J Biol Chem* **276**(19): 15876-80.

Reddy, G., E. I. Golub and C. M. Radding (1997). "Human Rad52 protein promotes single-strand DNA annealing followed by branch migration." *Mutat Res* **377**(1): 53-9.

Rice, M. C., S. T. Smith, F. Bullrich, P. Havre and E. B. Kmiec (1997). "Isolation of human and mouse genes based on homology to REC2, a recombinational repair gene from the fungus Ustilago maydis." *Proc Natl Acad Sci U S A* **94**(14): 7417-22.

Rijkers, T., J. Van Den Ouweland, B. Morolli, A. G. Rolink, W. M. Baarends, P. P. Van Sloun, P. H. Lohman and A. Pastink (1998). "Targeted inactivation of mouse RAD52 reduces homologous recombination but not resistance to ionizing radiation." *Mol Cell Biol* **18**(11): 6423-9.

Ristic, D., C. Wyman, C. Paulusma and R. Kanaar (2001). "The architecture of the human Rad54-DNA complex provides evidence for protein translocation along DNA." *Proc Natl Acad Sci U S A* **98**(15): 8454-60.

Saparbaev, M., L. Prakash and S. Prakash (1996). "Requirement of mismatch repair genes MSH2 and MSH3 in the RAD1-RAD10 pathway of mitotic recombination in Saccharomyces cerevisiae." *Genetics* **142**(3): 727-36.

Schild, D., Y. Lio, D. W. Collins, T. Tsomondo and D. J. Chen (2000). "Evidence for simultaneous protein interactions between human Rad51 paralogs." *J Biol Chem* **275**(22): 16443-9.

Shao, X. and N. V. Grishin (2000). "Common fold in helix-hairpin-helix proteins." *Nucleic Acids Res* **28**(14): 2643-50.

Shen, Z., K. G. Cloud, D. J. Chen and M. S. Park (1996). "Specific interactions between the human RAD51 and RAD52 proteins." *J Biol Chem* **271**(1): 148-52.

Shen, Z., K. Denison, R. Lobb, J. M. Gatewood and D. J. Chen (1995). "The human and mouse homologs of the yeast RAD52 gene: cDNA cloning, sequence analysis, assignment to human chromosome 12p12.2-p13, and mRNA expression in mouse tissues." *Genomics* **25**(1): 199-206.

Shen, Z., S. R. Peterson, J. C. Comeaux, D. Zastrow, R. K. Moyzis, E. M. Bradbury and D. J. Chen (1996). "Self-association of human RAD52 protein." *Mutat Res* **364**(2): 81-9.

Shinohara, A., H. Ogawa, Y. Matsuda, N. Ushio, K. Ikeo and T. Ogawa (1993). "Cloning of human, mouse and fission yeast recombination genes homologous to RAD51 and recA." *Nat Genet* **4**(3): 239-43.

Shinohara, A., H. Ogawa and T. Ogawa (1992). "Rad51 protein involved in repair and recombination in S. cerevisiae is a RecA-like protein." *Cell* **69**(3): 457-70.

Shinohara, A. and T. Ogawa (1995). "Homologous recombination and the roles of double-strand breaks." *Trends Biochem Sci* **20**(10): 387-91.

Shinohara, A. and T. Ogawa (1998). "Stimulation by Rad52 of yeast Rad51-mediated recombination." *Nature* **391**(6665): 404-7.

Shinohara, A., M. Shinohara, T. Ohta, S. Matsuda and T. Ogawa (1998). "Rad52 forms ring structures and co-operates with RPA in single-strand DNA annealing." *Genes Cells* **3**(3): 145-56.

Shu, Z., S. Smith, L. Wang, M. C. Rice and E. B. Kmiec (1999). "Disruption of muREC2/RAD51L1 in mice results in early embryonic lethality which can Be partially rescued in a p53(-/-) background." *Mol Cell Biol* **19**(12): 8686-93.

Sigurdsson, S., S. Van Komen, W. Bussen, D. Schild, J. S. Albala and P. Sung (2001). "Mediator function of the human Rad51B-Rad51C complex in Rad51/RPA- catalyzed DNA strand exchange." *Genes Dev* **15**(24): 3308-18.

Song, B. and P. Sung (2000). "Functional interactions among yeast Rad51 recombinase, Rad52 mediator, and replication protein A in DNA strand exchange." *J Biol Chem* **275**(21): 15895-904.

Sonoda, E., M. S. Sasaki, J. M. Buerstedde, O. Bezzubova, A. Shinohara, H. Ogawa, M. Takata, Y. Yamaguchi-Iwai and S. Takeda (1998). "Rad51-deficient vertebrate cells accumulate chromosomal breaks prior to cell death." *Embo J* **17**(2): 598-608.

Stasiak, A. Z., E. Larquet, A. Stasiak, S. Muller, A. Engel, E. Van Dyck, S. C. West and E. H. Egelman (2000). "The human Rad52 protein exists as a heptameric ring." *Curr Biol* **10**(6): 337-40.

Sugawara, N., E. L. Ivanov, J. Fishman-Lobell, B. L. Ray, X. Wu and J. E. Haber (1995). "DNA structure-dependent requirements for yeast RAD genes in gene conversion." *Nature* **373**(6509): 84-6.

Sugiyama, T. and S. C. Kowalczykowski (2002). "Rad52 protein associates with RPA-ssDNA to accelerate Rad51-mediated displacement of RPA and presynaptic complex formation." *J Biol Chem* **19**: 19.

Sugiyama, T., J. H. New and S. C. Kowalczykowski (1998). "DNA annealing by RAD52 protein is stimulated by specific interaction with the complex of

replication protein A and single-stranded DNA." *Proc Natl Acad Sci U S A* **95**(11): 6049-54.

Sugiyama, T., E. M. Zaitseva and S. C. Kowalczykowski (1997). "A single-stranded DNA-binding protein is needed for efficient presynaptic complex formation by the Saccharomyces cerevisiae Rad51 protein." *J Biol Chem* **272**(12): 7940-5.

Sung, P. (1994). "Catalysis of ATP-dependent homologous DNA pairing and strand exchange by yeast RAD51 protein." *Science* **265**(5176): 1241-3.

Sung, P. (1997). "Function of yeast Rad52 protein as a mediator between replication protein A and the Rad51 recombinase." *J Biol Chem* **272**(45): 28194-7.

Sung, P. (1997). "Yeast Rad55 and Rad57 proteins form a heterodimer that functions with replication protein A to promote DNA strand exchange by Rad51 recombinase." *Genes Dev* **11**(9): 1111-21.

Sung, P. and D. L. Robberson (1995). "DNA strand exchange mediated by a RAD51-ssDNA nucleoprotein filament with polarity opposite to that of RecA." *Cell* **82**(3): 453-61.

Swagemakers, S. M., J. Essers, J. de Wit, J. H. Hoeijmakers and R. Kanaar (1998). "The human RAD54 recombinational DNA repair protein is a double-stranded DNA-dependent ATPase." *J Biol Chem* **273**(43): 28292-7.

Takata, M., M. S. Sasaki, E. Sonoda, C. Morrison, M. Hashimoto, H. Utsumi, Y. Yamaguchi-Iwai, A. Shinohara and S. Takeda (1998). "Homologous recombination and non-homologous end-joining pathways of DNA double-strand break repair have overlapping roles in the maintenance of chromosomal integrity in vertebrate cells." *Embo J* **17**(18): 5497-508.

Takata, M., M. S. Sasaki, S. Tachiiri, T. Fukushima, E. Sonoda, D. Schild, L. H. Thompson and S. Takeda (2001). "Chromosome instability and defective recombinational repair in knockout mutants of the five Rad51 paralogs." *Mol Cell Biol* **21**(8): 2858-66.

Tan, T. L., J. Essers, E. Citterio, S. M. Swagemakers, J. de Wit, F. E. Benson, J. H. Hoeijmakers and R. Kanaar (1999). "Mouse Rad54 affects DNA conformation and DNA-damage-induced Rad51 foci formation." *Curr Biol* **9**(6): 325-8.

Tanaka, K., T. Hiramoto, T. Fukuda and K. Miyagawa (2000). "A novel human rad54 homologue, Rad54B, associates with Rad51." *J Biol Chem* **275**(34): 26316-21.

Tebbs, R. S., Y. Zhao, J. D. Tucker, J. B. Scheerer, M. J. Siciliano, M. Hwang, N. Liu, R. J. Legerski and L. H. Thompson (1995). "Correction of chromosomal

instability and sensitivity to diverse mutagens by a cloned cDNA of the XRCC3 DNA repair gene." *Proc Natl Acad Sci U S A* **92**(14): 6354-8.

Thayer, M. M., H. Ahern, D. Xing, R. P. Cunningham and J. A. Tainer (1995). "Novel DNA binding motifs in the DNA repair enzyme endonuclease III crystal structure." *Embo J* **14**(16): 4108-20.

Thompson, L. H. and D. Schild (2001). "Homologous recombinational repair of DNA ensures mammalian chromosome stability." *Mutat Res* **477**(1-2): 131-53.

Tsuzuki, T., Y. Fujii, K. Sakumi, Y. Tominaga, K. Nakao, M. Sekiguchi, A. Matsushiro, Y. Yoshimura and MoritaT (1996). "Targeted disruption of the Rad51 gene leads to lethality in embryonic mice." *Proc Natl Acad Sci U S A* **93**(13): 6236-40.

Van Dyck, E., N. M. Hajibagheri, A. Stasiak and S. C. West (1998). "Visualisation of human rad52 protein and its complexes with hRad51 and DNA." *J Mol Biol* **284**(4): 1027-38.

Van Dyck, E., A. Z. Stasiak, A. Stasiak and S. C. West (1999). "Binding of double-strand breaks in DNA by human Rad52 protein." *Nature* **398**(6729): 728-31.

Van Dyck, E., A. Z. Stasiak, A. Stasiak and S. C. West (2001). "Visualization of recombination intermediates produced by RAD52-mediated single-strand annealing." *EMBO Rep* **2**(10): 905-9.

Van Komen, S., G. Petukhova, S. Sigurdsson, S. Stratton, and P. Sung (1999). " Superheilicity - driven homologous pairing by yeast recombination factors Rad51 and Rad54." *Mol Cell* **6**(3): 563-72.

Wold, M. S. (1997). "Replication protein A: a heterotrimeric, single-stranded DNA-binding protein required for eukaryotic DNA metabolism." *Annu Rev Biochem* **66**: 61-92.

Yamaguchi-Iwai, Y., E. Sonoda, J. M. Buerstedde, O. Bezzubova, C. Morrison, M. Takata, A. Shinohara and S. Takeda (1998). "Homologous recombination, but not DNA repair, is reduced in vertebrate cells deficient in RAD52." *Mol Cell Biol* **18**(11): 6430-5.

Zaitseva, E. M., E. N. Zaitsev and S. C. Kowalczykowski (1999). "The DNA binding properties of Saccharomyces cerevisiae Rad51 protein." *J Biol Chem* **274**(5): 2907-15.